DIATOMS AS	TROPICAL CYCLONE PA	LEOENVIRONMENTAI	LINDICATORS

THE GATHERING STORM? AN EXAMINATION OF DIATOMS AS PALEOENVIRONMENTAL INDICATORS OF TROPICAL CYCLONE ACTIVITY THAT MAY HAVE PRECIPITATED THE CLASSIC MAYA DECLINE

By KATELYN MOUNTJOY, BSc

A Thesis Submitted to the School of Graduate Studies in Partial Fulfilment of the Requirements for the Degree Master of Earth and Environmental Science

McMaster University © Copyright by Katelyn Mountjoy, September 2025

McMaster University MASTER OF EARTH AND ENVIRONMENTAL SCIENCE (2025) Hamilton, Ontario (School of Earth, Environment and Society)

TITLE: The gathering storm? An examination of diatoms as paleoenvironmental indicators of tropical cyclone activity that may have precipitated the Classic Maya Decline

AUTHOR: Katelyn Mountjoy, BSc (McMaster University)

SUPERVISOR: Dr. E.G. Reinhardt

NUMBER OF PAGES: xi, 65

Lay Abstract

A warming climate has been linked to more severe storms, which may have similarly occurred in the past and been a contributing factor to the decline of the ancient Maya civilisation that inhabited the Yucatan Peninsula, as severe storms have been found to increase the salt content of the region's major freshwater source—which floats atop ocean water in an underground aquifer—by increasing the mixing between them. This study analysed microfossils known as diatoms from the aquifer from May 2012—May 2017, during which time several major storms affected the region: Ingrid, Dolly, Hanna, and Bill. This study found that the diversity of diatom species showed a general decrease after these storms, while the proportion of diatoms that reside closer to the bottom of the aquifer showed a general increase. These largely consistent responses to storms demonstrate diatoms could be used to examine past changes in the aquifer.

Abstract

As the increase in the intensity and frequency of tropical cyclones has been linked to a warming climate, this provides support for the hypothesis that the ancient Maya civilisation that inhabited the Yucatan Peninsula during the Late Classic Period—concurrent with another period of elevated global temperatures—may have been similarly affected by climate change-driven changes in tropical cyclone activity. Furthermore, this may have negatively impacted the peninsula's major freshwater source, which is a coastal aguifer that is anchialine in nature (i.e., a freshwater lens or meteoric water mass is stratified atop a denser, more saline marine water mass below), as tropical cyclones have been found in previous studies to be a direct cause of salinizing the freshwater lens and negatively affecting its potability. Accordingly, this study examined possible paleoenvironmental indicators of hurricane activity by analysing diatom microfossils, which are very sensitive to changes in water quality. The diatoms were obtained from sediment samples in the Yax Chen aquifer cave system from May 2012– May 2017, during which time several tropical cyclones affected the region: Ingrid, Dolly, Hanna, and Bill. This study found that the Shannon Diversity Index values showed a general decrease after tropical cyclone activity whereas the relative abundance of benthic diatoms showed a general increase, implying vertical mixing of the water column and increasing salinization of the meteoric water mass. Therefore, these largely consistent responses to tropical cyclones provide a foundation for utilising diatoms as paleoenvironmental indicators to examine tropical cyclone activity during the Terminal Classic Period/Medieval Warm Period.

Acknowledgements

I would like to thank Dr. Riley Steele for her tremendous guidance and support regarding the diatom sample preparation techniques that were used in this study. I would also like to acknowledge my supervisor Dr. Eduard Reinhardt for the interesting experience that constituted my graduate studies at McMaster University, not unlike that of so many other women in STEM; it was illuminating on many different levels. Last but not least, I would like to thank Dr. Sang-Tae Kim and Dr. Joe Boyce for being a part of my supervisory committee and Dr. Gita Ljubicic for chairing my thesis defense.

Table of Contents

Abstract	iv
Acknowled gements	v
List of Figures.	viii
List of Tables	ix
List of Abbreviations and Symbols	x
Declaration of Academic Achievements.	xi
1. Introduction	1
1.1. Physical geography	1
1.1.1. Yax Chen	2
1.2. Salination risks	4
1.3. Climate	5
1.3.1. Tropical cyclones	7
1.3.1.1. Instrumental record	7
1.3.1.2. Future projections	8
1.4. The Medieval Warm Period/Terminal Classic Period	9
1.4.1. Archaeological record	9
1.4.2. Paleoclimate studies	11
1.4.2.1. Drought	11
1.4.2.2. Tropical cyclones	12
1.5. Compound extremes	13
1.6. Paleoenvironmental indicators	13
1.6.1. Diatoms	14

1.7. Study Objectives
2. Methods
3. Results
3.1. Dominant species and ecological preferences
3.2. Spatial results
3.3. Temporal results
3.4. Si/Ti ratio and precipitation
3.5. Clustering analyses
4. Discussion
4.1. Time period
4.1.1. Precipitation and Si/Ti ratio
4.1.2. SDI values
4.1.3. Percentage of benthic diatoms
4.2. Spatial
5. Conclusions
5.1 Future research directions
5.1.1. Yax Chen
5.1.2. Broader upwelling and ocean circulation patterns
5.2. Concluding remarks
References Cited
Appendix45

List of Figures

Fig. 1. Locations of sediment trap sampling stations along Yax Chen
Fig. 2a–i. Fig. 2. Fractional relative abundances separated by upstream (sampling stations 2 and 7) and downstream (sampling stations 12 and 17). The first number denotes station number, while "M" and "D" represent May and December, respectively, followed by sampling year. a) <i>Thalassiosira spinulata</i> (planktonic). b) <i>Cyclotella meneghiniana</i> (planktonic and benthic). c) <i>Terpsinoe musica</i> (benthic). d) <i>Paralia sulcata</i> (benthic). e) <i>Navicula arvensis</i> var. maior Lange-Bertalot (benthic). f) <i>Nitzchia</i> sp. (benthic). g) <i>Denticula kuetzingii</i> Grunow (benthic). h) <i>Hemidiscus</i> sp. (benthic). i) <i>Thalassiosira</i> weissflogii (planktonic)
Fig. 3a–b. The first number of the legend denotes station number, while "M" and "D" represent May and December, respectively, followed by sampling year. a) Shannon Diversity Index (SDI) values at upstream (sampling stations 2 and 7) and downstream (sampling stations 12 and 17) stations. b) percentage of benthic diatoms at upstream (sampling stations 2 and 7) and downstream (sampling stations 12 and 17) stations
Fig 4a–d. Data plotted through time (May 2012–May 2017) and by station (upstream to downstream locations): the first number denotes station number, while "M" and "D" represent May and December, respectively, followed by sampling year. a) <i>Thalassiosira weissflogii</i> (planktonic) and <i>Thalassiosira spinulata</i> (planktonic). b) <i>Paralia sulcata</i> (benthic) and <i>Terpsinoe musica</i> (benthic). c) <i>Nitzchia</i> sp. (benthic) and <i>Navicula arvensis</i> Lange-Bertalot (benthic). d) <i>Hemidiscus</i> sp. (benthic) and <i>Denticula kuetzingii</i> Grunow (benthic).
Fig 5a–d. Data plotted through time (May 2012–May 2017) and by station (upstream to downstream locations): the first number denotes station number, while "M" and "D" represent May and December, respectively, followed by sampling year. a) Shannon Diversity Index (SDI). b) percentage of benthic diatoms. c) Si/Ti ratio. d) total precipitation over each 6-month sampling period (mm)
Fig. 6. Si/Ti ratio and total precipitation over each 6-month sampling period (mm)
Fig. 7a–d. Diatom concentration and Si/Ti ratio. a). sampling station 2. b) sampling station 7. c) sampling station 12. d) sampling station 17
Fig. 8a–d. Percentage of benthic diatoms and Si/Ti ratio. a) sampling station 2. b) sampling station 7. c) sampling station 12. d) sampling station 17
Fig. 9. Total precipitation during each 6-month sampling period (mm) and diatom concentrations
Fig 10a-b. R-mode global clustering analysis/clusters of species for all stations and time periods and Q-mode clusters of samples
Fig. 11a–d. Dominant species cluster analysis. The "P" beside taxa delineates planktonic diatoms and the "B" delineates benthic species

List of Tables

Table 1. Summary of TCs during the study period (May 2012–May 2017)	16
Table 2. Ecological preferences of the most abundant species	18

List of all Abbreviations and Symbols

 $\mu XRF\text{-}CS$: micro X-ray fluorescence core scanner

Ca: calcium

Cr-HE: Cr heavy element

DOC: dissolved organic carbon

ENSO: El Nino-Southern Oscillation

GHG: greenhouse gas

IPCC: Intergovernmental Panel on Climate Change

ITCZ: Intertropical Convergence Zone

MeWM: meteoric water mass

MWM: marine water mass

MWP: Medieval Warm Period

NAO: North Atlantic Oscillation

OM: organic matter

PP: primary productivity

SDI: Shannon Diversity Index

Si: silica

SSR: Sequential Sediment Reservoir

SST: sea surface temperature

TC: tropical cyclone

TCP: Terminal Classic Period

Ti: titanium

Declaration of Academic Achievement

K. Mountjoy was responsible for the diatom sample preparation and data analysis as well as the literature review and writing of the manuscript. K. Mountjoy and E.G. Reinhardt were both responsible for data visualisation. E.G. Reinhardt carried out the study conceptualisation, editing of the manuscript, and data collection with other students in his lab.

1. Introduction

A recent study found that the salinity levels of freshwater greatly impacted tourism and resulted in an economic loss to a coastal North Carolina tourist destination as tourists were less likely to consider visiting if the drinking water tasted salty (Whitehead et al. 2024). The Yucatan Peninsula of Mexico, and in particular Quintana Roo on the eastern coast, is a popular tourist destination and part of the most-visited region in all of Latin America (Mejia-Ortiz et al 2022b), receiving tens of millions of tourists annually (McNeill-Jewer et al. 2019). Popular tourist destinations include Cancun, established in 1970, and the Maya Riviera established in the 1990s (Mejia-Ortiz et al. 2022b), and the Mexican government has recently invested significantly in tourism in the region, including implementing major infrastructure projects such as the Yucatan railway line; however, the future of freshwater in Mexico remains uncertain due to the fact the country is currently facing several water crises (Godinez Madrigal et al. 2018), and the Yucatan Peninsula is not exempt as the geology and topography of the region contribute to scarcity of surface water over the peninsula (Gelting 1995). Moreover, the groundwater of the peninsula is at risk of increased salination, to be discussed in greater detail below.

1.1. Physical geography

The states of Quintana Roo, Campeche, and Yucatan compose the Yucatan Peninsula, which is bordered by the Caribbean Sea in the east and the Gulf of Mexico to the west and north (Rodriguez-Gonzalez & Cerezo-Mota 2025). The topography is relatively flat (except for some foothills in the south around Campeche) due to the flat beds of limestone, known as karst, that predominate the Yucatan Peninsula (Gelting 1995); most of the peninsula is typically at elevations less than 50 m above sea level (Rodriguez-Gonzalez & Cerezo-Mota, 2025), although the southernmost portion of the peninsula transitions to a non-karstic landscape as the limestone is mixed with other types of rock (Gelting 1995), and foothills result in a slightly higher elevation of up to 390 m (Rodriguez-Gonzalez & Cerezo-Mota 2025).

The karst that composes the Yucatan Peninsula is very porous, which leads to infiltration of precipitation to the subsurface resulting in very little surface waters (Gelting 1995; Rodriguez-Gonzalez & Cerezo-Mota, 2025; van Hengstum et al. 2008) with no rivers or streams (Pohlman et al. 1997), particularly in the northern portion of the peninsula. The southern portion does contain some surface water as clay and other more impermeable materials have accumulated amongst the limestone, resulting in some lakes, swamp lands, and the Rio Hondo (Gelting 1995).

The carbonic acid present in precipitation promotes weathering of the limestone, which leads to faults or fractures that further facilitate the subsurface flow of water (Gelting 1995); this limestone dissolution has resulted in an extensive cave network that acts as a conduit for groundwater (Pohlman et al. 1997). The collapse of portions of the cavern ceiling as a result of dissolution results in cenotes (Collins et al. 2015), also known as sinkholes or karst windows (Gelting 1995), which number in the thousands across the peninsula and connect the surface to the subterranean cave network and aquifer (van Hengstum et al. 2008).

Anchialine caves are common features of tropical volcanic and karstic coastal regions, and the Yucatan Peninsula is home to the largest anchialine cave network globally (Pohlman et al. 1997), which contains the largest source of freshwater in the Yucatan Peninsula (Gelting 1995) and the country, with

Quintana Roo housing the best-conserved reservoir (Mejia-Ortiz et al. 2022b). Anchialine aquifers are characterized by a density-stratified water column of a freshwater lens or meteoric water mass (MeWM) that flows overtop of a marine water mass (MWM) (Collins et al. 2015). The marine water mass and meteoric water mass are divided by the halocline, a mixing zone of the water layers (Mejia-Ortiz et al. 2022b). The halocline is of intermediate salinity that is affected by storms, tidal mixing, wet/dry cycles, and sea level (Coutino et al. 2017; Kovacs et al. 2017; McNeill-Jewer et al. 2019), while the aquifer's water level is affected by droughts, seasonal rainfall, and tides (McNeill-Jewer et al. 2019). The temperature and dissolved organic carbon (DOC) present in the water column are directly related to halocline depth, and generally decrease as depth increases (Mejia-Ortiz et al. 2022b). Anchialine ecosystems are often oligotrophic with low dissolved O, and can become anoxic and eutrophic if organic matter (OM) increases (Mejia-Ortiz et al. 2022b; Pohlman et al. 1997).

Notably, water also flows through the aquifer very quickly toward the ocean compared to aquifers of other rock types, leading to a very shallow meteoric water mass or freshwater lens (Gelting 1995), although it becomes wider farther from the coast (Mejia-Ortiz et al. 2022b); saline and freshwater have been found to travel through the aquifer system at 1–10 km per day (van Hengstum et al. 2008).

Anchialine environments are made up of interconnected groundwater habitats (Mejia-Ortiz et al. 2022a) as tropical forest and mangrove ecosystems are connected to the aquifer system and establish connections with the surrounding areas (Collins et al. 2015; Mejia-Ortiz et al. 2022b), although only in the past 20 years have anchialine caves been recognized as important biological habitats (Pohlman et al. 1997). Many cave-adapted organisms can be found in them, including invertebrates, and the greatest species richness occurs in the marine water just beyond the halocline (Mejia-Ortiz et al. 2022a). Other fauna that have been found in anchialine environments include amphipods, remipedes, fish, shrimp, isopods, mysids, ostracods, and crustaceans (Pohlman et al 1997), and primary producers reported in the Yucatan Peninsula's cenotes include thecamoebians and foraminifera (van Hengstum et al. 2008) as well as diatoms (McNeill-Jewer et al. 2019).

As a result of the predominantly karstic landscape, sediment such as sand and silt typically produced from weathering of other types of rock are not present in the region (Gelting 1995), and studies have found little sedimentation in the cave network (Collins et al. 2015; McNeill-Jewer et al. 2019) with the exception of organic matter (OM), which is a result of primary productivity (PP) having occurred within the sunlit cenotes themselves or transported from surrounding land areas (Collins et al. 2015). Primary productivity and cenote size, which is directly related to primary productivity, were found to be important controlling factors for sedimentation in anchialine cave systems as well as surrounding vegetation type, as the mangroves typically found farther downstream result in higher PP and sedimentation, slowing percolation and retaining water for longer, whereas the tropical forests found farther inland enable rainfall to immediately infiltrate through the limestone and are less dependant on cenotes for percolation (Collins et al. 2015).

1.1.1. Yax Chen

Yax Chen is part of the larger Ox Bel Ha cave network, approximately 496,804 m in length, the longest cave network in Quintana Roo (Quintana Roo Speleological Survey 2025), and is on average 10 m wide and 6 m high (Coutino et al. 2017). It is oriented in a NW direction with its conduits positioned

perpendicular to the coastline, and seven large cenotes are located along the main channel ranging in size from 1600–9000 m² (McNeill-Jewer et al. 2019). The meteoric water mass or freshwater lens was found to have minimal salinity (1–7 psu) compared to 35 psu for the marine water mass, and the temperature of the freshwater lens was also found to be more stable, at around 25 °C compared to 25.5–28 °C for the marine water mass (Collins et al. 2015). Yax Chen is part of an ongoing monitoring project that began in 2011 (McNeill-Jewer et al. 2019), and is displayed in Figure 1 with the locations of the sediment trap sampling stations (McNeill-Jewer et al. 2019).

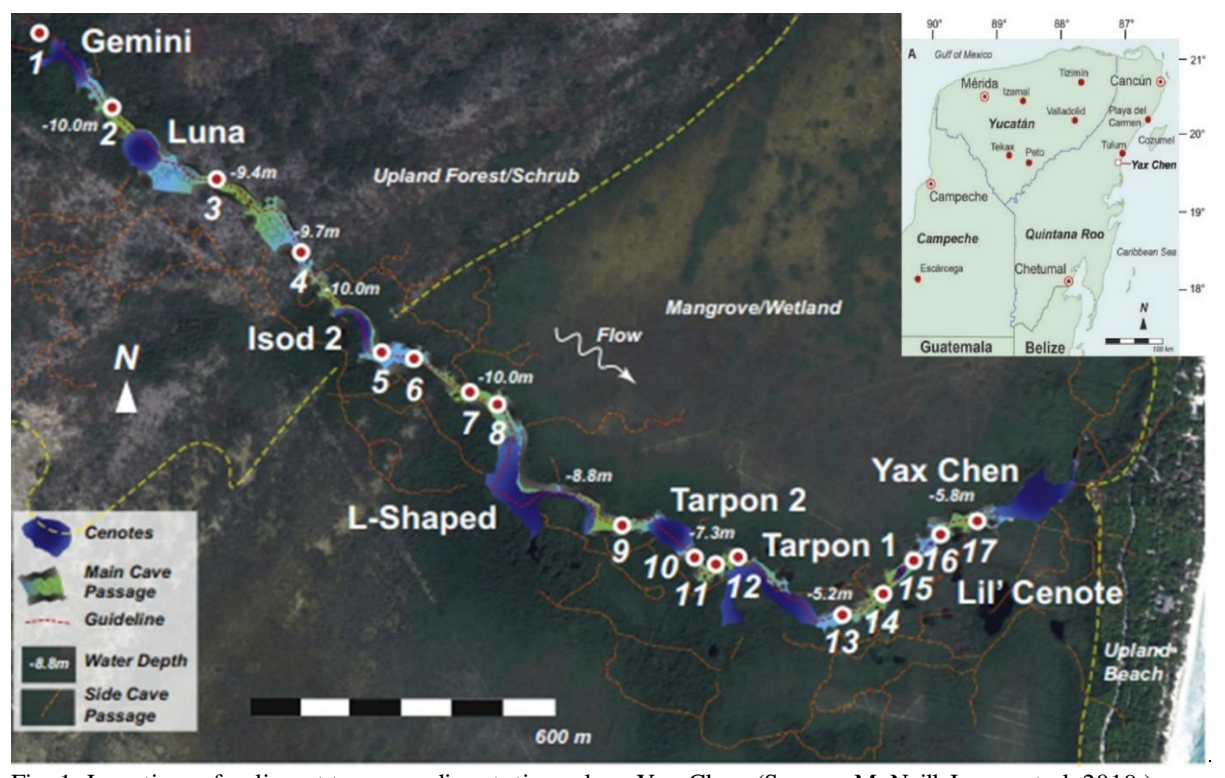


Fig. 1. Locations of sediment trap sampling stations along Yax Chen. (Source: McNeill-Jewer et al. 2019.)

Significant sediment accumulation is absent in most of the caves, although Yax Chen was found to have substantial organic sediment (McNeill-Jewer et al. 2019). As mentioned previously, PP largely determines the sediment flux, as larger cenotes and the presence of mangroves surrounding them were found to increase sediment flux: cenotes were found to decrease in size with distance from the coast, and the vegetation type transitioned from mangrove to lowland tropical forest approximately 100 m upstream of sampling stn. 7 (Collins et al. 2015). Accordingly, Collins et al. (2015) found that sediment flux rates showed a strong correlation with upstream cenote size (r²=0.7), and little sedimentation was found by areas surrounded by lowland tropical forest and with few cenotes, upstream of sampling stn. 1. Stns. 2–8 exhibited moderate sediment flux, and were surrounded by some mangroves, while stns. 13–17 had the highest sediment flux, three times higher than stns. 2–8, and were located in an area predominated by mangroves. OM content was fairly consistent year-over-year during the study, but sediment flux showed greater variations, which was greater in the downstream portions (stns. 13–17, 0.15 mg/cm²/day) than areas farther upstream (0.5 mg/cm²/day) (Collins et al. 2015).

The study by Collins et al. (2015) also examined the effects of Hurricane Ingrid on sedimentation, which occurred in September 2013 and resulted in rainfall in excess of 320 mm over a

24-hour period (McNeill-Jewer et al. 2019) that led to substantial flooding of the study area; however, it was found that Hurricane Ingrid affected the water table but did not have an immediate significant impact on sediment flux rate, although it resulted in increased nutrients and PP in cenotes for months following the hurricane (Collins et al. 2015). This was posited to be because during large precipitation events, water has a short residence time in cenotes due to higher flow within the MeWM and less time for PP, while as the water level subsides into the dry season, mangrove nutrients help promote increased PP (McNeill-Jewer et al. 2019) and water has longer residence times (Collins et al. 2015). Accordingly, Hurricane Ingrid did not significantly affect the yearly sediment flux rate in 2013, although it increased in the months following as Dec 2013 had low sediment flux rates that increased significantly in May 2014; however, this change was more pronounced in the downstream areas of Yax Chen, as sedimentation in the upper region was more constant throughout the year (Collins et al. 2015).

These findings corresponded to subsequent work done by McNeill-Jewer et al. (2019), which found that lithogenic-derived elements such as Ti/K were directly correlated with precipitation, whereas biogenic-derived elements (Si/Ti) only showed a response after large precipitation events such as Hurricane Ingrid and other TCs, and also displayed a lagged response or latency period of approximately 6–12 months. A plankton tow of Yax Chen cenote showed that the organic matter is predominated by an abundance of diatom frustules (50–60%), which corresponds with the high Si content found in sediment trap samples (McNeill-Jewer et al. 2019) as Si is the primary component of diatoms, incorporated into their frustules (Williams 2020), and thus is an indicator of diatom abundance (McNeill-Jewer et al. 2019). Interestingly, mangroves have been reported to facilitate diatom abundance and diversity (Lopez Fuertes et al. 2010), which may also be a contributing factor to the higher PP and sedimentation in downstream, mangrove-dominated areas of the aquifer.

Anchialine ecosystems have traditionally been considered stable environments, although there is growing evidence they are affected by external oceanic, hydrological, and meteorological conditions, and as a result may be more vulnerable to environmental change than considered previously (Mejia-Ortiz et al. 2022a), including salination (Coutino et al. 2017; Kovacs et al. 2017).

1.2. Salination risks

Freshwater demand in the Yucatan Peninsula is supplied from drilled wells accessorised with electric pumps, although over-withdrawal of groundwater can lead to saltwater intrusions of the freshwater lens (Gelting 1995). The increasing tourism sector, which has led to the Yucatan Peninsula, and Quintana Roo in particular, being recognized as the most visited tourist destination region in all of Latin America (Mejia-Ortiz et al 2022b) in addition to population growth—in part resulting from government policies to develop areas such as Quintana Roo that has outstripped the rest of the country—are resulting in increased freshwater demand that increases the risk of over-withdrawal (Gelting 1995).

In addition, sea level rise is also associated with saltwater intrusions into freshwater aquifers (Whitehead et al. 2024), and the Gulf of Mexico is experiencing some of the highest rates of sea level rise globally, far outpacing the global average of 1.7–1.8 mm/year (Rosenzweig et al. 2007), as sea level rise along the Gulf coast has been rapidly accelerating since 2010 with rates at over 10 mm/yr⁻¹ (Dangendorf et al. 2023). However, the accretion rates of mangroves have been found to generally compensate for sea level rise (Rosenzweig et al. 2007), which are prevalent along the coast of the Yucatan Peninsula (Collins et al. 2015).

Sea level rise and low elevations make areas particularly susceptible to the effects of hurricanes, notably storm surge (Rosenzweig et al. 2007), and the Yucatan Peninsula is a prime example of an area with particularly low elevations and high sea level rise, and is also prone to frequent hurricane activity as it has the highest rates of landfalling hurricanes in Mexico (Appendini et al. 2019). Climate change is resulting in an increased intensity and frequency of tropical cyclones (TCs), including hurricanes in the North Atlantic region (Seneviratne et al. 2021), which also directly increases groundwater salinity within anchialine aquifers.

In particular, Kovacs et al. (2017) conducted the first long-term study in the Yucatan Peninsula of groundwater salinity between 2012 and 2016 and found that turbulent mixing with the underlying water mass and precipitation affected the salinity of groundwater, which was controlled by rainfall intensity (Kovacs et al. 2017). Specifically, they found that the salinity of the meteoric water mass increased after large precipitation events as it triggered mixing with the marine water mass: the study found seasonal variations in groundwater salinity from 6.5–7.25 ppt over the rainy and dry seasons as well as tidal mixing, which occurred on diurnal scales. The study also found that the salinity increased quickly after large precipitation events, with more intense rainfall events corresponding with larger, longer-lasting changes in groundwater salinity (Kovacs et al. 2017). Coutino et al. (2017) analysed the hydrodynamics after TCs and found that the water column was unstable for several months following the 2013 TCs Ingrid and Manuel, finding a strong correlation between TCs and changes in salinity and temperature above the halocline, with mixing preferentially occurring along the periphery of the halocline/pycnocline (Coutino et al. 2017).

Computer modelling of groundwater flow or groundwater flow models are used in some areas for improved water management and to avoid saltwater intrusions by modelling the flows of the two water masses; however, this is often difficult in karstic environments because of the karst geology, which leads to multiple possible flow paths (Gelting 1995). Desalination plants have been used on a small-scale in Mexico since the 1960s, although the costs to operate them are quite high (Gelting 1995).

1.3. Climate

The Yucatan Peninsula is classified as having a warm, sub-humid climate, which is amplified through evapotranspiration from the abundant vegetation (Rodriguez-Gonzalez & Cerezo-Mota 2025), and temperatures typically range between 20–25 degrees °C (Mejia-Ortiz et al. 2022b). The Yucatan Peninsula also experiences 35% more rainfall on average than the rest of the country, with most of it occurring from May–September during the rainy season, which also contributes to the humid climate (Gelting 1995).

The latitude of the Intertropical Convergence Zone (ITCZ) shifts seasonally together with subtropical high-pressure cells that affect moisture availability in most of Mesoamerica, with the northerly position of the ITCZ corresponding to high precipitation during the summer (Gill et al. 2007; Rodriguez-Ramirez et al. 2015): the Yucatan Peninsula lies at the northernmost edge of the ITCZ (Fagan 2004), and thus precipitation over the peninsula is most strongly controlled by the ITCZ as well as the North Atlantic High, as it receives very little precipitation from the Pacific with the exception of some winter storms (Gill et al. 2007). The North Atlantic High is the descending branch of the more general Hadley circulation cell, and its position varies slightly annually from a southwest to northeast direction,

implying contraction and expansion of the Hadley cell, which has been found to in turn influence the position of the ITCZ: when it is located more to the northeast, implicating an expansion of the Hadley cell (Gill et al. 2007)— which is currently occurring with Hadley cells in general as a result of a warming climate (Seneviratne et al. 2021)—there is greater rainfall in Mesoamerica, and when in the southwest, it implies contraction of the Hadley cell, bringing the North Atlantic High closer to Mesoamerica which in turn results in the ITCZ remaining to the south and fuelling drought conditions (Gill et al. 2007).

The North Atlantic High is part of the broader North Atlantic Oscillation (NAO) atmospheric circulation pattern resulting from sea-level pressure differences between the North Atlantic High and corresponding Icelandic Low (Rodriguez-Gonzalez & Cerezo-Mota 2025), which affects winter precipitation and temperatures in Eurasia and North America as well as the winter storm track, particularly in the North Atlantic (Mann 2021). For the last 30 years, the NAO has been in more of a positive phase (Visbeck et al. 2001), characterized by a North Atlantic High (and corresponding Icelandic Low) of increased strength (Lindsey & Dahlman 2009): a positive NAO results in prevailing westerly winds that are stronger than average over the mid-latitudes (Visbeck et al. 2001) and storms are driven farther north (Lindsey & Dahlman 2009). Rodriguez-Gonzalez and Cerezo-Mota (2025) found that in the Yucatan Peninsula, a positive NAO is associated with increases in rainfall and extreme rainfall events, as an analysis of weather station data from 1980–2010 across the Yucatan Peninsula found a 50% increase in total precipitation during the positive NAO phase as well as an increased frequency of days with extreme, consecutive rainfall, with the strongest influence during winter (Rodriguez-Gonzalez & Cerezo-Mota 2025).

The width, strength, and position of the ITCZ determine the seasonality and location of the tropical rain belt (Douville et al., 2021), and as a result of the movement of the ITCZ to its northernmost extent, the Yucatan Peninsula also experiences a distinct rainy season (Fagan 2004), lasting from June-November when tropical phenomena such as tropical cyclones (TCs) and easterly waves occur (Rodriguez-Gonzalez & Cerezo-Mota, 2025). The rainy season is also generally interrupted by a midsummer drought of minimal precipitation in July and August, termed canicula, before experiencing a more pronounced dry season from November-May (Rodriguez-Gonzalez & Cerezo-Mota, 2025), although some infrequent rains may still occur (191 mm on average) (Mejia-Ortiz et al. 2022b). Rodriguez-Gonzalez and Cerezo-Mota (2025) also found that summer rainfall typically accounts for over 40% of total precipitation while winter rainfall typically accounts for 10–15%, and the maximum typically occurs in September and minimum in March. The researchers also found that significant rainfall events, often as a result of TCs, are on the rise; for example, in 2020, many weather stations received over half of their annual average rainfall over six days from TC Cristobal, as TCs are among the most extreme rainfall events in the tropics and subtropics (Frappier et al. 2014). Moreover, in Sept., Oct., and Nov. of 2020, there were precipitation increases in the northeastern portion of the peninsula (Rodriguez-Gonzalez & Cerezo-Mota 2025), which corresponds with hurricane season. Most areas of the states of Yucatan and Campeche also experienced increased extreme rainfall events from 1980-2010, with the coast of Campeche and the eastern portion of the state of Yucatan experiencing the strongest trends in increased extreme rainfall events (Rodriguez-Gonzalez & Cerezo-Mota 2025).

However, rainfall is spatially and temporally variable across the peninsula (Gill et al. 2007), and is affected by geography in addition to climate (Rodriguez-Gonzalez & Cerezo-Mota 2025): although precipitation across the peninsula can range from 150–4000 mm (Gill et al. 2007), the northwest coast of

the Yucatan Peninsula is the driest (Hodell et al. 2005), and the coastline along the northern Yucatan typically has an average annual rainfall of 600–1200 mm (Rodriguez-Gonzalez & Cerezo-Mota 2025), while the south receives more precipitation (Hodell et al. 2005), as southwestern Campeche typically receives the highest with an average annual rainfall of over 1200 mm (Rodriguez-Gonzalez & Cerezo-Mota 2025). Rainfall also varies spatially east to west in the northern portion of the peninsula owing to the easterly trade winds, with more precipitation generally observed in the east (1400 mm/yr), which decreases west (Hoddell et al. 2005).

Yax Chen also experienced highly variable precipitation between May 2012 and May 2017 (the study period): May 2012–May 2013 received 1026 mm of rain which then nearly doubled in May 2013–May 2014 to 2031 mm largely as a result of Hurricane Ingrid, where over 320 mm of precipitation was recorded in a 24-hr period and significant flooding of the study site occurred (Collins et al. 2015). The following 2014 rainy season was limited and relatively dry, although TCs Dolly and Hanna occurred; the 2015 rainy season had frequent rainfalls and larger events that extended into March 2016 (peaking in Oct. and Nov. of 2015); and the 2016 rainy season did not have large rainfall events and was similar to 2014 in that it was short (McNeill-Jewer et al. 2019).

As a result of its geography, Mexico is particularly vulnerable to extreme hydrometeorological events (Andrade-Velazquez et al. 2021), although a knowledge gap currently exists pertaining to the impacts and regional processes of extreme precipitation events in the Yucatan Peninsula: this is especially true in Quintana Roo, where weather stations are scarcer than in other parts of the peninsula and have exhibited contrasting patterns between stations so trends pertaining to the intensity and frequency of rainfall are unclear (Rodriguez-Gonzalez & Cerezo-Mota 2025).

1.3.1. Tropical cyclones 1.3.1.1. Instrumental record

Attribution science has linked the warming climate to an increase in the intensity and frequency of many extreme weather events, including tropical cyclones (TCs), which comprise low pressure systems such as hurricanes, tropical storms, tropical depressions, etc. (Seneviratne et al. 2021). Since 1980, an increase in the proportion of category 3–5 TCs has been well documented (Knutson et al. 2021; NOAA 2023; Seneviratne et al. 2021). To properly reflect the increases in intensity that are being witnessed, scientists have also proposed adding a category 6 to the Saffir-Simpson scale (Mann 2024). Another factor that is increasing TC intensity is the increase in rapid intensification rates (Knutson et al. 2021; Seneviratne et al. 2021), defined as when winds intensify very quickly, usually 35 mph or greater within a 24-hour time period (Gonzalez 2024).

TCs constitute some of the costliest and most destructive natural disasters (Miles et al. 2017; Wang & Toumi 2021), which tends to increase with increased TC intensity (Emanuel 2020). Coastal areas have been found to be prone to meteorological extreme events such as wind and precipitation extremes that often accompany TCs (Seneviratne et al. 2021), and many coastal regions are being doubly affected by an increased intensity of TCs in addition to sea level rise (Rosenzweig et al. 2007). Wang and Toumi (2021) examined TC activity in coastal regions between 1982 and 2018 and found that there is increased activity of TCs by coastal regions and the maximum intensity is occurring closer to land, decreasing by about 30 km each decade. Moreover, while rapid intensification events in the open

ocean have not changed significantly, there has been a threefold increase in coastal areas (within 400 km of shore) between 1980 and 2020, and the Gulf of Mexico has been reported to be an area particularly susceptible to rapid intensification events (Li et al. 2023). The increased rapid intensification rates of Atlantic TCs in recent decades have been found to be highly abnormal and cannot be accounted for by natural variability alone (Knutson et al. 2021).

Although the global frequency of TCs has not changed much in recent decades (Knutson et al. 2021), one other abnormality of North Atlantic TCs is the increased frequency that has been observed, which has been attributed to a reduction in anthropogenic aerosols in the region since the 1970s (Murakami et al. 2020; Seneviratne et al. 2021). For example, the 2020 hurricane season had the most recorded (i.e., named) storms since 1878, including six that were category 3–5 and five that were category 4–5, as well as 22 that were of longer duration (Knutson et al. 2021).

Anthropogenic aerosols are thought to impact sea surface temperatures (SSTs) (Seneviratne et al. 2021), as sea surface warming is posited to be the driving force behind the changes in TC activity (Knutson et al. 2021). SSTs have increased significantly since 1900 in the Gulf of Mexico and tropical Atlantic (NOAA 2023) as the average SST in the Atlantic TC main development region has increased by 1 °C over the last century and 0.6 °C over the last 50 years (Masters 2021), and 2023 and 2024 experienced the warmest SSTs on record (Klotzbach et al. 2024). Marine heat waves (i.e., when SSTs surpass a threshold for more than five days) have also been implicated in fuelling more intense TCs by increasing evaporation and atmospheric moisture, increasing the likelihood of rapid intensification events by 50% in the Gulf of Mexico and Caribbean Sea, and one study found that the duration of marine heat waves is increasing and pinpointed the Bay of Campeche and Yucatan Channel—both adjacent to the Yucatan Peninsula—as two of three hot spots in the region that are particularly susceptible to marine heat waves (Gonzalez 2024), highlighting how susceptible the Yucatan Peninsula is to TC activity. Another study found that the frequency of TCs is also highly dependant on the latitude of the warmest SSTs, as northerly shifts result in a northern shift of the ITCZ, which in turn results in an increased frequency of TCs (Burnett et al. 2021).

The Yucatan Peninsula has the highest rates of landfalling hurricanes within Mexico (Appendini et al. 2019), and between 1920 and 2020 experienced 112 TCs, 18 of which were major hurricanes, and 72% made landfall above 18.25°N, which corresponds to the northern Maya lowlands (Sullivan et al. 2022). From 1951–2006, Quintana Roo and northern Yucatan experienced 18 hurricanes, representing a 3.3-year recurrence interval (Frappier et al. 2014), and during the particularly active North Atlantic hurricane season of 2020 (Knutson et al. 2021), four TCs directly hit the Yucatan Peninsula (Cristobal, Gamma, Delta, and Zeta) (Rodriguez-Gonzalez & Cerezo-Mota 2025).

1.3.1.2. Future projections

An increase in peak TC wind speeds by approximately 3% is expected in the future with further warming (NOAA 2023) in addition to an increase in the proportion of the most intense TCs (Seneviratne et al. 2021), as a 10% increase in the proportion of category 4 and 5 TCs has been projected (NOAA 2023), accompanying an increased duration (Knutson et al. 2021). Increased stalling of TCs over land and moisture in the atmosphere have also been projected to result in higher precipitation rates accompanying TCs (Seneviratne et al. 2021) by about 15% (NOAA 2023), as the Clausius—Clapeyron relation states that 7% more water vapour will be present in a tropical atmospheric column per every degree of warming of the surface (Knutson et al. 2021). It has also been projected that storm surge

resulting from a rise in sea level will increase between 2 and 3 ft by the end of the century (NOAA 2023), and flooding in coastal areas has been stated to be one of the greatest projected impacts of TCs (Knutson et al. 2023).

The change in TC frequency is more highly debated: while many studies have projected the total frequency of TCs to decrease with climate change and increased greenhouse gas (GHG) concentrations (Murakami et al. 2020; Seneviratne et al 2021) by approximately 15% (NOAA 2023), there is uncertainty and results have been mixed (Knutson et al. 2021) as other studies have projected an increase in TCs alongside increased GHGs (Emanuel 2020). There is also great uncertainty in changes to storm tracks, TC size, and formation location (NOAA 2023).

One of the problems in examining the relationship between climate change and TCs is that the observational record is very limited (Murakami et al. 2020). For example, the observational record only goes back as far as 1900 for US landfalling TCs that are category 3 or above, and data from most other areas is far more limited (Knutson et al. 2021). For Atlantic hurricanes, there is typically not an observed record long enough to examine centennial-scale trends, and in cases where they do exist, clear trends are typically not discernible (NOAA 2023).

Moreover, as experts agree that it is difficult to examine the relationship between climate change and recent trends in hurricane activity given that temperatures have only shown strong increases in the last few decades (Rosenzweig et al. 2007), one approach to examine the relationship is to study an analogous historical period characterized by above-average temperatures, such as the Medieval Warm Period, which coincided with a notable period in history, the Terminal Classic Period (TCP) or Classic Maya Decline.

1.4. The Medieval Warm Period/Terminal Classic Period

The Classic Maya (collapse, or) Decline (800–900 CE) marked the Terminal Classic Period (TCP) (800–950 CE) (Smyth et al. 2017) and has been well-studied in paleoclimate records as it represents an intriguing case study in that rarely have declines of well-developed civilizations been so pronounced in the archaeological record (Gill et al. 2007). Notably, the Terminal Classic Period overlaps neatly with the beginning of the Medieval Warm Period (Smyth et al. 2017), also often referred to as the Medieval Climatic Anomaly (Fagan 2004), which was a period of elevated temperatures throughout much of the world spanning 800–1300 CE with a peak in temperature occurring at about 1050 CE (Idso 2009).

1.4.1. Archaeological record

Maya civilization is often regarded as among the most advanced in the world during the Classic Period (250–850 CE) (Grodsky 2024), noted for its architecture, art, calendrical system, mathematics, astronomy, and fully developed writing system of hieroglyphic script (Jobbova et al. 2018). Its societal organization was akin to theocratic city-states led by divine rulers who combined religion with government, and the legitimacy of Maya leaders was often founded through the provision of crucial goods, and in particular water (Grodsky 2024).

Pyramids and much of the other monumental architecture in urban centres doubled as rain-collection structures, showing how closely tied control of water was to urbanisation and centralised power centres in ancient Maya societies (Smyth et al. 2017), although the Maya are also known to have obtained freshwater from the caves and cenotes that dot the peninsula (Gelting 1995). At Chichen Itza, for example, a higher number of chultuns, or household water storage vessels, near cenotes suggests they were relied on to source water for the chultuns (Smyth et al. 2017). Chultuns were also the characteristic method for storing water during the Terminal Classic Period in the Puuc region, and were not found in the earlier Preclassic period (Smyth et al. 2017), suggesting an increased reliance on cenotes to source water may have increased Maya society's vulnerability to changes in the aquifer. Moreover, Maya rulers' divine kingship and emphasis on water provision may have simultaneously resulted in their civilization being particularly vulnerable to extreme weather events (Grodsky 2024), and the archaeological record documenting the abandonment of sites and political decline is so closely coupled with climate records that it has often been suggested they were intrinsically linked (Wu et al. 2017).

Jobbova et al. (2018) presented some interesting evidence in support of increased climatic stress during the Terminal Classic Period through an analysis of Terminal Classic Maya records (800–900 CE), which largely do not mention social upheavals or warfare that have been suggested from archaeological evidence as a cause of the Classic Maya Decline. Instead, they largely focus on the proper performance of key ceremonies, a marked change from the texts of the earlier part of the Classic Period (250–800 CE), which documented rulers and royal life more, including warfare, marriages, enthronements, royal births, etc. In addition, from 800–850 CE, the texts record former adversaries visiting each other to perform joint rituals aimed at maintaining order, as war narratives largely disappear (Jobbova et al. 2018).

This may offer some insight into the concerns that preoccupied Maya society, as rituals are often widespread during periods of climatic stress and were particularly related to water in the Yucatan Peninsula (Jobbova et al. 2018); for example, Smyth et al. (2017) found that a cave system at the Maya centre of Xcoch was used for rain-related rituals and visited for centuries after its population decline in 850 CE—well into the Medieval Warm Period—as cenotes held great ritual importance to the Maya (Mejia-Ortiz et al. 2022b). More broadly, throughout Mesoamerica, caves were seen as the "first temple of the world", and it was a common belief that rain originated within caves (Brady & Peterson 2008). In addition, *Chaahk*, an ancient Maya deity associated with rain and clouds and personified as thunder, has been linked to a present-day rainmaking ceremony called *Ch'a-chaak* that is especially known throughout the Yucatan as well as in north and central Belize (Jobbova et al. 2018), and the term "hurricane" is derived from one of the Maya creator gods, *Hurakan* (Frappier et al. 2014). However, there were only two direct references to drought amongst the thousands of Classic Period Maya texts: one was prophetic rather than historical, and the historical drought that was mentioned occurred in the eight century CE (Jobbova et al. 2018), before the onset of the TCP, and texts that may have recorded the dates of hurricanes were destroyed (Frappier et al. 2014).

Jobbova et al. (2018) also noted that support for climatic stress in Maya society can also be seen in stelae, as in one stela from 879 CE in Jimbal, *Chaahk* is also mentioned with the "Paddler gods", two ancient Maya deities whose names are not decipherable (known as the Old Jaguar paddler and Stingray paddler instead) but stated to be two *Chaahk* entities that personify rain and thunder. The Paddlers gods are often associated with the glyphs *y-at-ij* throughout Maya society, which has some debate surrounding its translation but roughly means "the Paddler gods bathed". This statement is most

prevalent during the Terminal Classic Period, with a sharp increase from 850–900 CE, even though the number of texts decreased significantly, and a high frequency of this statement is recorded in June, October, and November, corresponding with some of the wettest periods of the year (Jobbova et al. 2018).

By 890 CE, there was a significant halt in activity in the archaeological record and only three monuments were created during the TCP thereafter: the last recorded date on a TCP Maya monument occurred in 909 CE, by which point none were recorded again until 1200 CE in Mayapan (Gill et al. 2007), offering a glimpse into the extent of the disruption that must have shaken the very foundations of Maya society during the Terminal Classic Period.

1.4.2. Paleoclimate studies

1.4.2.1. Drought

While the independent role of climate was not widely accepted in Maya archaeology as a cause of the Classic Maya Decline (Gill et al. 2007) as drought was never historically considered a plausible explanation for the stark demographic changes that impacted Maya civilization during the Terminal Classic Period (Fagan 2004), several studies have since found evidence of recurring major drought throughout the Common Era, with the most severe droughts coinciding with the Classic Maya Decline. For example, a marine core from the Cariaco Basin in Venezuela found evidence of intense prolonged droughts at 810, 860, and 910 CE amidst generally drier conditions in the region (Haug et al. 2003), which coincided precisely with when Maya cities were abandoned in 810 (affected mostly the southwestern and western regions), 860 (affected mostly the southeast), and 910 CE (affected mostly the north and central regions) (Gill et al. 2007). Further studies were done with lake sediment cores extracted from Lake Chichancanab in the northcentral Yucatan Peninsula, which analysed the gypsum content and found that drought conditions occurred from 770-870 CE and 920-1100 CE, which were termed the "Terminal Classic Drought" (Hodell et al. 2005). Rodriguez-Ramirez et al. (2015) used diatoms to analyse climate conditions over a 2000-year period and found a dry interval from 500–1000 CE stretching from western Mexico to the Yucatan Peninsula with peak intensity from 600–800 CE (Rodriguez-Ramirez et al. 2015).

Droughts as the sole cause of the Classic Maya Decline have remained controversial as it is seen as an oversimplification of numerous interacting factors and many of the studies that found evidence of drought relied predominantly on summer precipitation proxy records (Wu et al. 2017), and water level has been found to have marked seasonal variations (Collins et al. 2015). Additionally, as many of these studies utilised lake sediment cores, there were limitations with accurate dating as they rely on finding organic matter within the samples that can be radiocarbon dated and assume a constant sedimentation rate (Gill et al. 2007). The core from the Cariaco Basin has also been noted to be quite a distance from the Yucatan Peninsula, and may not accurately reflect the regional climate changes that were occurring there (Fagan 2009).

In addition, although the position of the North Atlantic High has been implicated in determining drought regimes over the Yucatan Peninsula by limiting the northward extent of the ITCZ and its accompanying precipitation—as paleoclimate evidence has been used to posit the ITCZ remained to the south from the ninth to early tenth centuries as the North Atlantic High was located in the southwest, preventing precipitation (Gill et al. 2007)—it is also important in steering the paths taken by hurricanes,

particularly the winter storm track in the North Atlantic (Mann 2021), and a positive North Atlantic Oscillation phase (NAO) has been found to steer storms farther north (Lindsey & Dahlman 2009). A positive NAO has been found to result in an increase in extreme precipitation events in the Yucatan Peninsula (Rodriguez-Gonzalez & Cerezo-Mota 2025), and changes in hurricane paths can influence the moisture balance (Rodriguez-Ramirez et al. 2015). Notably, the NAO was also found to be in a predominantly positive phase during the Medieval Warm Period (Trouet et al. 2009), which would imply the Yucatan Peninsula was susceptible to increased storm activity, and more recent paleoclimate studies have begun to find evidence of increased TC activity during the TCP or Medieval Warm Period, discussed below.

1.4.2.2. Tropical cyclones

Mann et al. (2009) used sedimentary records and a statistical model to examine hurricane activity in the Atlantic over the past 1500 years and found hurricane frequency peaked during the Medieval Warm Period around 1000 CE, with a frequency similar to or even surpassing today's trends. An ice core used to examine climate conditions in Greenland and the North Atlantic throughout the Medieval Warm Period also found increased levels of Ca during the TCP, indicating increased storm activity over land surfaces (Gill et al. 2007).

One study that examined speleothem laminae at a cave nearby the Maya settlement of Xcoch in the Puuc Hills in northern Yucatan found that speleothem deposition rates of calcite, which act as a proxy for precipitation, reached some of their highest levels from 797–892 CE amidst the entire period analysed (300–1500 CE), with deposition rates 14 mm greater than for the following period (972–1014 CE). Additionally, evidence of a series of cave flooding from 841–845 CE was inferred from surface soil sediment deposited on the speleothem, which immediately preceded a population decline in 850 CE (Smyth et al. 2017).

This corresponds closely with a study by Hodell et al. (2005) at Lake Chichancanab in northcentral Yucatan that found that prolonged dry periods (which are collectively referred to as the "Terminal Classic Drought" and lasted from 770–1100 CE) were interspersed with relatively wetter conditions, including from 870–920 CE (Hodell et al. 2005). A study by Sullivan et al. (2022) that examined sediment from Cenote Muyil in the northeastern portion of the peninsula (nearby Yax Chen) spanning 2200 years interpreted coarse carbonate amongst fine-grain autogenic carbonate as a paleoenvironmental indicator of hurricane activity and found above-average hurricane activity occurred from 700–1450 CE, with a particularly high frequency beginning in 800 CE, concurrent with the beginning of the Terminal Classic Period (Sullivan et al. 2022).

Frappier et al. (2014) examined cave flooding events using speleothems from Cenote Chaltun in Huhi, Yucatan, and also concluded that TCs likely affected the Yucatan Peninsula frequently during the TCP, as they found evidence of 13 cave flooding events throughout the TCP representing a recurrence interval of 11. 6 yrs. However, the researchers also noted that TC events were likely under-recorded based on present-day comparisons, and suggested that TC activity during the TCP was unparalleled to anything the region has ever experienced.

1.5. Compound extremes

The Intergovernmental Panel on Climate Change (IPCC) concluded in their latest assessment report that regional changes in extreme weather events affecting both the frequency and intensity generally correlate to increased global warming, as even very small changes in temperature can result in significant changes to extreme weather events over large regions, particularly regarding the increase in temperature extremes, heavy precipitation including that associated with TCs, as well as increased drought severity in some regions (Seneviratne et al. 2021). Their latest report also concluded that the probability of compound events, or extreme weather events occurring simultaneously, has increased as a result of global warming and has been projected to increase as global warming continues alongside the land area that compound extremes affect (Seneviratne et al. 2021).

Understanding of how the ITCZ is affected by a warming climate has also increased in the IPCC's Sixth Assessment Report (2021), as it has been found that convection becomes stronger and more intense within the core of the ITCZ, leading to increased drying on the equatorward edges and more moisture within the core of the ITCZ (Douville et al. 2021). The IPCC also found that a strengthening and tightening of the ITCZ has resulted in greater extremes between wet and dry (Douville et al. 2021). Moreover, in the IPCC's previous (Fifth) Assessment Report (2013), they found that the contrast in precipitation between wet and dry seasons and regions was expected to increase with a warming climate, which they assessed with high confidence. They also projected that intense precipitation events would increase in frequency while the total number of precipitation events would decrease in frequency, which led to a paradoxical projection of an increase in both droughts and floods (Collins et al. 2013). This provides a theoretical foundation for the notion that the Yucatan Peninsula may have experienced concurrent extremes of droughts and storms throughout the Medieval Warm Period/Terminal Classic Period, which can be particularly destabilising (Smyth et al. 2017).

For example, a study by Rodriguez-Gonzalez & Cerezo-Mota (2025) of precipitation changes in the Yucatan Peninsula from 1980–2010 found that parts of the Yucatan Peninsula, including northern Campeche and the state of Yucatan, had an increase in the frequency and intensity of extreme precipitation events, although precipitation occurred fewer days over the year, leading to a simultaneous increase in the frequency and intensity of dry periods. Trends in Quintana Roo were more difficult to assess as weather stations are fewer in number and showed contrasting patterns, although both extreme precipitation events and droughts can negatively impact groundwater supplies (Rodriguez-Gonzalez & Cerezo-Mota 2025).

1.6. Paleoenvironmental indicators

It has been noted that more prolonged extreme weather events that cover a large area, such as droughts, are easier to discern in the paleoclimate record than extreme weather events more limited in time and scale such as tropical cyclones (Seneviratne et al. 2021), which could help to account for the fact that few climate reconstructions focused only on hurricane activity currently exist, although they are needed to better examine the relationship between changes in their frequency and Maya civilization (Sullivan et al. 2022). Furthermore, the locations where paleoclimate studies of TCs have been conducted are limited (Seneviratne et al. 2021), and paleo-reconstructions over the past millennium have produced widely varying results regarding TC frequency, finding for example, large differences in storm frequencies in neighbouring Belize (Sullivan et al. 2022). This has resulted in low confidence by the

IPCC in concluding changes in extreme weather events obtained from the paleoclimate record (Seneviratne et al. 2021).

However, better understanding past climate events has been stated as critical for attributing causes and effects of environmental changes in the future as well as understanding modern environmental processes (Rodriguez-Ramirez et al. 2015), which is particularly relevant for hurricanes, as how they are affected by climate change is still not fully understood (Méndez-Tejeda & Hernández-Ayala, 2023). In particular, the paleoclimate studies that found a higher frequency of TCs during the Terminal Classic Period seemingly dispel the notion reported by some researchers that the recent uptick in TCs in the North Atlantic is a "course correction" due to reductions in anthropogenic aerosols after the 1970s (Knutson et al. 2023; NOAA 2023; Seneviratne et al. 2012), and suggests that other factors may be responsible for their increased frequency which warrants further study.

The IPCC also concluded that better insights are garnered about recent extreme weather events where multiple paleoclimate studies have been undertaken or where multiple proxies have been utilised spanning large areas (Seneviratne et al. 2021). It was also noted that using the sedimentary record to examine extreme weather events of short duration is complex and thus clear comprehension of the natural processes involved is required; for example, when reconstructing paleoclimate events using proxies such as diatom assemblages, a clear comprehension of physical mechanisms and sediment sources is required (Seneviratne et al. 2021), which is one of the major aims of the current study. Less is known about the processes affecting anchialine cave systems than proxy records and sediment cores from lakes and oceans (Collins et al. 2015), although they typically experience less bioturbation and thus provide better temporal records, and can therefore serve as important sources of information for paleoenvironmental records (Steele et al. 2022).

Scant information currently exists regarding how climate change affects groundwater in anchialine aquifers over the long-term, as no proxies have been developed and only short-term instrumental monitoring exists (Collins et al. 2015), although even small changes in the intensity, frequency, and timing of TCS are expected to majorly affect coastal wetland processes, including on biotic structure (Michener et al. 1997); thus, a major aim of this study was to examine whether diatoms show a response to TCs that can be used as a paleoenvironmental indicator to examine TC activity over a longer timescale.

1.6.1. Diatoms

Diatoms are used extensively in paleoclimate reconstructions as they are often well preserved in the fossil record due to their silica frustules (Williams 2020), which render them fairly resistant to acids and heat (Cristobal et al. 2020). They can be found in fossil records dating as far back as the Jurassic, although they are more prevalent beginning in the Cretaceous, when centric diatoms were the earliest forms from which pennate diatoms later evolved (Saraswati & Srinivasan 2016). In addition, diatoms are excellent at modelling environmental change due to their high sensitivity, and thus are seen as useful in studying changes in past environments (Williams 2020). A diatom community's composition is often closely related to physicochemical conditions of the surrounding environment (Cristobal et al. 2020), and temperature, salinity, and light are often regarded as important controlling factors for their distribution (Saraswati & Srinivasan 2016). Diatoms have also been stated to be the most representative group of the phytobenthos, making them excellent bioindicators of water quality (Cristobal et al. 2020).

Species estimates of diatom diversity vary widely as their taxonomy is still evolving (Williams 2020), although there are around 10,000 currently recognised species (Cristobal et al. 2020; Krayesky et al. 2009). Surveys of diatom populations in the Gulf of Mexico and surrounding areas beginning since 1954 have yielded an estimate of nearly 1,000 different species (Krayesky et al. 2009). Recent surveys of benthic diatoms have also confirmed that coastal areas in Mexico have a high floristic potential, identifying 397 taxa with genera that include *Nitzchia, Cocconeis, Navicula, Amphora, Diploneis*, and *Grammatophora* (Siqueiros Beltrones et al. 2021). Mangrove environments have also been found to support high species diversity, as 520 taxa from mangrove environments in NW Mexico have been reported (Lopez-Fuertes et al. 2010).

The Yucatan Peninsula has not been particularly well studied, although one study of the northern coast reported the genera *Cocconeis, Petroneis, Oestrupia, Climaconeis, Licmophora, Talaroneis*, and *Synedrosphenia* were present (Hernandez-Almeida et al. 2013). Steele et al. (2023) analysed diatom taxa from sediment in a cave system near Yax Chen and reported 32 taxa, including the genera *Amphora, Diploneis, Cyclotella, Craticula, Hyalosynedra*, and *Grammatophora*. The study also noted that the diatoms found in the sampling stations positioned within the cave could only have resulted from taphonomic transport as diatoms are photosynthetic and require access to sunlight, and therefore originated in the cenotes or surrounding environment before being transported throughout the rest of the cave system, so assemblage changes reflect changes to the epikarst environments/cenotes (low-relief terrain on the karst landscape), as not much organic matter originates within the cave habitats (Steele et al. 2023).

1.7. Study Objectives

As knowledge gaps currently exist regarding how the Yucatan Peninsula was affected by TCs during the TCP as well as gaps in knowledge regarding how groundwater in anchialine aquifers is affected by climate change on long-term timescales as no proxies have been developed (Collins et al. 2015), the main objective of this study was to better understand the response of diatoms to TC activity within the Yax Chen anchialine aquifer cave system and in particular, to determine whether they exhibited a measurable, reliable response to TCs that would warrant their use as a paleoenvironmental indicator of TC activity during the TCP in order to examine paleo-tempest records. The difference between the assemblages upstream and downstream of the forest—mangrove transition was also examined to this end.

2. Methods

The diatoms used in this study were collected from sediment trap samples positioned along the Yax Chen aquifer cave system (Fig. 1), which were collected approximately every May following the dry season and December following the rainy season: an exception is the 2012–2013 sampling period, when only one sample was collected in May 2013 (i.e., there is no Dec. 2012), as the monitoring project initially began with annual sample collections but became more frequent on a biannual scale to better examine the effects of hurricane activity on the aquifer (McNeill-Jewer et al. 2019). Each sampling station is comprised of three sediment traps positioned along the width of the cave system.

For this study, the sediment trap samples from sediment trap stations 2, 7, 12, and 17 (n = 33 samples total as three stations were missing samples) were used spanning the time period May 2012—May 2017, and four TCs affected the peninsula during this time period: Ingrid in Sept. 2013, Dolly in Sept. 2014, Hanna in Oct. 2014, and Bill in Jun. 2015, as summarised in Table 1.

		•	υ	J 1	` '	,
TC	Date	Location	Location	Peak	Direction	Source
name		formation	where low-	intensity	of travel	
			pressure			
			area formed			
Ingrid	Sept	19.3°N,	northwestern	75 kt	W-NW	(Beven 2014)
	12-	92.2°W	Caribbean			
	17,		Sea			
	2013					
Dolly	Sept	19.2°N,	Yucatan	45 kt	N-NW,	(Beven 2015)
	1–3	92.3° W	Peninsula		shifted	
	2014				NW on	
					Sept. 2	
Hanna	Oct	19.2°N,	Veracruz	35 k	Е	(Cangialosi 2014)
	22-	91.3°W				
	28					
	2014					
Bill	Jun	27°N,	northern	50 kt	NW	(Berg 2015)
	16-	94.3° W	Belize and			
	18		Yucatan			
	2015					

Table 1. Summary of TCs during the study period (May 2012–May 2017).

The samples in this study were prepared following the diatom analysis preparation method outlined by the Paleoecological Environmental and Research Laboratory (PEARL) (2021), which was also used by Steele et al. (2023) to prepare diatom samples from the nearby Boca Paila cave: sediment samples (~0.5 g) were treated with 10% HCl for 24 h to remove excess calcium carbonate and then were rinsed until a neutral pH was reached before 35% H₂O₂ was added for several weeks to remove excess organic matter (a heat bath was also used to expedite this process) and were then rinsed again until a neutral pH was reached. Afterwards, 0.5 mL of microspheres were mixed with each sample, and 1 mL of each sample was then subsequently plated onto slides using Naphrax®. Once dry, samples were examined under an oil immersion binocular microscope (Nikon Optiphot) at 100x magnification for diatom counts, where at least 300 specimens were counted per sample.

Diatoms were identified to the species-level in most cases using illustrated databases and references of diatoms (e.g., Lopez-Fuerte et al. 2010; Park et al. 2017; Siqueros Beltrones et al. 2021; Spaulding et al. 2021; Taylor et al. 2007). From here, the most abundant diatom species across samples were identified, which were those with at least 1–2 % relative abundance in most of the samples; photographs of the most prevalent diatom species found throughout the samples can be found in Appendix 3.

Data on precipitation and elemental composition of sediment within the aquifer was obtained from earlier work by McNeill-Jewer et al. (2019): the weather data was obtained from the nearby Cozumel weather station, and water level data was collected using a ReefNet Sensus Ultra dive logger that had been positioned near sampling station 7 in the meteoric water mass with a surface-deployed

sensor that was used to correct for atmospheric barometric change (Kovacs et al. 2017; McNeill-Jewer et al. 2019).

A Cox ITRAX µXRF-CS (micro X-ray fluorescence core scanner), which has a very high resolution that is able to examine data on a biannual scale, was used in earlier work by McNeill-Jewer et al. (2019) to analyse the elemental composition of the sediment trap samples: the three samples from each sampling station were combined and spread onto a Sequential Sediment Reservoir (SSR) with a spatula before analysing the sequential cuvettes (~1 cm³) utilising the X-ray source's (step size: 1 mm, exposure time: 15 s, 28 mA, 30 Kv) Cr heavy element (Cr-HE). Data was recorded as the total counts spanning the 15 s integration time, and the averaged value of ten measurements per sample reservoir taken from the central portion were used (McNeill-Jewer et al. 2019). These same samples were used for obtaining diatom samples in the current study.

The Shannon Diversity Index (SDI) values, percentage of benthic diatoms, relative abundance of each species, and overall diatom concentrations were calculated for each sample in this study as well as the Si/Ti ratio: because Si can result from biogenic sources or as a weathering product, Ti was used to help normalise the data as it is also a weathering product of limestone with a dissolution rate that is roughly equal to that of Si; therefore, a high Si/Ti ratio indicates high primary productivity (Steele et al. 2023).

As mentioned above, the most dominant taxa were identified as those having the highest total relative abundances (at least 1–2 % relative abundance across most samples) relative to other taxa, which were then used for statistical analyses and plotting relationships. Hierarchical dendrograms showing the grouping of species were obtained with R-mode clustering analyses (Ward's Method) using the PAST software package in order to examine clustering at each sampling station. Two analyses for each station were carried out: one with all of the previously mentioned most abundant species (at least 1–2% relative abundance across the majority of stations) and a more condensed clustering analysis using the most predominant species across stations (relative abundances of far greater than 1–2% across most samples, often composing most of the diatoms in the samples), as discussed in Fishbein and Patterson (1993). A global clustering analysis and Q-mode clustering analysis displaying a hierarchical dendrogram of samples were also completed.

3. Results

3.1. Dominant species and ecological preferences

The results of the diatom analyses are displayed in Supplementary Information 1, Figs. 1–11, and Appendices 1 and 2. The most dominant species found in this study were *Thalassiosira weissflogii*, *Thalassiosira spinulata*, *Paralia sulcata*, *Hemidiscus* sp., *Terpsinoe musica*, *Navicula arvensis* var. *maior* Lange-Bertalot, *Cyclotella meneghiniana*, *Denticula kuetzingii* Grunow, and *Nitzchia* sp., the ecological preferences of which are displayed in Table 2.

Table 2. Ecological preferences of the most abundant species.

Taxa	Planktonic/Benthic	Ecology	Source
Thalassiosira weissflogii	Planktonic	Halophilic, riverine	(Taylor et al. 2007)
Thalassiosira spinulata	Planktonic	Common in low salinity, high turbulence conditions	(Park et al. 2017)
Paralia sulcata	Benthic	Common in vertical mixing/upwelling zones	(Abrantes 1988; McQuoid & Nordberg 2003)
		Tychopelagic, benthic, marine, commonly found in plankton that is neritic	(Lopez Fuerte et al. 2010)
Terpsinoe musica	Benthic	Freshwater, brackish, and marine (cosmopolitan). Common in warm mineral waters	(Spaulding et al. 2021)
Navicula arvensis var. maior Lange-Bertalot	Benthic	Cosmopolitan; waters with mid- to elevated-electrolytes	(Taylor et al. 2007)
Cyclotella meneghiniana Kutzing	Planktonic and Benthic	Benthos and plankton of electrolyte-rich, eutrophic streams	(Taylor et al. 2007)
Denticula kuetzingii Grunow	Benthic	Waters with mid- to elevated-electrolytes, freshwater to brackish	(Taylor et al. 2007)
Nitzchia	Benthic	Cosmopolitan	(Lopez Fuerte et al. 2010)

3.2. Spatial results

Fig. 2a–i displays the species distributions of some of the most prevalent species found throughout the analysis. *Thalassiosira weissflogii* (Fig. 2i), *Thalssiosira spinulata* (Fig. 2a), *Cyclotella menghiniana* (Fig 2b), and *Terpsinoe musica* (Fig. 2c) generally have higher relative abundances in the sampling stations upstream of L-shaped cenote (i.e., sampling stations 2 and 7), which decrease in proportion at the downstream stations (i.e., stations 12 and 17). *Paralia sulcata* (Fig. 2d), *Navicula arvensis* var. *maior* Lange-Bertalot (Fig. 2e), *Nitzchia* sp. (Fig. 2f), *Denticula kuetzingii* Grunow (Fig, 2g), and *Hemidiscus* sp. (Fig. 2h) show an inverse trend, with higher relative abundances found in the downstream stations, while a lower proportion found upstream. Fig. 3a shows the Shannon Diversity Index (SDI) values and Fig. 3b displays the proportion of benthic diatoms, which are also generally higher in the downstream stations compared to the sampling stations located farther upstream.

3.3. Temporal results

Fig. 4a–d shows that these species responded differently to TC activity depending on the sampling station, with some showing increases and some decreases. In Fig. 4a, both *Thalassiosira weissflogii* and *Thalassiosira spinulata* show a decrease in relative abundance at stns. 2, 7, and 17 (the samples for stn. 12 were missing for this sampling period) immediately following TC Ingrid, although the decrease in *Thalassiosira weissflogii* is quite modest. The decrease in these species was also seen after TCs Dolly and Hanna in 2014 with the exception of stn. 2, where a significant increase in *Thalassiosira spinulata* is observed. Conversely, increases are seen in both of these species after TC Bill at all stations except for 17, where a small decrease in both species is observed.

Fig. 4b depicts the response of *Paralia sulcata* and *Terpsinoe musica* to TC activity during the study period. *Terpsinoe musica* increases at stn. 2, 7, and 17 following TC Ingrid (data from stn. 12 is missing), while *Paralia sulcata* only shows an increase at stns. 2 and 7, as a slight decrease at stn. 17 following TC Ingrid is observed. The trends after TCs Dolly and Hanna are more variable, as a decrease in both species is seen at stn. 2, while increases in both species are observed at stns. 7, 12, and 17. After TC Bill, decreases in both species are seen at stns. 2 and 7, while increases are seen at stns. 12 and 17.

Fig. 4c depicts the relative abundances of *Nitzchia* sp. and *Navicula arvensis* var. *maior* Lange-Bertalot during the study period. *Navicula arvensis* var. *maior* Lange-Bertalot shows a decrease at stns. 2, 7, and 17 following TC Ingrid, whereas *Nitzchia* sp. decreases at stn. 2 and increases slightly at stn. 17. After TCs Hanna and Dolly, a slight decrease in *Navicula arvensis* var. *maior* Lange-Bertalot is observed at stn. 2, while increases in both species are seen at stns. 7 and 17. The response to TC Bill is the most uniform, with both species showing decreases across stations.

Fig. 4d shows the response of *Hemidiscus* sp. and *Denticula kuetzingii* Grunow. After TC Ingrid, *Denticula kuetzingii* Grunow shows a decrease at stn. 2. and increases at stns. 7 and 17 (the data for stn. 12 was missing). *Hemidiscus* sp. does not show major changes, except at stn. 17 where a slight decrease is observed following TC Ingrid. After TCs Dolly and Hanna, *Denticula kuetzingii* Grunow increases at all stations except 17, where a slight decrease occurs, while *Hemidiscus* sp. increases at stns. 12 and 17. After TC Bill, *Denticula kuetzingii* Grunow decreases at all stns. except 12, where an increase is observed. Similarly, *Hemidiscus* sp. also decreases at all stns. except for stn. 7, where an increase is observed.

Seasonality (i.e., wet or dry) also does not show strong trends with relative abundance in Fig. 4a–d. Fig. 5a shows that virtually all SDI values across sampling stations decrease after each TC. As shown in Fig. 5b, the effect of TCs on the percentage of benthic diatoms has mixed results, with virtually all sampling stations showing an increase after TCs Ingrid, Hanna, and Dolly, although a decrease is seen after TC Bill. However, the percentage of benthic diatoms does show an increase in subsequent sampling periods following TC Bill (in May 2016 for stns. 7 and 12, and Dec. 2016 at stns. 2 and 17). Seasonality does not appear to show any clear trends regarding the relative abundance of benthic diatoms.

3.4. Si/Ti ratio and precipitation

Fig. 5c displays the Si/Ti ratios for each sample throughout the study period, while Fig. 5d shows the total precipitation over each 6-month sampling period (mm). Fig. 6 is a scatter plot showing the precipitation and Si/Ti ratio for each sample, with r² values of 0.0154, -0.3679, -0.3586, and -0.1707 for stations 2, 7, 12, and 17, respectively. Overall, the Si/Ti values do not show much of a relationship with precipitation, and the sampling period with very minimal precipitation (May 2015) is further skewing the results. There is a tendency for lower Si/Ti with precipitation, which may be a result of the productivity lag found in McNeill-Jewer et al. (2019). Fig. 7a–d displays the Si/Ti ratio and diatom concentrations across sampling stations, with r² values of 0.0385, -0.0071, 0.0057, and 0.3348 at sampling stations 2, 7, 12, and 17, respectively. Fig. 8a–d display the Si/Ti ratio in relation to the benthic diatom proportions, with r² values of 0.1009, 0.1005, 0.4428, and -0.0271 at stations 2, 7, 12, and 17, respectively. Fig. 9 displays total precipitation during each 6-month sampling period and diatom concentrations, with r² values of 0.1186, -0.0021, -0.3376, and 0.0156 for sampling stations 2, 7, 12, and 17, respectively.

3.5. Clustering analyses

The global clustering analysis and Q-mode clustering analysis are displayed in Fig. 10a-b. In Fig. 10b, most visible is that sampling station 17 from Dec 2014–Dec 2016 are clustered closely together, following Hurricane Ingrid and encompassing all TCs that occurred during the study period. During this same time period, the upstream stations 2 and 7 also cluster quite closely except for May 2015, which is more distant from this cluster although stations 2, 7, and 12 for May 2015 are clustered quite closely, May 2015 being the sampling period that followed a period of minimal precipitation (719 mm). Taken together, this suggests that the stations seem to show a response to precipitation extremes.

When looking at the R-mode global clustering analysis (Fig. 10a), many of the species that are considered to occupy a cosmopolitan ecological niche are very similar (e.g., *Guinardia striata, Nitzchia frustulum* (Kutzing) Grunow, *Sellaphora pupula, Nitzchia amphibia*, etc.). In addition, the species in the genus *Cocconeis* are also clustered closely together. *Terpsinoe musica* and *Thalassiosira weissflogii* are also clustered closely together, which is also observed at many of the individual stations. This is also seen with *Hemidiscus* sp. and *Nitzchia* sp. (discussed in greater detail below.)

The results of the individual clustering analyses are shown in Fig. 11 a–d, which displays the most predominant species, as well as Appendix 2a–2d, which shows the results of a more expanded analysis. Some significant clusters emerged in the expanded analysis, as *Aulacoseira ambigua* (Grunow) Simonsen, *Aulacoseira granulata* var. *angustissima* (Grunow) Simonsen, *Fragilaria capucina* var. *vaucheriae* (Kutzing) Lange-Bertalot, and *Guinardia striata* were closely clustered together at all sampling stations except for station 17.

In addition, *Planothidium rostratum* (Oestrup) Round & Bukhityarova and *Melosira* varians Agardh are also closely clustered together across sampling stations, and are also closely associated with the aforementioned cluster (i.e., *Aulacoseira ambigua* (Grunow) Simonsen, *Aulacoseira granulata* var. *angustissima* (Grunow) Simonsen, *Fragilaria capucina* var. *vaucheriae* (Kutzing) Lange-Bertalot, and *Guinardia striata*) at most of the stations.

Sellaphora pupula (Kutzing), Hemidiscus sp., and Nitzchia sp. also form another closely related cluster at half of the sampling stations (i.e., sampling stations 2 and 12), whereas more distance is evident between them at sampling stations 7 and 17. In addition, Appendix 2a–2d and Fig. 11a–d of the most dominant species also show that a combination of two or more of Terpsinoe musica, Thalassiosira spinulata, and Thalassiosira weissflogii are often closely clustered at most of the sampling stations. Terpsinoe musica and in particular Thalassiosira spinulata often appear as a single leaf or simplicifolious in the dendrograms, indicating they are more dissimilar from the other species.

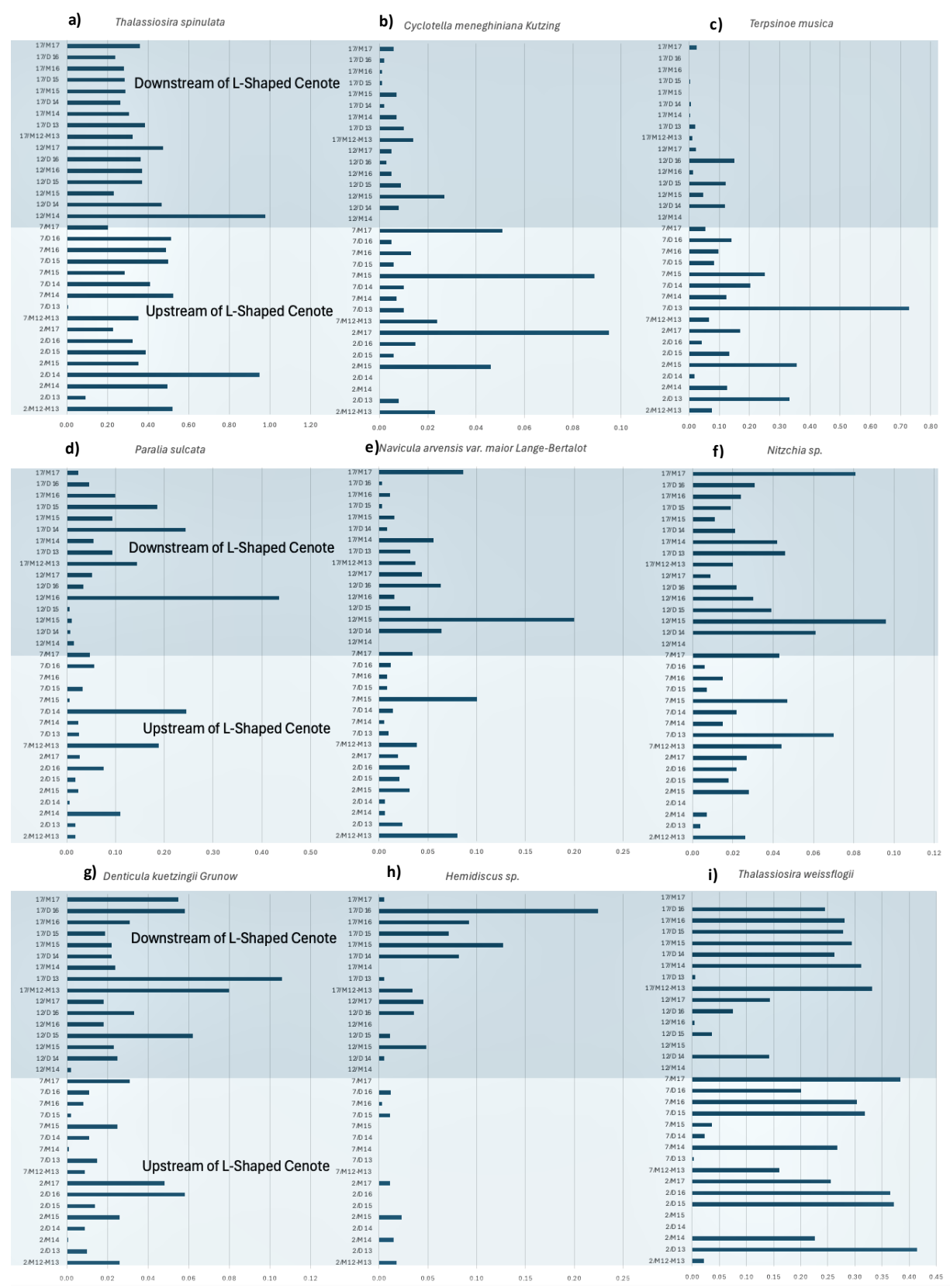


Fig. 2. Fractional relative abundances separated by upstream (sampling stations 2 and 7) and downstream (sampling stations 12 and 17). The first number denotes station number, while "M" and "D" represent May and December, respectively,

followed by sampling year. a) Thalassiosira spinulata (planktonic). b) Cyclotella meneghiniana (planktonic and benthic). c) Terpsinoe musica (benthic). d) Paralia sulcata (benthic). e) Navicula arvensis var. maior Lange-Bertalot (benthic). f) Nitzchia sp. (benthic). g) Denticula kuetzingii Grunow (benthic). h) Hemidiscus sp. (benthic). i) Thalassiosira weissflogii (planktonic).

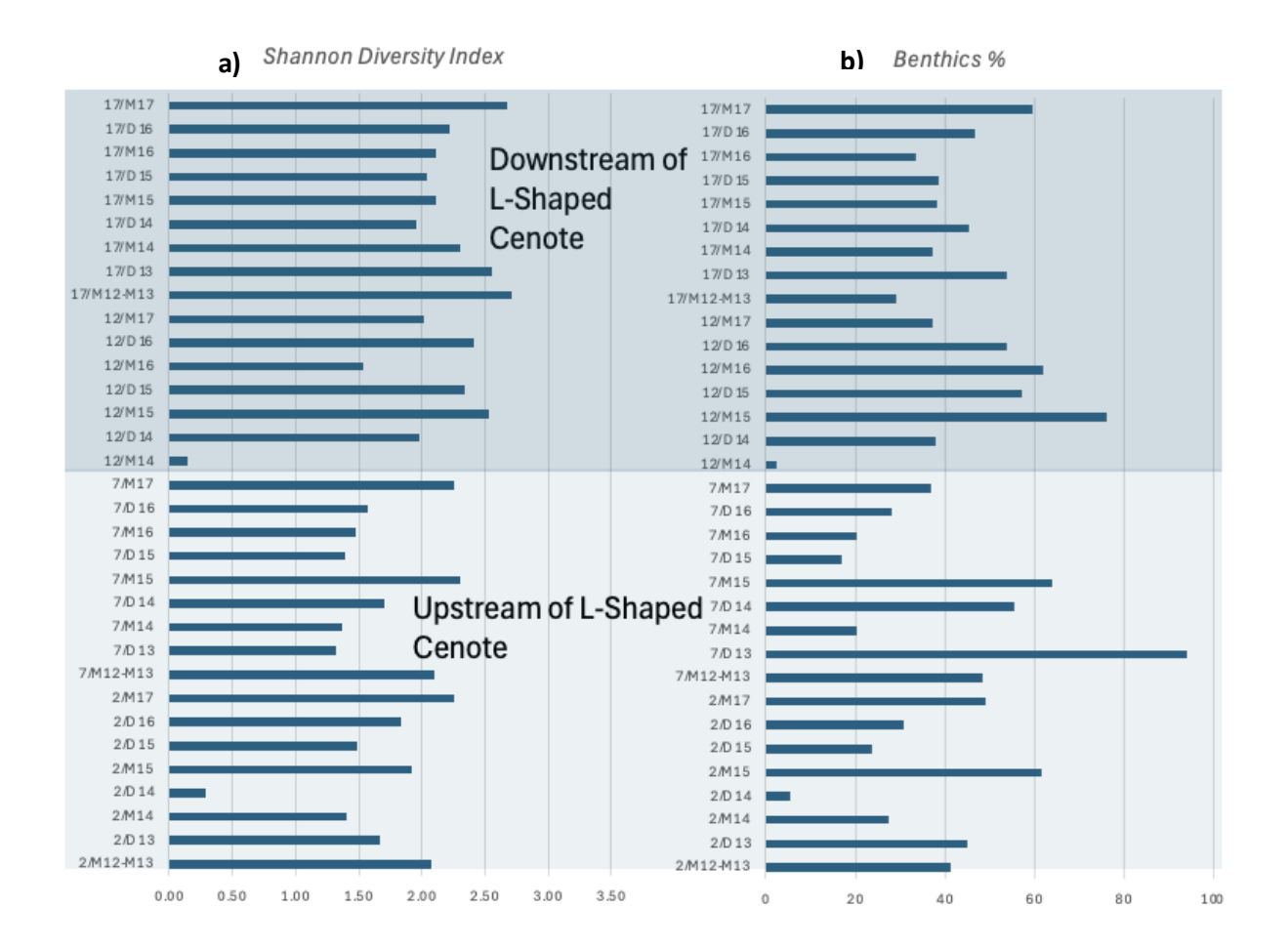


Fig. 3. The first number of the legend denotes station number, while "M" and "D" represent May and December, respectively, followed by sampling year. a) Shannon Diversity Index (SDI) values at upstream (sampling stations 2 and 7) and downstream (sampling stations 12 and 17) stations. b) percentage of benthic diatoms at upstream (sampling stations 2 and 7) and downstream (sampling station 12 and 17) stations.

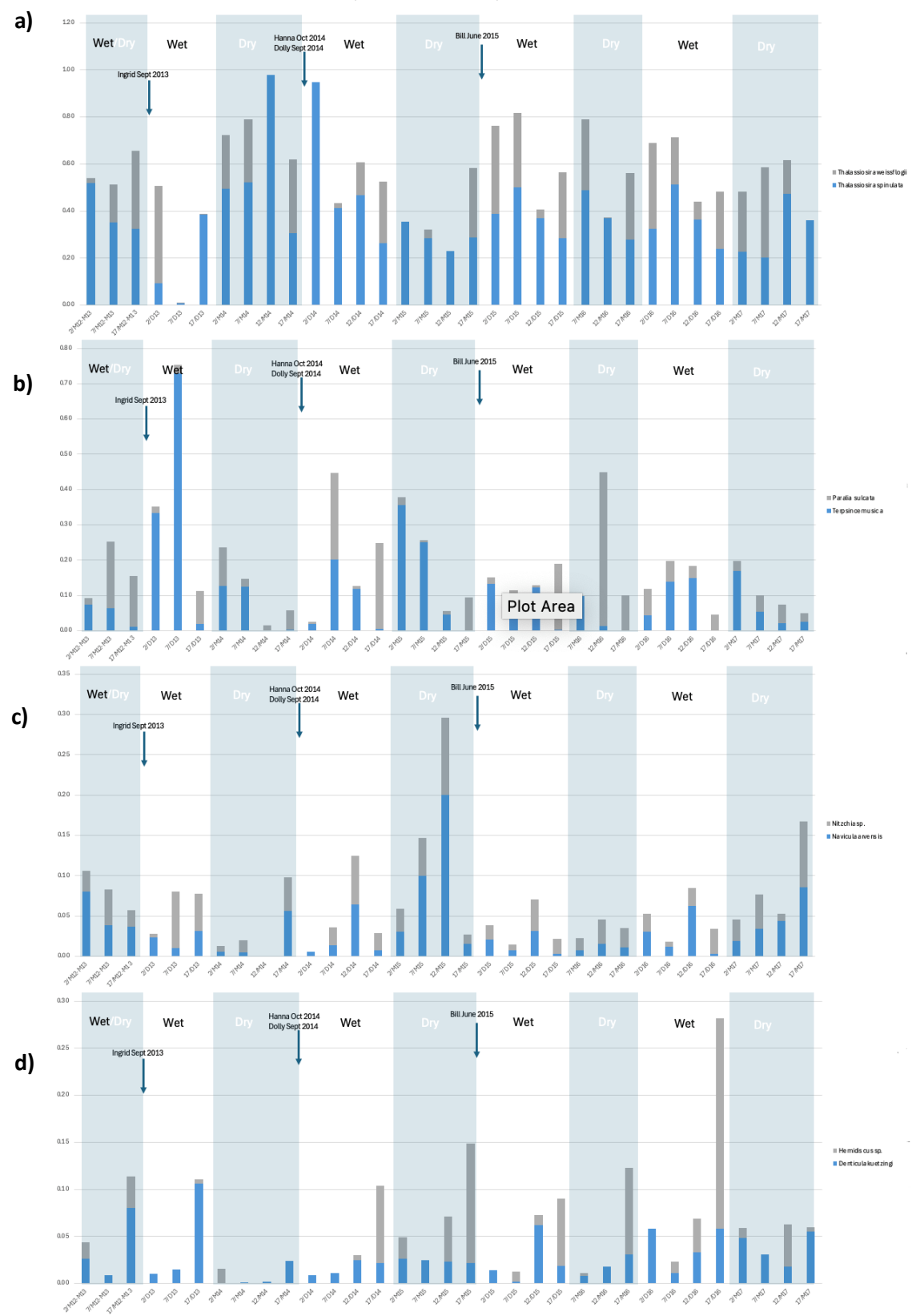


Fig 4. Data plotted through time (May 2012–May 2017) and by station (upstream to downstream locations): the first number denotes station number, while "M" and "D" represent May and December, respectively, followed by sampling year.

a) Thalassiosira weissflogii (planktonic) and Thalassiosira spinulata (planktonic). b) Paralia sulcata (benthic) and Terpsinoe musica (benthic). c) Nitzchia sp. (benthic) and Navicula arvensis Lange-Bertalot (benthic). d) Hemidiscus sp. (benthic) and Denticula kuetzingii Grunow (benthic).

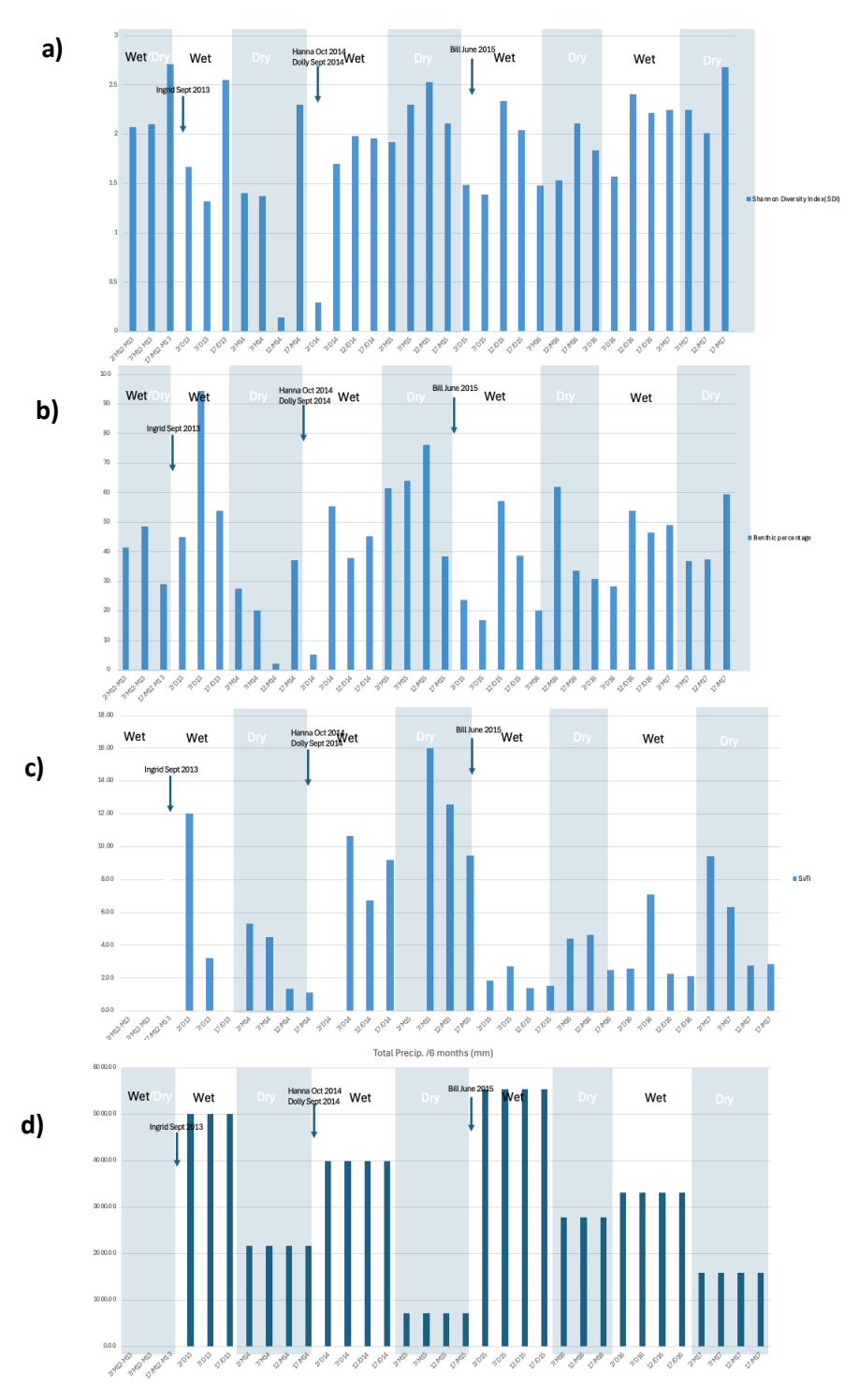


Fig 5. Data plotted through time (May 2012–May 2017) and by station (upstream to downstream locations): the first number denotes station number, while "M" and "D" represent May and December, respectively, followed by sampling year.

a) Shannon Diversity Index (SDI). b) percentage of benthic diatoms. c) Si/Ti ratio. d) total precipitation over each 6-month sampling period (mm).

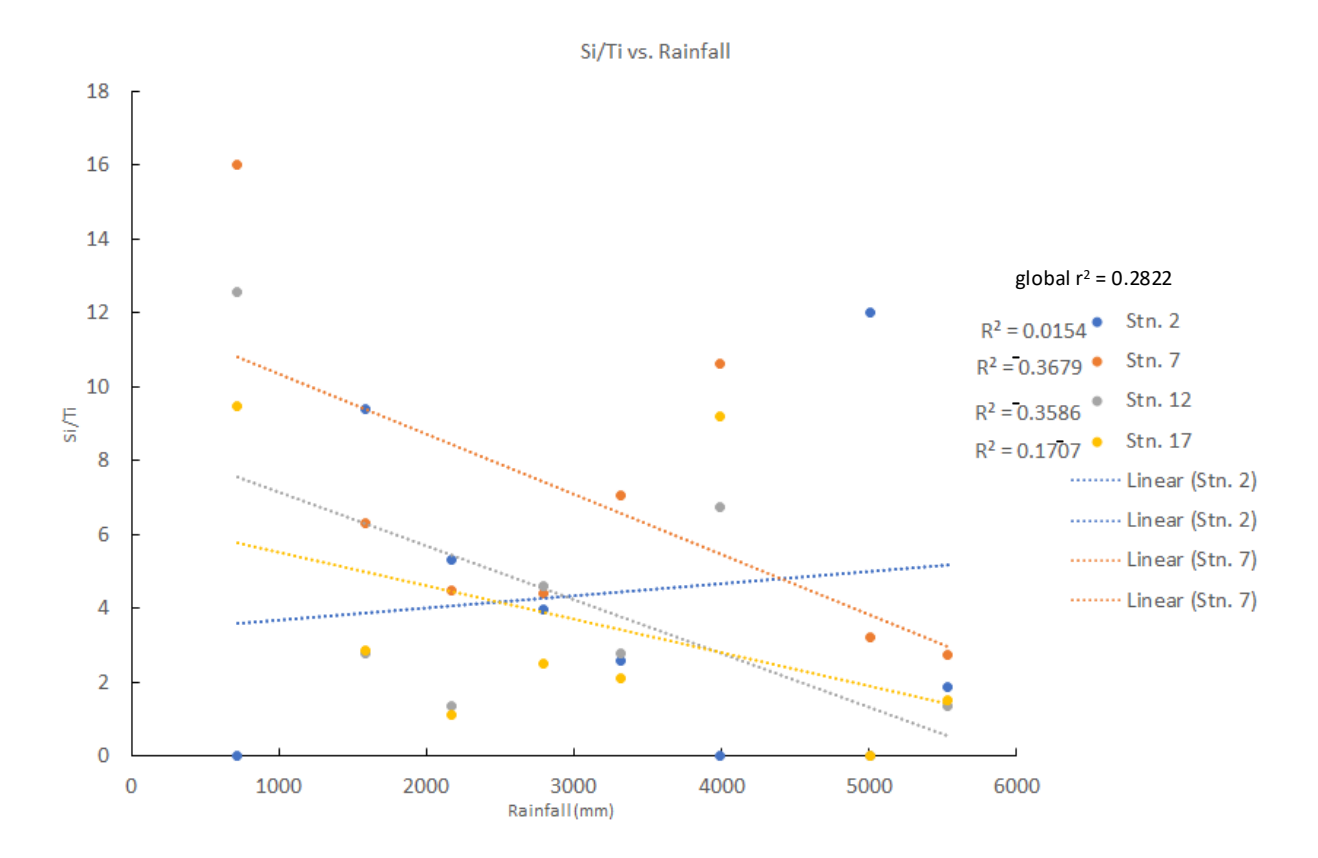


Fig. 6. Si/Ti ratio and total precipitation over each 6-month sampling period (mm).

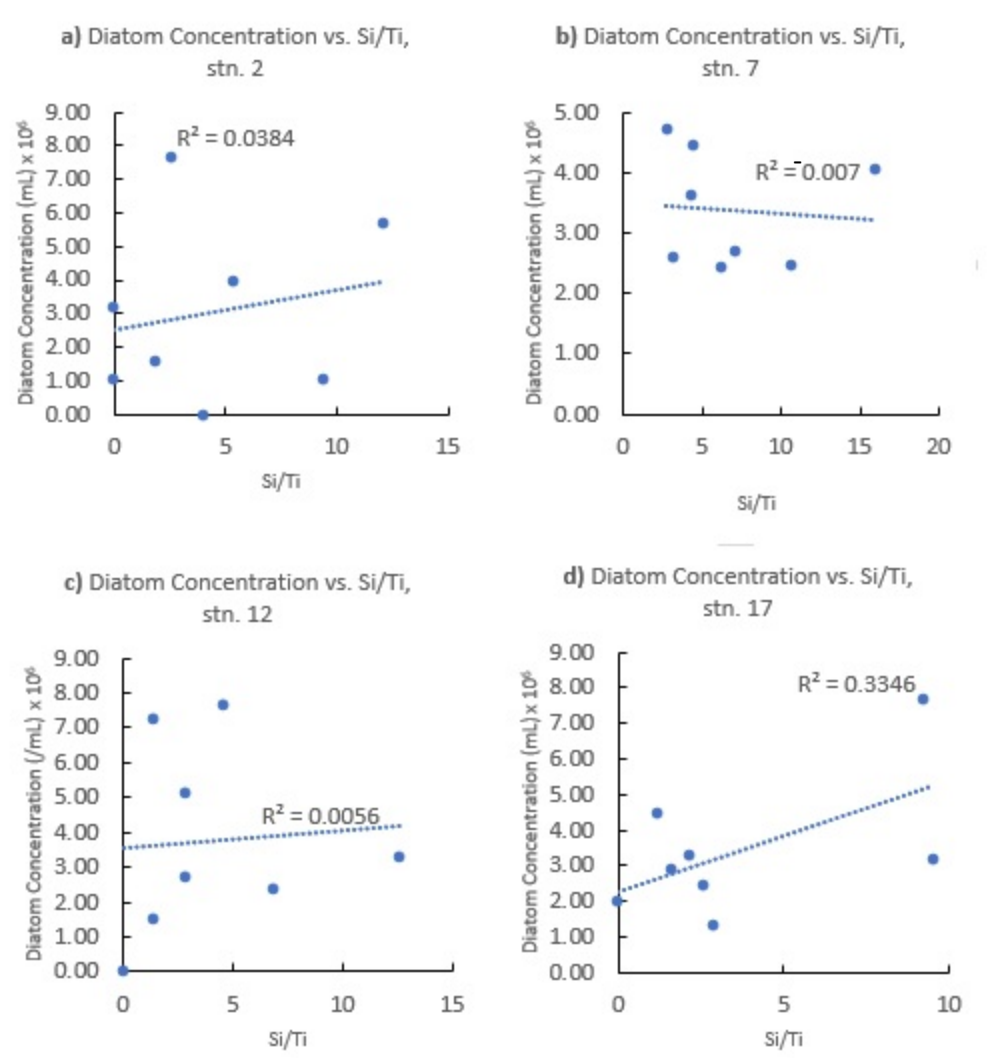


Fig. 7. Diatom concentration and Si/Ti ratio. a). sampling station 2. b) sampling station 7. c) sampling station 12. d) sampling station 17.

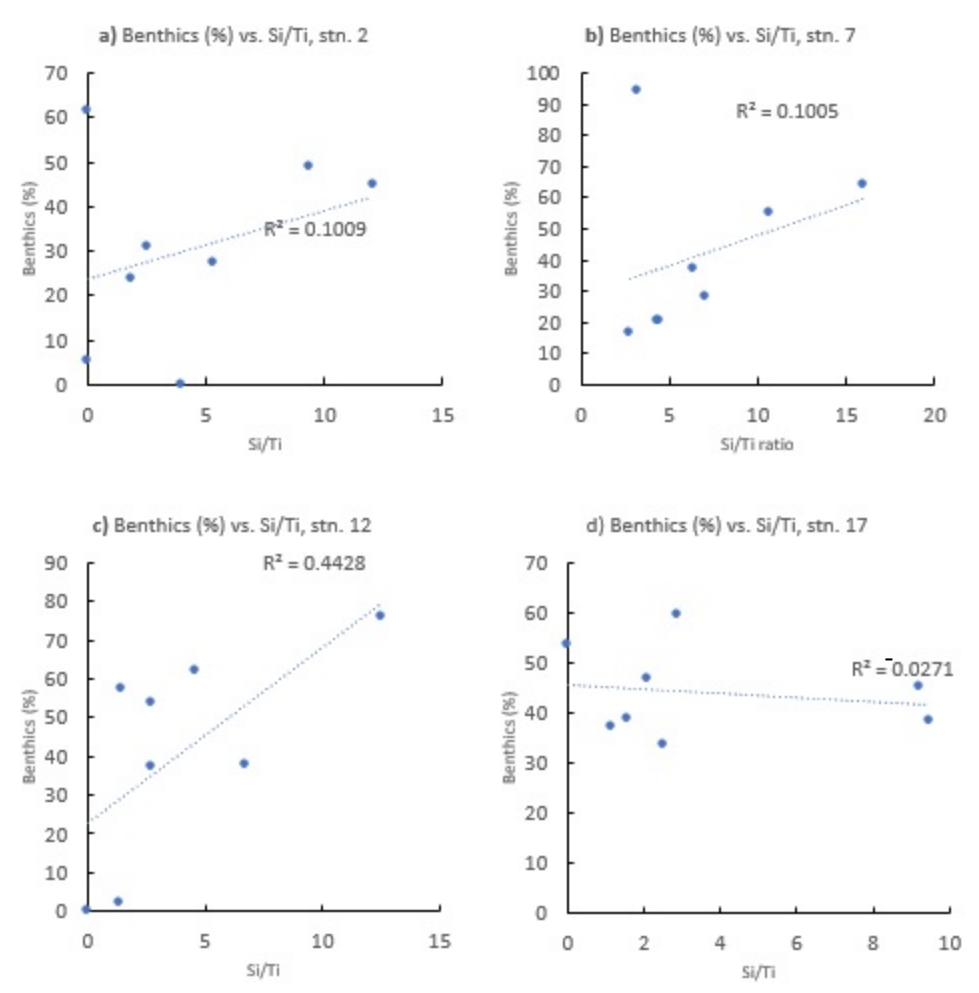


Fig. 8. Percentage of benthic diatoms and Si/Ti ratio. a) sampling station 2. b) sampling station 7. c) sampling station 12. d) sampling station 17.

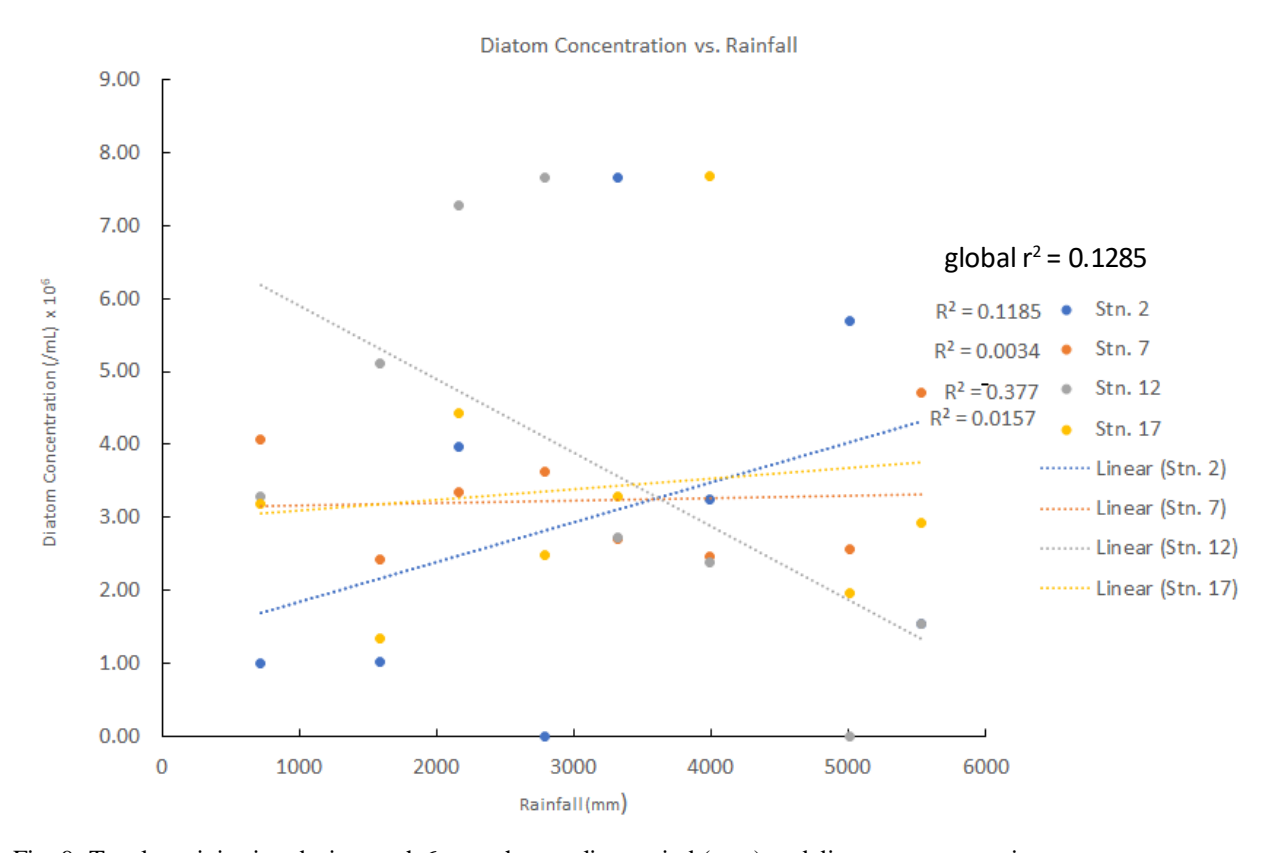


Fig. 9. Total precipitation during each 6-month sampling period (mm) and diatom concentrations.

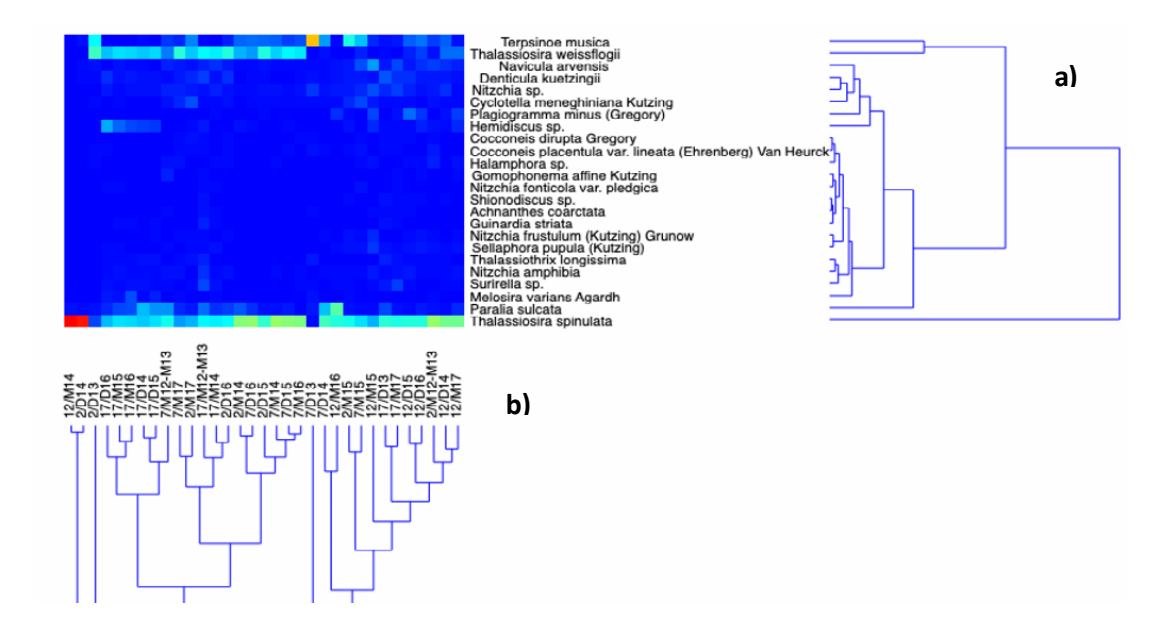


Fig. 10a) R-mode global clustering analysis/clusters of species for all stations and time periods. b) Q-mode clusters of samples.

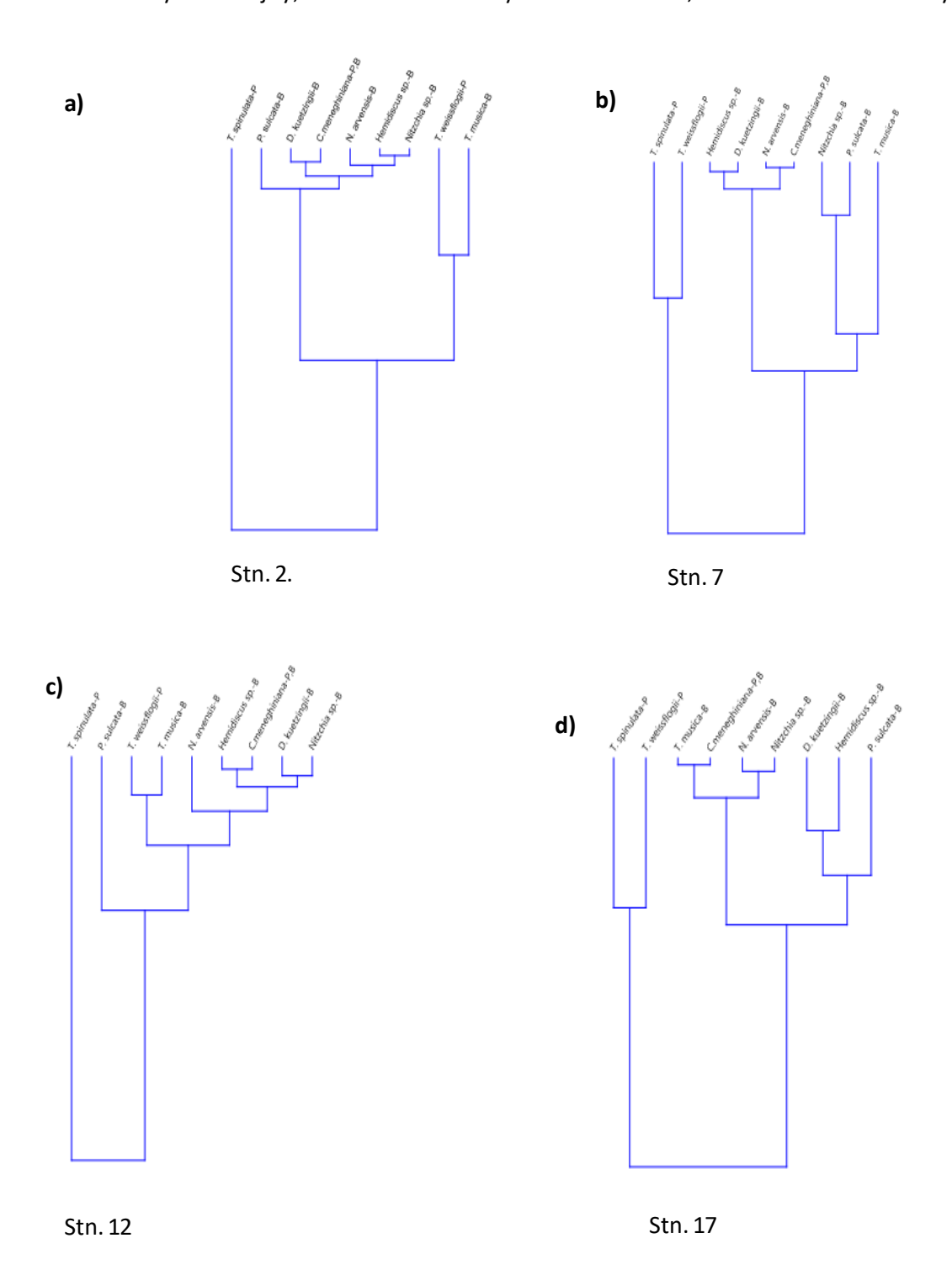


Fig. 11. Dominant species cluster analysis. The "P" beside taxa delineates planktonic diatoms and the "B" delineates benthic species.

4. Discussion

4.1. Time period

4.1.1. Precipitation and Si/Ti ratio

Diatoms generally showed a stronger response to individual TC events as opposed to precipitation, and the correlations between diatom concentrations and precipitation were generally quite weak; however, oftentimes there was a delayed response or latency period of approximately 6–12 months for the diatom response (i.e., increase) to register after TC activity (e.g., *Thalassiosira weissflogii, Thalassiosira spinulata*, etc.).

These findings correspond with prior studies of the aquifer by Collins et al. (2015) and McNeill-Jewer et al. (2019), which found that primary productivity (PP) was not immediately affected by large hurricane events, but rather during the months following each TC event, becoming more pronounced during the following dry season due to higher nutrient inputs and residence times in cenotes (Collins et al. 2015; McNeill-Jewer et al. 2019). Specifically, the significant rainfall events associated with TCs lead to higher nutrient input in the cenotes, particularly in cenotes surrounded by mangroves (Collins et al. 2015), which results in increased PP that can then also travel downstream after subsequent rainfall events, affecting diatom concentrations. This complex interrelationship and lagged response of PP likely contributes to the weak correlations between diatom concentrations and precipitation.

Similarly, McNeill-Jewer et al. (2019) specifically examined the Si/Ti ratio as an indicator of biological productivity in Yax Chen and found that although it had a weak correlation to overall rainfall events (lithogenic-derived elements were more strongly correlated), there was a response to hurricanes, albeit a lagged response of approximately 6–12 months, which the researchers concluded was likely due to a latency period pertaining to biological growth as well as the six-month sampling period, which may have obscured some of the results (McNeill-Jewer et al. 2019).

This result also corresponds to a similar study by Sullivan et al. (2022), who interpreted coarse carbonate amongst fine grain autogenic carbonate as evidence of local hurricane activity in Cenote Muyil, which is nearby Yax Chen, and also noted a disconnect between rainfall and hurricane proxies, noting that paleo-rainfall events may not accurately depict hurricane activity in the past (Sullivan et al. 2022), and similarly in this study, stronger, more discernible responses are seen in response to hurricane activity, discussed in more detail below. Interestingly, however, this finding would actually ease data analysis for utilising proxies such as diatoms to examine paleo-tempest records as it enables TC activity in the paleoenvironmental record to be more readily teased out from other rainfall events.

Similar to precipitation, the Si/Ti ratios also showed a weak correlation to diatom concentration, which is a somewhat surprising result as diatoms are predominantly silica-based organisms, although there may be variations between species in Si uptake as the correlations between Si/Ti ratio and benthic diatoms were generally higher.

4.1.2. SDI values

The general decrease in Shannon Diversity Index values after TC activity shown in Fig. 5a exemplifies a traditional concept in ecological studies that natural disturbances affecting habitat result in a decrease in biodiversity (Thieniemann 1918); however, natural disturbances can also result in greater development of species that survive (Thienemann 1918), which was particularly evident after Hurricane Ingrid in 2013: the following year in 2014 had extremely low SDI values at two of the stations owing to the predominance of *Thalassiosira spinulata* (i.e., 97.7% of the sample at stn. 12 in May 2014 and 94.7% at station 2 in Dec 2014).

Thalassiosira spinulata is often reported in rivers of high turbulence (Park et al. 2017), and not only have anchialine aquifers been noted to possess particularly fast flow rates (Gelting 1995), which increase turbulence, but Hurricane Ingrid resulted in extreme precipitation levels and flooding of the study site that likely resulted in higher turbulence resulting from shorter residence times in the corresponding cenotes (Collins et al. 2015). In addition, species within the *Thalassiosira* genus that are smaller in size, which is a defining characteristic of *Thalassiosira* spinulata, have been noted to inhabit areas with more constant upwelling (Abrantes 1988), which likely was present in the aquifer as studies by Kovacs et al. (2017) and Coutino et al. (2017) found increased vertical mixing of the water layers occurred after Hurricane Ingrid.

The *Thalassiosira* genus is also noted for its almost exclusive ability to produce chitin (*Cyclotella* is the only other genus where this has been reported), which leads to changes in buoyancy and sinking further down into the water column, and has been hypothesised as an adaptation mechanism to surface disturbances and fluctuating water conditions (Durkin et al. 2009) such as tropical cyclones, which might help to account for the near total dominance of this species at two of the sampling stations following Hurricane Ingrid.

During large rainfall events, the water level rises and can flood the surrounding environment, which was particularly evident after Hurricane Ingrid in 2013 (Collins et al. 2015). Diatoms from the surrounding terrestrial areas can then be transported into cenotes and subsequently farther downstream as the water recedes, which might lead one to expect an immediate increase in SDI values after TCs, contrary to this study's findings. However, these processes could help influence the increase in benthic diatoms and SDI values generally seen downstream, which could be affected by the input of species from terrestrial environments (i.e., shallow wetland environments and forested areas as opposed to open water cenotes) and the aforementioned lagged response/latency period in biological productivity.

4.1.3. Percentage of benthic diatoms

The significant proportion of benthic diatoms found in the samples corresponds to observations from van Hengstum et al. (2008), who investigated cenotes in the surrounding vicinity of Yax Chen and noted the presence of thick algal mats in the benthic environment. This finding also agrees with Hernandez-Almeida et al. (2013), who reported re-suspension of benthic diatoms was occurring along the Yucatan Peninsula's northern coast. The most important influencing factors of bentho-pelagic diatom distributions in the water column are re-suspension and sinking processes as algal species often sediment out of water during periods of less turbulence, and then become resuspended with high

turbulence, and wind has been cited to be one of the most important factors in coastal areas for turbulence and mixing processes of certain benthic species (Shchekinova et al. 2018).

Accordingly, the percentage of benthic diatoms increased at virtually all sampling stations following TC activity, with the exception of Bill in 2015 when a decrease occurred in the sampling period immediately following (i.e., Dec 2015). James et al. (2008) reported that the duration of storms was one of the strongest controlling factors for changes in sediment disturbance and re-suspension as storms of longer duration caused more bottom shear stress that increase total suspended solids in the water column, and Bill was a very short-lived TC (Jun 16–18, 2015), resulting in the year 2015 having the shortest duration of TC activity throughout the study period, as shown in Table 1, which could account for the difference in benthic activity. Interestingly, the proportion of benthic diatoms did still increase in the following sampling periods (in May 2016 for stns. 7 and 12, and Dec. 2016 at stns. 2 and 17), indicating the benthic population still showed a response, although the shorter TC duration could have resulted in a longer period of time for the increase to register, perhaps associated with the delayed biological response to TC events discussed in McNeill-Jewer et al. (2019).

The finding of generally increased benthic abundances after TC activity corresponds with previous studies that have reported the presence of the benthic species *Paralia sulcata* in the water column after storms and tidal mixing (e.g., Gebuhr et al. 2009; Smith et al. 1985), suggesting the relative abundance of benthic diatoms could be a reliable proxy for hurricane activity in paleo-tempest records.

4.2. Spatial

Differences emerged between the downstream (i.e., stns. 12 and 17) and upstream stations (i.e., stns. 2 and 7) for each sampling period, which is likely related to surrounding vegetation, as the downstream stations are surrounded by relatively more mangrove, as shown in Fig. 1, whereas the upstream stations are surrounded by more lowland tropical forest, which a study by Collins et al (2015) found has a significant influence on sediment flux, as after Hurricane Ingrid the stations surrounded by mangrove had higher sedimentation. Not only do mangroves result in greater nutrient inputs, but also greater habitat diversity (Lopez Fuerte et al. 2010), which likely accounts for the generally greater SDI values as well as proportion of benthic diatoms found in the downstream stations. This finding corresponds with a previous study that found mangrove environments support high benthic species diversity (Lopez-Fuerte et al. 2010).

This finding by Lopez-Fuerte et al. (2010) is reflected in the species distributions at the upstream vs. downstream stations, as *Paralia sulcata, Navicula arvensis* var. *maior* Lange-Bertalot, *Nitzchia* sp., *Denticula kuetzingii* Grunow, and *Hemidiscus* sp—which are all considered benthic species—had generally higher relative abundances in the downstream stations, whereas *Thalassiosira weissflogii*, *Thalassiosira spinulata*, *Cyclotella meneghiniana*, and *Terpsinoe musica*—which are largely considered planktonic—all had generally higher relative abundances in the upstream stations. One exception is *Terpsinoe musica*, which is a benthic diatom that was more prevalent in the upstream stations, although a prior study by Luttenton et al. (1986) reported this species was predominantly found on submerged roots and branches of a forest growing beside a river in Oklahoma, which could suggest this species prefers the forested environment found farther upstream around Yax Chen.

33

Interestingly, most of the planktonic species in this study have been commonly reported in freshwater to brackish rivers and streams—analogous to the aquifer's conditions—including the genus *Cocconeis* (Saraswati & Srinivasan 2016), *Cyclotella menghiniana* Kutzing (Taylor et al. 2007), *Thalassiosira weissflogii* (Kipp et al. 2023), *Thalassiosira lacustris* (Taylor et al. 2007), and *Thalassiosira spinulata* (Park et al. 2017), whereas the most commonly reported benthic species in this study, in contrast, were generally cosmopolitan in nature and adapted to a range of salinity preferences, as shown in Table 2.

Given that the salinity of the water column changes relatively quickly between the meteoric water mass, halocline, and marine water mass, this environment would favour species that are able to tolerate a range of salinity conditions when being routinely transported upwards and re-suspended into the water column as a result of TC activity. Interestingly, some of the dominant species found in this study are also tychopelagic, and have often been reported to prefer habitats delineated by coastal upwelling and/or vertical mixing zones, including *Paralia sulcata* (McQuoid & Nordberg 2003), as well as smaller species of *Thalassiosira* (Abrantes 1988) that might include *Thalassiosira spinulata*, further illustrating the mixing of the water column that has been reported to take place in the aquifer, particularly after TC activity (Coutino et al. 2017; Kovacs et al. 2017).

The divide between the upstream—downstream diatoms is also seen in the clustering analysis (Fig. 11), as the species that are more abundant upstream (i.e., mostly planktonic) were generally more closely clustered together or else were simplicifolious, and likewise the diatoms that were most abundant downstream (i.e., benthic) were also often closely clustered in the analysis—one exception to this was *Cyclotella meneghiniana* Kutzing (which is more abundant upstream), which was also often closely clustered with some of the benthic diatoms, although this can be accounted for by the fact that this species can be both planktonic and benthic (Taylor et al. 2007). Interestingly, the greater abundance upstream of the genera *Cyclotella* and *Thalassiosira* may be related to their exclusive ability among diatoms to produce chitin, posited to aid in avoiding adverse surface conditions (Durkin et al. 2009).

The distinct differences found in this study between planktonic and benthic diatoms could also be useful for sea-level studies where one might expect a transition from upstream to downstream diatom assemblages concurrent with sea level rise, as for example, a core analysis may show an upstream assemblage transitioning to a downstream assemblage indicating sea level rise.

5. Conclusions

In summary, the results of this study agree with previous findings from Yax Chen by Collins et al. (2015) and McNeill-Jewer et al. (2019) in that PP—or diatom concentration in this study—was not well correlated with precipitation. In addition, many of the variables measured (e.g., Si/Ti, etc.) had overall poor correlations with diatom concentrations, although nonetheless some potentially useful findings were still obtained from this study: in particular, the SDI values as well as the proportion of benthic diatoms were generally found to be higher in the downstream stations, which has also been reported in previous studies where the presence of mangrove was found to be an important controlling factor on sedimentation of OM (Collins et al. 2015) that also supports benthic diatom biodiversity (Lopez-Fuerte et al. 2010), and hence the differences in upstream and downstream diatom assemblages could potentially be used to reconstruct sea-level rise in the paleoclimate record. This study also found

34

that SDI values showed a general decrease after TC activity whereas the relative abundance of benthic diatoms showed a general increase, implying vertical mixing of the water column, and thus these metrics might also represent a promising paleoenvironmental indicator for examining TC activity during the TCP/Medieval Warm Period.

5.1. Future research directions

5.1.1. Yax Chen

A sediment core sample was extracted by cave divers for future paleoclimate studies from nearby sediment trap station 17 as it is in the downstream portion of the aquifer where the greatest sedimentation occurs, which the results of this study show is an optimal location as this is also where the greatest proportion of benthic diatoms and diversity occurs, which are two metrics that also responded quite consistently to TCs.

Changes in extreme winds have been linked to changes in storms, including TCs, and geographical distributions, frequencies, and intensities of TC-related extreme wind events are expected to change with TCs (Seneviratne et al. 2021), so further studies to better understand the response of benthic diatoms to wind-related changes will also aid in refining the use of diatoms as a reliable paleoenvironmental indicator. In addition, changes in phytoplankton communities in the North Atlantic have been associated with changes in temperature in the Northern Hemisphere and the NAO index (Rosenzweig et al. 2007), which as discussed earlier, have been found to be important in controlling storm activity over the Yucatan Peninsula, so a better understanding of how benthic diatoms respond to these changing conditions would also strengthen their reliability as a paleoenvironmental proxy.

5.1.2. Broader upwelling and ocean circulation patterns

Diatoms in general have been recognised as effective indicators of the intensity of paleo-upwelling (Saraswati & Srinivasan 2016), including species reported in this study such as *Paralia sulcata* (McQuoid & Nordberg 2003). As such, benthic diatoms could be used to further explore broader upwelling and ocean circulation patterns throughout the Terminal Classic Period and Postclassic/Medieval Warm Period, which could account for some of the demographic changes that occurred amongst the Maya. In particular, dependence on maritime economies and trade networks in the Yucatan Peninsula became more robust during the Terminal Classic Period, including at Chichen Itza (Glover et al. 2011), and increased further during the Postclassic (Steele et al. 2023; Sullivan et al. 2022). As well, the majority of coastal settlements were located on the eastern coast of the peninsula (Andrews 1993), and the emergence of new centres including Tulum—which is in the vicinity of Yax Chen—also occurred during this period (Sullivan et al. 2022), and could signify increased ocean upwelling in this area and greater abundance of maritime resources, as upwelling zones account for approximately 1% of the ocean's surface yet are responsible for 50% of fish landings due to the rich supply of nutrients brought from the seafloor (Fagan 2004).

Evidence of increased ocean upwelling in this region is supported by findings from one study that found SSTs were significantly cooler in the North Atlantic during the Terminal Classic Period (Wu et al. 2017), which is characteristic of increased ocean upwelling (Fagan 2004). Additionally, tropical cyclones have been found to result in significant upwelling in the deep ocean, and although coastal areas

35

have not received as much attention, a study of Hurricane Sandy found that strong winds parallel to the coastline occurred for nearly 48 hours before making landfall, resulting in upwelling of colder nearbottom water (Miles et al. 2017). Dorian in 2019 also travelled along the coastline for a lengthy period of time before making landfall (Wang & Toumi 2021), also suggesting changed TC activity and ocean upwelling.

More evidence of broader changing ocean upwelling circulation patterns can be found in a comparable case study discussed by Fagan (2004) off the Santa Barbara Channel in southern California, where researchers found that upwelling increased during the Medieval Warm Period, becoming particularly intense from 950–1300 CE, which also corresponded to evidence of several severe droughts throughout the region and resulted in a shift by the local Chumash population toward a greater reliance on fishing subsistence (Kennett & Kennett 2000): archaeological settlements increased along the coastline and became larger, and evidence of more extensive maritime trade was found farther inland as the expanded maritime economy is believed to have helped buffer against the adverse effects of the droughts, and interdependence among settlement groups also increased (Fagan 2004). Wind speed and the El Nino–Southern Oscillation (ENSO) were noted to help influence this upwelling zone (Fagan 2004), although it is also possible that the effects of contemporaneous increased storm activity helped fuel this upwelling.

5.2. Concluding remarks

As evidence of tropical cyclones in the paleoclimate record is currently limited and difficult to interpret compared to most other paleoclimatic extreme events (Seneviratne et al. 2021), the findings from this study present a promising paleoenvironmental indicator to better examine paleo-tempest records. Hence, the findings from this project will provide a paleoclimatic context for better understanding TC activity during the TCP, which can be used to infer resulting hydrological changes to the peninsula's extensive anchialine aquifer. Moreover, as the TCP occurred during a similar period of elevated global temperatures (i.e., the Medieval Warm Period), the findings will also provide a comparable historical analogue for future projections of TC activity on the peninsula that may help to clarify some of the ambiguities in the current literature, and may also yield important insights into freshwater management of coastal aquifers in today's changing climate.

References Cited

- Abrantes F (1988). Diatom assemblages as upwelling indicators in surface sediments off Portugal. *Marine Micropaleontology*, 35(1–2): 91–103. https://doi.org/10.1016/0025-3227(88)90082-5
- Andrade-Velazquez M, Medrano-Perez OR, Montero-Martinez MJ, Alcudia-Aguilar A (2021). Regional climate change in Southeast Mexico-Yucatan Peninsula, Central America and the Caribbean. *Applied Science*. 211: 8284.
- Andrews AP (1993). Late postclassic lowland Maya archaeology. *Journal of World Prehistory*, 7(1): 35e69. https://doi.org/10.1007/BF00978220.
- Appendini CM, Meza-Padilla R, Abud-Russell S, Proust S, Barrios RE, Secaira-Fajardo F (2019). Effect of climate change over landfalling hurricanes at the Yucatan Peninsula. *Climate Change*, 157: 469–482.
- Berg R (2015). Tropical Storm Bill. National Hurricane Centre Tropical Cyclone Report, National Hurricane Center, NOAA, https://coast.noaa.gov/hurricanes/ [Accessed 10 April, 2025]
- Beven JL II (2014). Hurricane Ingrid. National Hurricane Centre Tropical Cyclone Report, National Hurricane Center, NOAA, https://coast.noaa.gov/hurricanes/ [Accessed 10 April, 2025]
- Beven JL II (2015). Tropical Storm Dolly. National Hurricane Centre Tropical Cyclone Report, National Hurricane Center, NOAA, https://coast.noaa.gov/hurricanes/ [Accessed 10 April, 2025]
- Brady JE, Peterson PA (2008). Re-envisioning ancient Maya ritual assemblages. *KIP Articles*, 36: 7364.
- Burnett AC, Sheshadri A, Silvers LG, Robinson T (2021). Tropical cyclone frequency under varying SSTs in aquaplanet simulations. *Geophysical Research Letters*, 48: e2020GL091980. https://doi.org/10.1029/2020GL091980
- Cangialosi JP (2014). Tropical Storm Hanna. National Hurricane Centre Tropical Cyclone Report, National Hurricane Center, NOAA, https://coast.noaa.gov/hurricanes/ [Accessed 10 April, 2025]
- Collins M, Knutti R, Arblaster J, Dufresne J-L, Fichefet T, Friedlingstein P, Gao X, Gutowski WJ, Johns T, Krinner G, Shongwe M, Tebaldi C, Weaver AJ, Wehner M (2013). *Long-term Climate Change: Projections, Commitments and Irreversibility*. In Stocker TF, Qin D, Plattner G-K, Tignor M, Allen SK, Boschung J, Nauels A, Xia Y, Bex V, Midgley PM (eds.) *Climate Change 2013: The Physical Science Basis. Contribution of Working Group I to the Fifth Assessment Report of the Intergovernmental Panel on Climate Change*. Cambridge University Press: Cambridge, United Kingdom and New York. pp. 1029–1136.
- Collins SV, Reinhardt EG, Werner CL, Le Maillot C, Devos F, Meachum SS (2015).

- Regional response of the coastal aquifer to Hurricane Ingrid and sedimentation flux in the Yax Chen cave system (Ox Bel Ha) Yucatan, Mexico. *Palaeogeography, Palaeoclimatology, Palaeoecology*, 438: 226–238. http://dx.doi.org/10.1016/j.palaeo.2015.07.030 0031-0182/
- Coutino A, Stastna M, Kovacs S, Reinhardt E (2017). Hurricanes Ingrid and Manuel (2013) and their impact on the salinity of the Meteoric Water Mass, Quintana Roo, Mexico, *Journal of Hydrology*, 551: 715–729.
- Cristobal G, Blanco S, Bueno G (2020). Overview: Antecedents, Motivation, and Necessity. In: Cristobal G, Blanco S, Bueno G. (eds.) *Modern Trends in Diatom Identification: Fundamentals and Applications. Developments in Applied Phycology* (10th edition). Cham, Switzerland: Springer Nature Switzerland. p. 34–36.
- Dangendorf S, Hendricks N, Sun Q, Klinck J, Ezer T, Frederikse T, Calafat FM, Wahl T, Tornqvist TE (2023). Acceleration of U.S. Southeast and Gulf coast sea-level rise amplified by internal climate variability. *Nature Communications*, 14(1935): 1–11. https://doi.org/10.1038/s41467-023-37649-9
- Douville H, Raghavan K, Renwick J, Allan RP, Arias PA, Barlow M, Cerezo-Mota R, Cherchi A, Gan TY, Gergis, J, Jiang D, Khan A, Pokam Mba W, Rosenfeld D, Tierney J, Zolina O (2021). *Water Cycle Changes*. In Masson-Delmotte V, Zhai P, Pirani A, Connors SL, Péan C, Berger S, Caud N, Chen Y, Goldfarb L, Gomis MI, Huang M, Leitzell K, Lonnoy E, Matthews JBR, Maycock TK, Waterfield T, Yelekçi O, Yu R, Zhou B (eds.) *Climate Change 2021: The Physical Science Basis. Contribution of Working Group I to the Sixth Assessment Report of the Intergovernmental Panel on Climate Change*. Cambridge University Press: Cambridge, United Kingdom and New York, pp. 1055–1210, doi:10.1017/9781009157896.010.
- Durkin CA, Mock T, Armbrust EV (2009). Chitin in diatoms and its association with cell walls. *Eukaryot Cell*, 8(7): 1038–1050. doi: 10.1128/EC.00079-09
- Emanuel K (2020). Response of global tropical cyclone activity to increasing CO₂: Results from Downscaling CMIP6 Models. *Journal of Climatology*, 34: 57–70.
- Fagan B (2004). *The Long Summer: How Climate Changed Civilization*. Basic Books: New York.
- Fishbein E, Patterson RT (1993). Error-weighted maximum likelihood (EWML): A new statistically based method to cluster quantitative micropaleontological data. *Journal of Paleontology*, 67(3): 475–486.
- Frappier, AB, Pyburn J, Pinkey-Drobnis AD, Wang X, Corbett DR, Dahlin BH (2014). Two millennia of tropical cyclone-induced mud layers in a northern Yucatán stalagmite: Multiple overlapping climatic hazards during the Maya Terminal Classic 'megadroughts'. *Geophysical Research Letters*, 41: 5148–57. https://doi.org/10.1002/2014GL059882

- Gebuhr C, Wiltshire KH, Aberle N, van. Beusekom JEE, Gerdts, G (2009). Influence of nutrients, temperature, light and salinity on the occurrence of *Paralia sulcata* at Helgoland Roads, North Sea. *Aquatic Biology*, 7: 185–197.
- Gelting RJ (1995). *Water and population in the Yucatan Peninsula*. International Institute for Applied Systems Analysis. WP-95-87.
- Gill RB, Mayewskib PA, Johan Nybergc J, Haugd GH, Petersone LC (2007).

 Drought and the Maya collapse. *Ancient Mesoamerica*. 18. New York: Cambridge University Press; p. 283–302.
- Glover JB, Rissolo D, Mathews JP (2011). The Hidden World of the Maritime Maya: Lost Landscapes Along the North Coast of Quintana Roo, Mexico. In Ford B (ed.) The Archaeology of Maritime Landscapes. When the Land Meets the Sea: vol 2. Springer: New York. pp. 195–216. https://doi.org/10.1007/978-1-4419-8210-0_1
- Godinez Madrigal J, van der Zaag P, van Cauwenbergh N (2018). A half-baked solution: drivers of water crises in Mexico. *Proceedings of the International Association of Hydrological Sciences* (IAHS), 376: 57–62.
- González R (2024). Marine heat waves make tropical storm intensification more likely, *Eos*, 105, https://doi.org/10.1029/2024EO240446.
- Grodsky B (2024). Political regimes and climate change: Learning from past civilisations. *Global Environment*, 17: 614–649. doi: 10.3828/whpge.63837646622499
- Haug GH, Gunther D, Peterson LC, Sigman DM, Hughen KA, Aeschlimann B (2003). Climate and the collapse of Maya civilization. *Science*, 299(5613): 1731–1735. https://doi.org/10.1126/science.1080444
- Hernandez-Almeida OU, Herrera-Silveira JA, Merino-Virgilio yF (2013). Nine new records of benthic diatoms of the genera *Climaconeis, Cocconeis, Licmophora, Talaroneis, Oestrupia, Petroneis* and *Synedrosphenia* from the northern coast of the Yucatan Peninsula, Mexico. *Hidrobiología*, 23(2): 154–168.
- Hodell DA, Brenner M, Curtis JH (2005). Terminal Classic drought in the northern Maya lowlands inferred from multiple sediment cores in Lake Chichancanab (Mexico). *Quaternary Science Reviews*, 24 (12–13): 1413–1427. https://doi.org/10.1016/j.quascirev.2004.10.013
- Idso, CD (2009). Paleoclimatic Indicators of Medieval Climate Change. In McKitrick R (ed.) Critical Topics in Global Warming: Supplementary Analysis of the Independent Summary for Policymakers. Fraser Institute Studies in Risk and Regulation: Vancouver, Canada. pp. 89–95.
- James RT, Chimney MJ, Sharfstein B, Engstrom DR, Schottler SP, East T, Jin K-R (2008).

- Hurricane effects on a shallow lake system, Lake Okeechobee, Florida (USA). *Fundamental and Applied Limnology (Archiv für Hydrobiologie*), 172(4): 273–287. doi: 10.1127/1863-9135/2008/0172-0273
- Jobbová E, Helmke C, Bevan A (2018). Ritual responses to drought: An examination of ritual expressions in Classic Maya written sources. *Human Ecology*, 46: 759–781.
- Kennett DJ, Kennett JP (2000). Competitive and cooperative responses to climate instability in coastal southern California. *American Antiquity*, 65(2): 379–395. doi:10.2307/2694065
- Kipp RM, McCarthy M, Fusaro A (2023). *Thalassiosira weissflogii* (Grunow) G. Fryxell & Hasle, (1896) 1977: U.S. Geological Survey, Nonindigenous Aquatic Species Database, Gainesville, FL, and NOAA Great Lakes Aquatic Nonindigenous Species Information System, Ann Arbor, MI, https://nas.er.usgs.gov/queries/greatlakes/FactSheet.aspx?Species_ID=1693&Potential=N&Type =0, Revision Date: 9/12/2019 [Accessed 22 October, 2023]
- Klotzbach PJ, Bell MM, DesRosiers AJ, Silvers LG. *Discussion of 2024 Atlantic hurricane* season to date and forecast thoughts on the rest of the season. Seasonal Hurricane Forecasting, Colorado State University Tropical Weather and Climate Research. https://tropical.colostate.edu/Forecast/2024_0903_seasondiscussion.pdf [Accessed 15 September, 2024]
- Knutson TR, Chung MV, Vecchi G, Sun J, Hsieh T-L, Smith AJP (2021). *ScienceBrief Review:* Climate change is probably increasing the intensity of tropical cyclones. In Le Quéré C, Peter Liss P, Forster P (eds.) Critical Issues in Climate Change Science. East Anglia, United Kingdom: University of East Anglia (UEA). p. 1–8.
- Kociolek P (2011). Thalassiosira weissflogii. *Diatoms of North America*. https://diatoms.org/species/46475/thalassiosira_weissflogii [Accessed 20 September, 2025]
- Kovacs SE, Reinhardt EG, Stastna M, Coutino A, Werner C, Collins CV, Devos F, Le Maillot C (2017). Hurricane Ingrid and Tropical Storm Hanna's effects on the salinity of the coastal aquifer, Quintana Roo, Mexico. *Journal of Hydrology*, 551: 704 714. https://doi.org/10.1016/j.jhydrol.2017.02.024
- Krayesky DM, del Castillo EM, Zamudio E, Norris JN, Fredericq S (2009). *Diatoms* (Bacillariophyta) of the Gulf of Mexico. In Felder DL, Camp DK (eds.) Gulf of Mexico: Its Origins, Waters, and Biota. I Biodiversity: Texas A&M University Press: Texas. pp. I 155–J85.
- Li Y, Tang Y, Wang S, Toumi R, Song X, Wang Q (2023). Recent increases in cyclone intensification events in global offshore regions. *Nature Communications*, 2014: 5167. https://doi.org/10.1038/s41467-023-40605-2

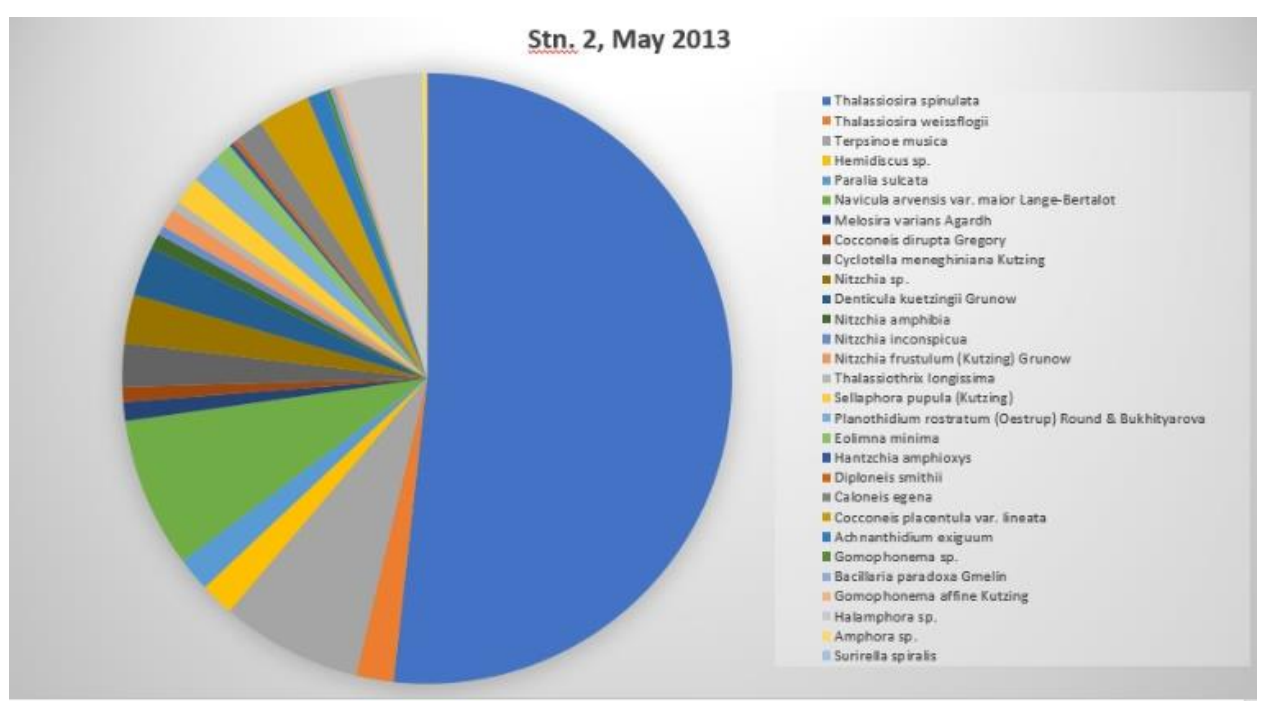
- Lindsey R, Dahlman L (2009). Climate variability: North Atlantic Oscillation. NOAA. https://www.climate.gov/news-features/understanding-climate/climate-variability-north-atlantic-oscillation [Accessed 18 May 2025]
- Lopez Fuerte FO, Siqueiros Beltrones DA, Navarros JN (2010). *Benthic Diatoms Associated with Mangrove Environments in the Northwest Region of Mexico*. Conabio: Mexico. pp. 1–204.
- Luttenton MR, Pfiester LA, Timpano P (1986). Morphology and growth habit of Terpsinoe musica Ehr. (Bacillariophyceae). *Castanea*, *51*(3): 175–182. http://www.jstor.org/stable/4033384
- Mann ME (2021). Beyond the hockey stick: Climate lessons from the Common Era. *PNAS*, 118(39): 1–9, e2112797118. https://doi.org/10.1073/pnas.2112797118
- Mann ME (2024). Cat 6 hurricanes have arrived. *PNAS*, 121(7): e2322597121 https://doi.org/10.1073/pnas.2322597121
- Mann ME, Woodruff JD, Donnelly JP, Zhang Z (2009). Atlantic hurricanes and climate over the past 1500 years. *Nature* 460: 880–883.
- Masters J. Why are there so many Atlantic-named storms? Five possible Explanations. Yale Climate Connections. https://yaleclimateconnections.org/2021/05/why-are-there-so-many-atlantic-named-storms-five-possible-explanations/ [Accessed 1 October 2023]
- McNeill-Jewer CA, Reinhardt EG, Collins S, Kovacs S, Chan WM, Devos F, Le Maillot C (2019). The effect of seasonal rainfall on nutrient input and biological productivity in the Yax Chen cave system (Ox Bel Ha), Mexico, and implications for µXRF core studies of paleohydrology. *Palaeogeography, Palaeoclimatology, Palaeoecology*, 534: 109289.
- McQuoid MR, Nordberg K (2003). The diatom *Paralia sulcata* as an environmental indicator species in coastal sediments. *Estuary Coastal Shelf Science*, 56(2): 339–354.
- Mejia-Ortiz LM, Chavez-Solis EM, Brankovits D (2022a). Editorial: The effects of environmental change on anchialine ecosystems. *Frontiers in Maritime Science*, 9:1029027. doi: 10.3389/fmars.2022.1029027
- Mejia-Ortiz LM, Collantes-Chavez-Costa AL, Lopez-Contreras C, Frausto-Martinez O (2022b). Subterranean waters in Riviera Maya of the Yucatan Peninsula: Vulnerability and the importance of monitoring. *Limnology The Importance of Monitoring and Correlations of Lentic and Lotic Waters, InTechOpen*, 1–16.
- Méndez-Tejeda R, Hernández-Ayala JJ (2023). Links between climate change and hurricanes in the North Atlantic. *PLOS Climate* 2(4): e0000186. https://doi.org/10.1371/journal.pclm.0000186
- Michener WK, Blood ER, Bildstein KL, Brinson MM, Gardner LR (1997). Climate change,

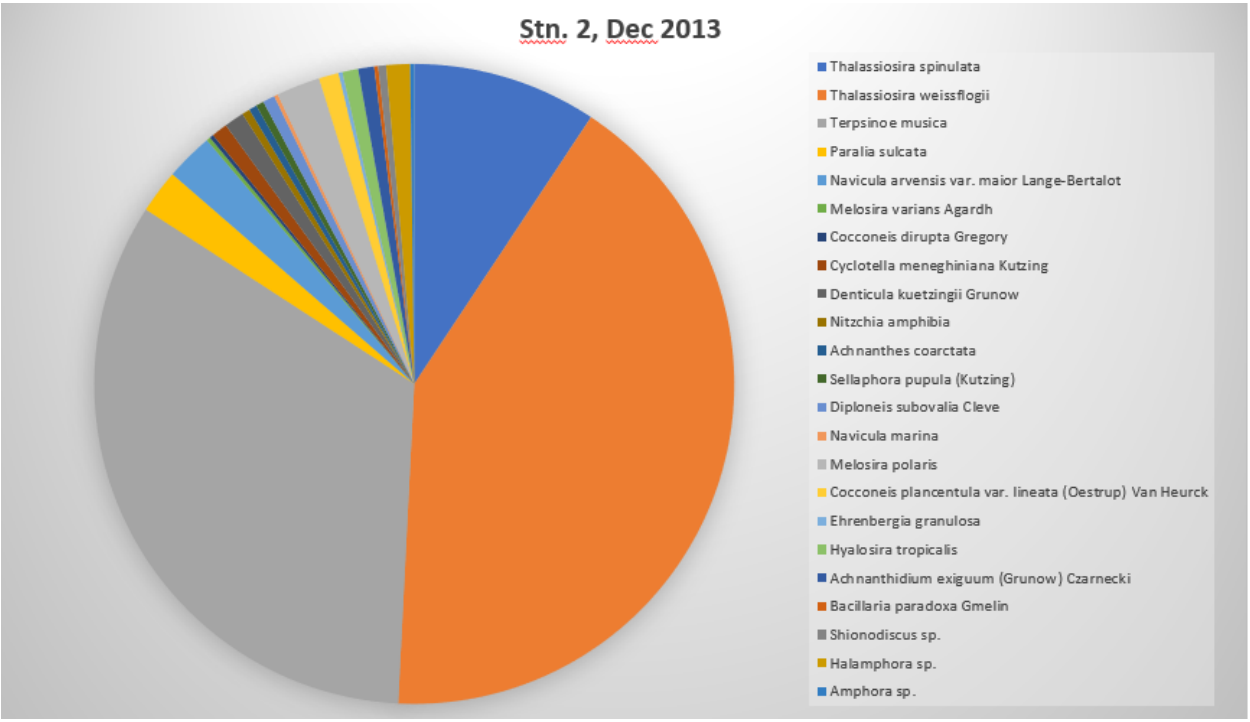
- hurricanes and tropical storms, and rising sea level in coastal wetlands. *Ecological Applications: Ecological Society of America*, 7(3): 770–801.
- Miles T, Seroka G, Glenn S (2017). Coastal ocean circulation during Hurricane Sandy. *Journal of Geophysical Research: Oceans*, 122: 7095–7114, doi:10.1002/2017JC013031
- Murakami H, Delworth TL, Cooke WF, Zhao M, Xiang B, Hsu P-C (2020). Detected climatic change in global distribution of tropical cyclones. *Proceedings of the National Academy of Science*, 117(20): 10706–10714.
- NOAA (2023). Atlantic hurricanes and climate change. NOAA. https://www.gfdl.noaa.gov/global-warming-and-hurricanes/ [Accessed 24 February, 2025]
- Paleoecological Environmental and Research Laboratory (PEARL) (2021). Sediment Sample Preparation Methods for Diatoms (Siliceous Microfossils). Department of Biology, Queen's University: Kingston, Canada. p. 1–8.
- Park JS, Jung SW, Ki J-S, Guo R, Kim HJ, Lee K-W, Lee JH (2017). Transfer of the small diatoms *Thalassiosira proschkinae* and *T. spinulata* to the genus *Minidiscus* and their taxonomic re-description. *PLoS ONE* 12(9): e0181980. https://doi.org/10.1371/journal.pone.0181980
- Pohlman JW, Iliffe TM, Cifuentes LA (1997). A stable isotope study of organic cycling and the ecology of an anchialine cave ecosystem. *Marine Ecology Progress Series*,155: 17–27.
- Quintana Roo Speleological Survey (2025). List of long underwater caves in Quintana Roo Mexico to 1500 meters. Quintana Roo Speleological Survey. https://qrss.caves.org/qrlong.htm [Accessed 25 July 2025]
- Rodriguez-Gonzalez MP, Cerezo-Mota R (2025). Trend analysis of extreme precipitation indices and climate oscillations over the Yucatan Peninsula for the period 1980–2010. *International Journal of Climatology*, 45(9): e8885. https://doi.org/10.1002/joc.8885
- Rodríguez-Ramírez A, Caballero M, Roy P, Ortega B, Vázquez-Castro G, Lozano-García S (2015). Climatic variability and human impact during the last 2000 years in western Mesoamerica: evidence of late Classic (AD 600–900) and Little Ice Age drought event. *Climatology of the Past*, 11: 1239–1248
- Rosenzweig C, Casassa G, Karoly DJ, Imeson A, Liu C, Menzel A, Rawlins S, Root TL, Seguin B, Tryjanowski P (2007). Assessment of observed changes and responses in natural and managed systems. In Parry ML, Canziani OF, Palutikof JP, van der Linden PJ, Hanson CE (eds.) Climate Change 2007: Impacts, Adaptation and Vulnerability. Contribution of Working Group II to the Fourth Assessment Report of the Intergovernmental Panel on Climate Change. Cambridge University Press: Cambridge, United Kingdom. p. 79–131.

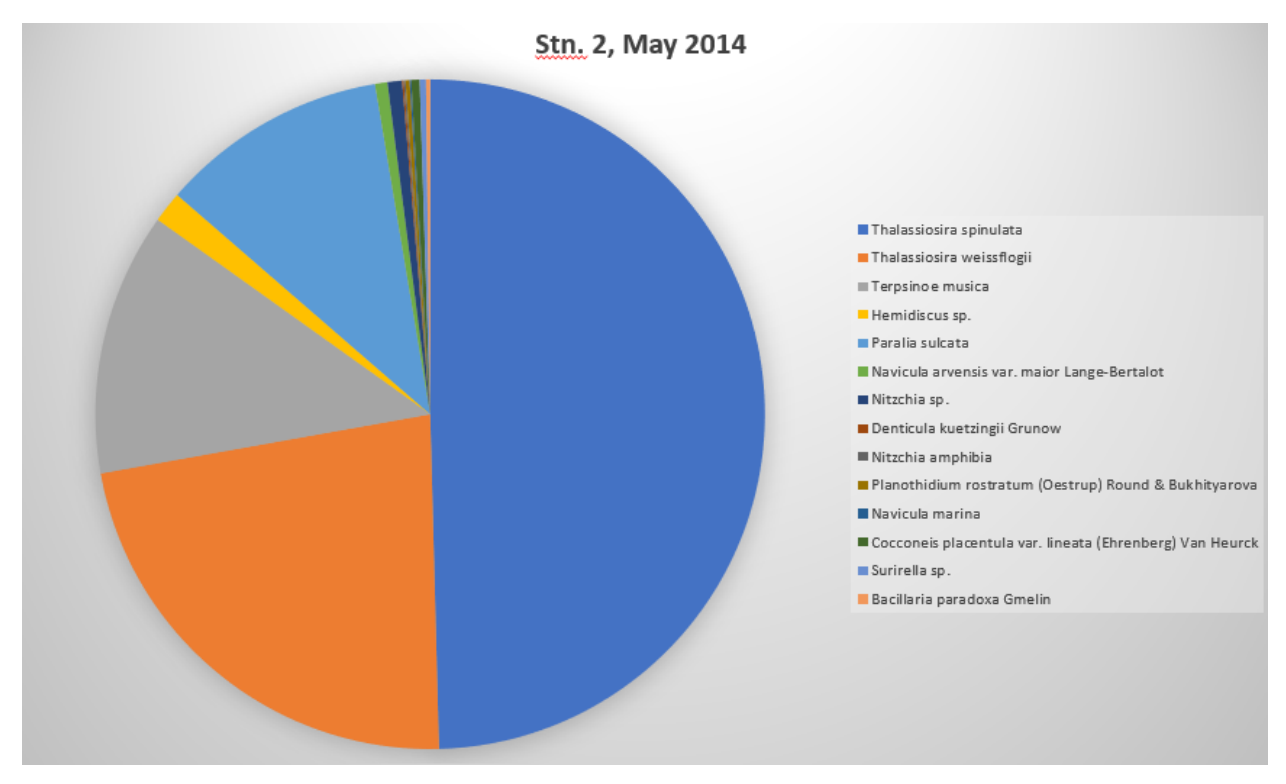
- Saraswati PK, Srinivasan MS (2016). *Micropaleontology: Principles and Applications*. Springer: Switzerland. doi: 10.1007/978-3-319-14574-7
- Seneviratne SI, Zhang X, Adnan M, Badi W, Dereczynski C, Di Luca A, Ghosh S, Iskandar I, Kossin J, Lewis S, Otto F, Pinto I, Satoh M, Vicente-Serrano SM, Wehner M, Zhou B (2021). Weather and Climate Extreme Events in a Changing Climate. In Masson-Delmotte V, Zhai P, Pirani A, Connors SL, Péan C, Berger S, Caud N, Chen Y, Goldfarb L, Gomis MI, Huang M, Leitzell K, Lonnoy E, Matthews JBR, Maycock TK, Waterfield T, Yelekçi O, Yu R, Zhou B. (eds.) Climate Change 2021: The Physical Science Basis. Contribution of Working Group I to the Sixth Assessment Report of the Intergovernmental Panel on Climate Change. Cambridge University Press: New York. p. 1513–1766.
- Shchekinova EY, Gebuhr C, Boersma M, Wiltshire KH (2018). Changes in sinking of plankton–like particle: comparison between observations and numerical model. arXiv:1804.00446 [physics.ao-ph]. https://doi.org/10.48550/arXiv.1804.00446
- Siqueiros Beltrones DA, López-Fuerte FO, Martínez YJ, Altamirano-Cerecedo MdC (2021). A first estimate of species diversity for benthic diatom assemblages from the Revillagigedo Archipelago, Mexico. *Diversity*, 13: 458. https://doi.org/10.3390/d13100458
- Smith DE, Cullingford RA, Haggart A (1985). A major coastal flood during the Holocene in eastern Scotland. *E & G Quaternary Science Journal*, 35(1): 109–118.
- Smyth MP, Dunning NP, Weaver EM, van Beynen P, Ortegón Zapata D (2017). The perfect storm: Climate change and ancient Maya response in the Puuc Hills region of Yucatán. *Antiquity*, 91(356): 490–550.
- Spaulding et al. (2021). Diatoms.org: Supporting taxonomists, connecting communities. *Diatom Research*, 36(4): 291–301. Diatoms of North America. https://doi.org/10.1080/0269249X.2021.2006790. [Accessed 20 February, 2023]
- Steele RE, Reinhardt EG, Devos F, Meacham S, Le Maillot C, Gabriel JJ, Rissolo D, Vera CA, Peros MC, Kim S-T, Marshall M, Zhu J (2023). Evidence of recent sea-level rise and the formation of a classic Maya canal system inferred from Boca Paila cave sediments, Sian Ka'an biosphere, Mexico. *Quaternary Science Reviews*, 310: 108117.
- Sullivan RM, van Hengstum PJ, Donnelly JP, Tamalavage AE, Tyler S. Winkler TS, Little SN, Mejia-Ortiz L, Reinhardt EG, Meacham S, Schumacher C, Korty R (2022). Northeast Yucatan hurricane activity during the Maya Classic and Postclassic periods. *Scientific Reports*, 12: 20107.
- Taylor, JC, Harding WR, Archibald CGM (2007). *An Illustrated Guide to Some Common Diatom Species from South Africa* (Report to the Water Research Commission: WRC Report TT 282/07), Water Research Commission: Praetoria. pp. 1–225.
- Thienemann A (1918). Lebensgemeinschaft und Lebensraum. *Naturwissenschaftliche Wochenschrift NF*, 17: 282–290, 297–303.

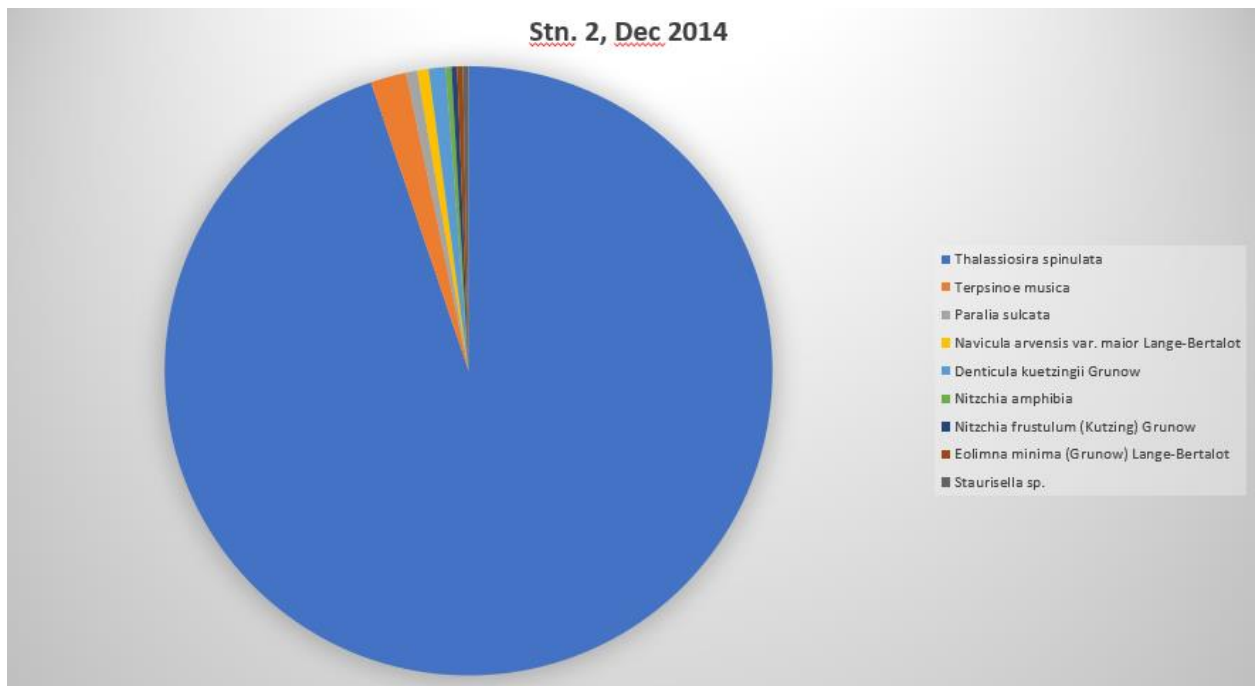
- Trouet V, Esper J, Graham NE, Baker A, Scourse JD, Frank DC (2009). Persistent positive North Atlantic Oscillation mode dominated the Medieval Climatic Anomaly. *Science*, 324(5923): 78–80. doi: 10.1126/science.1166349
- van Hengstum PJ, Reinhardt EG, Beddows PA, Huang RJ, Gabriel JJ (2008). Thecamoebians (testate amoeba) and foraminifera from three anchialine cenotes in Mexico: Low salinity (1.5–4.5 psu) faunal transitions. *Journal of Foraminiferal Research*, 38(4): 305–317.
- Visbeck MH, Hurrell JW, Polvani, L, Cullen HM (2001). The North Atlantic Oscillation: Past, present and future. *PNAS*, 98(23)" 12876–12877. www.pnas.org/cgi/doi/10.1073/pnas.231391598
- Wang S, Toumi R. (2021). Recent migration of tropical cyclones towards coasts. *Science*, 371: 514–517. 10.1126/science.abb9038
- Whitehead JC, Anderson WP Jr, Guignet D, Landry CE, Morgan OA (2024). Sealevel rise, drinking water quality and the economic value of coastal tourism in North Carolina. *Water Resources Research*, 60: e2023WR036440. https://doi.org/10.1029/2023WR036440
- Williams DM. (2020). *Diatom Classifications: What Purpose do they Serve?* In Cristobal G, Blanco S, Bueno G (eds.) *Modern Trends in Diatom Identification: Fundamentals and Applications. Developments in Applied Phycology* (10th ed.). Cham, Switzerland: Springer Nature Switzerland. p. 34–36.
- Wu S (2013). Terpsinoe musica. *Diatoms of North America*. https://diatoms.org/species/49374/terpsinoe_musica [Accessed 20 Sept 2025]
- Wu HC, Felis T, Scholz D, Giry C, Kolling M, Jochem KP, Scheffers SR (2017).
 Changes to Yucatán Peninsula precipitation associated with salinity and temperature extremes of the Caribbean Sea during the Maya civilization collapse. *Nature, Scientific Reports*, 7: 15825. doi:10.1038/s41598-017-15942-0

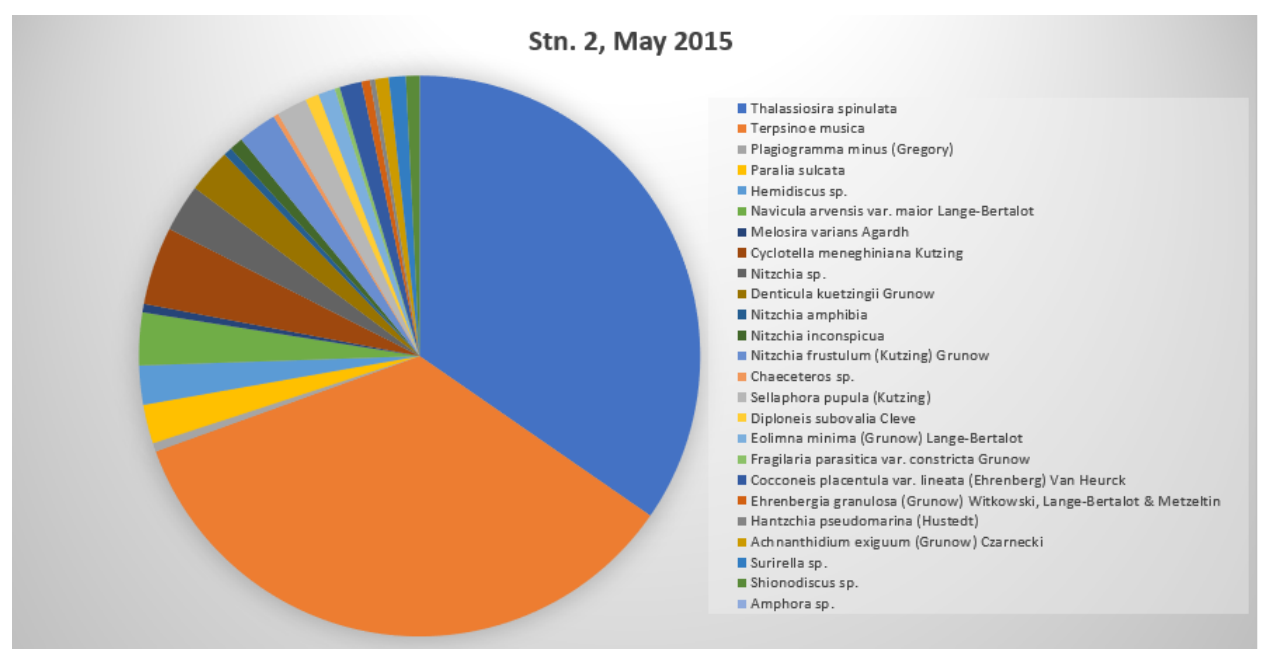
Appendix 1a. Stn. 2 population distributions.

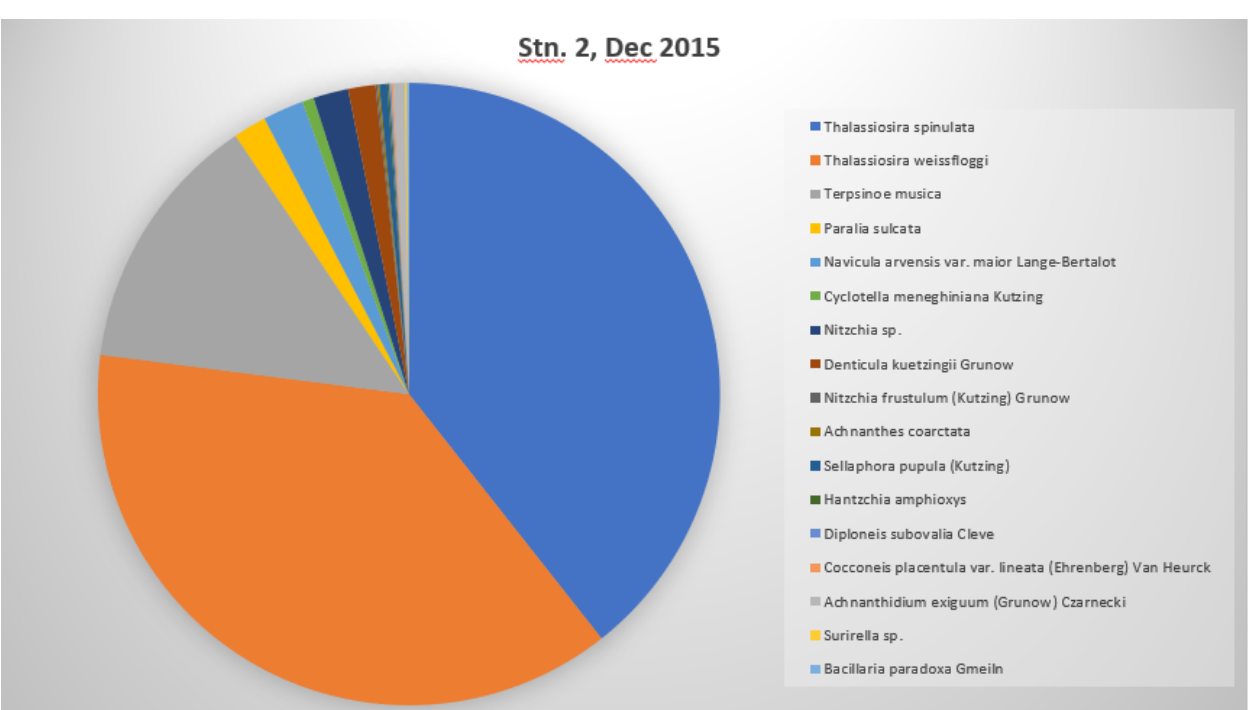


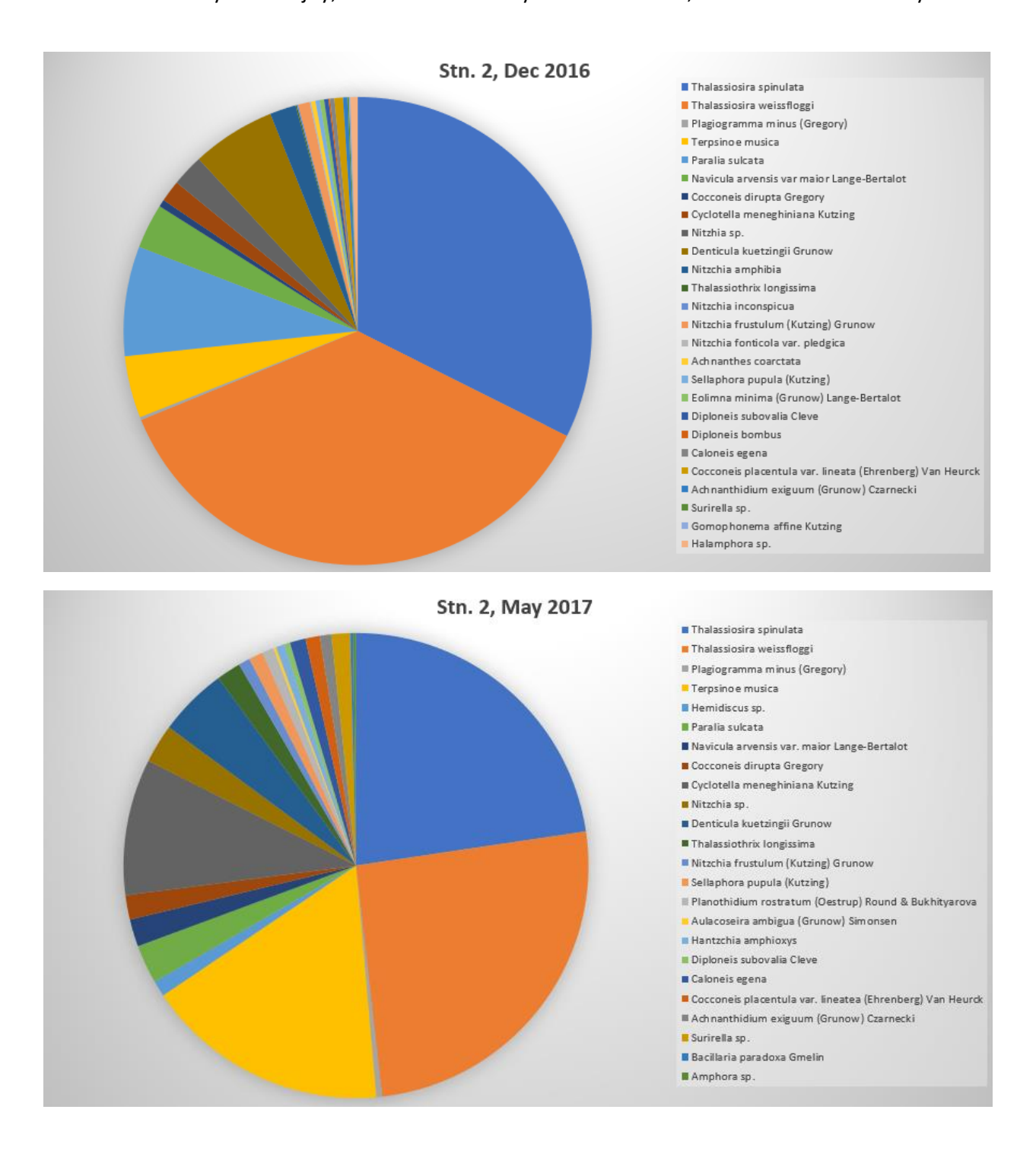




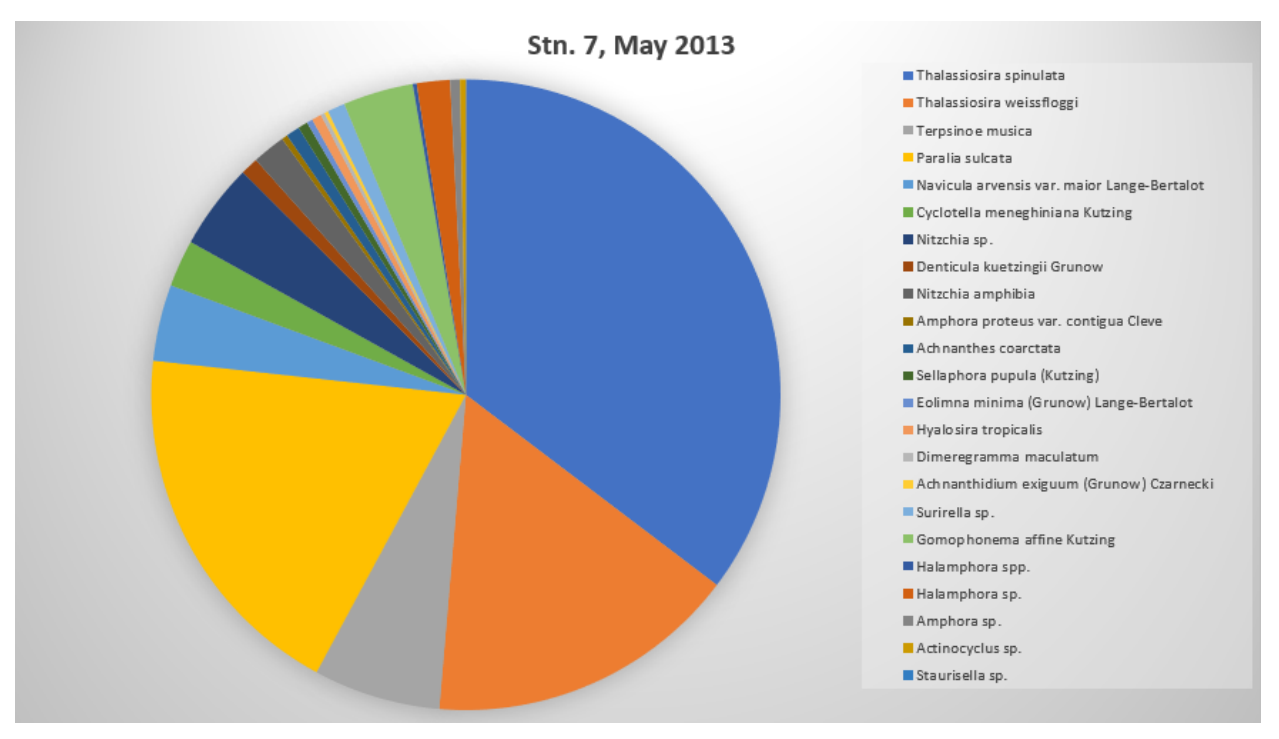


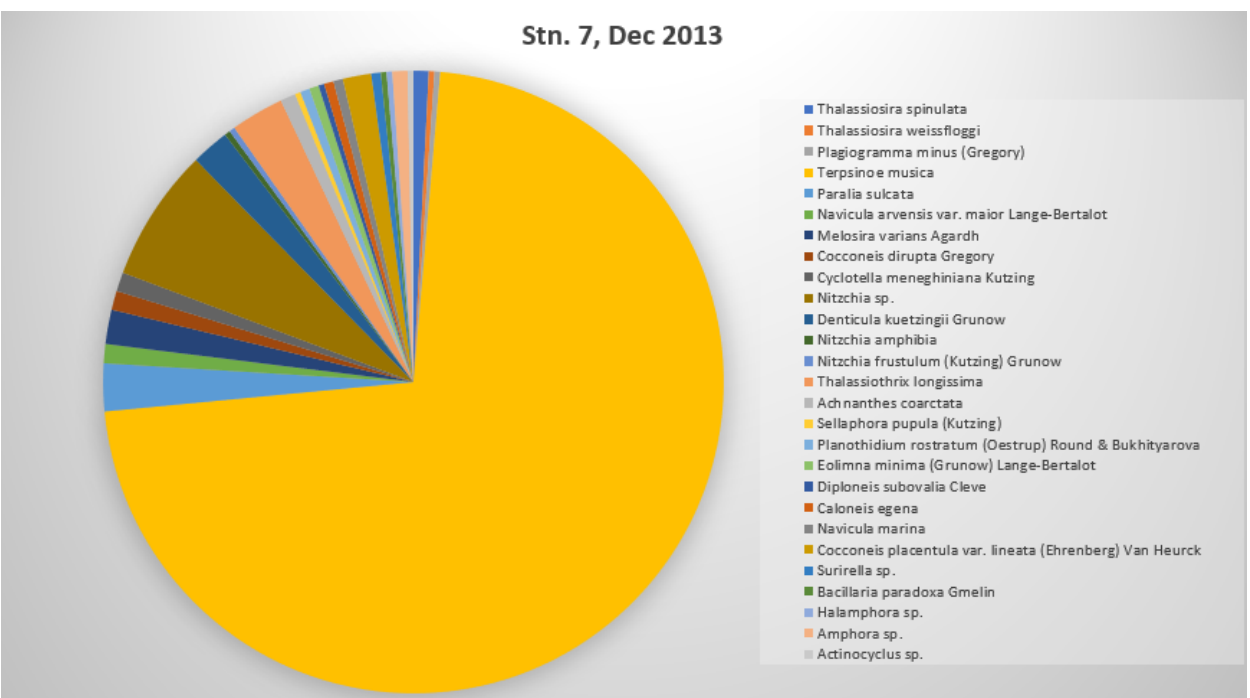


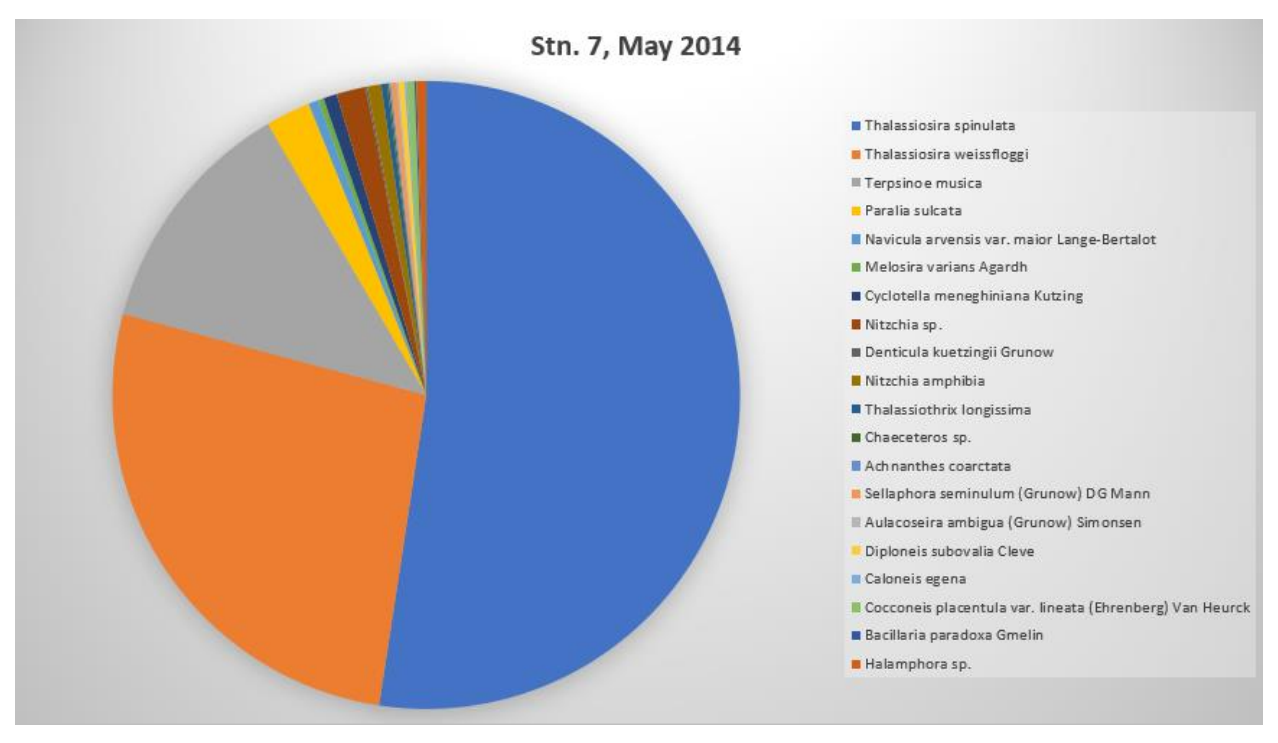


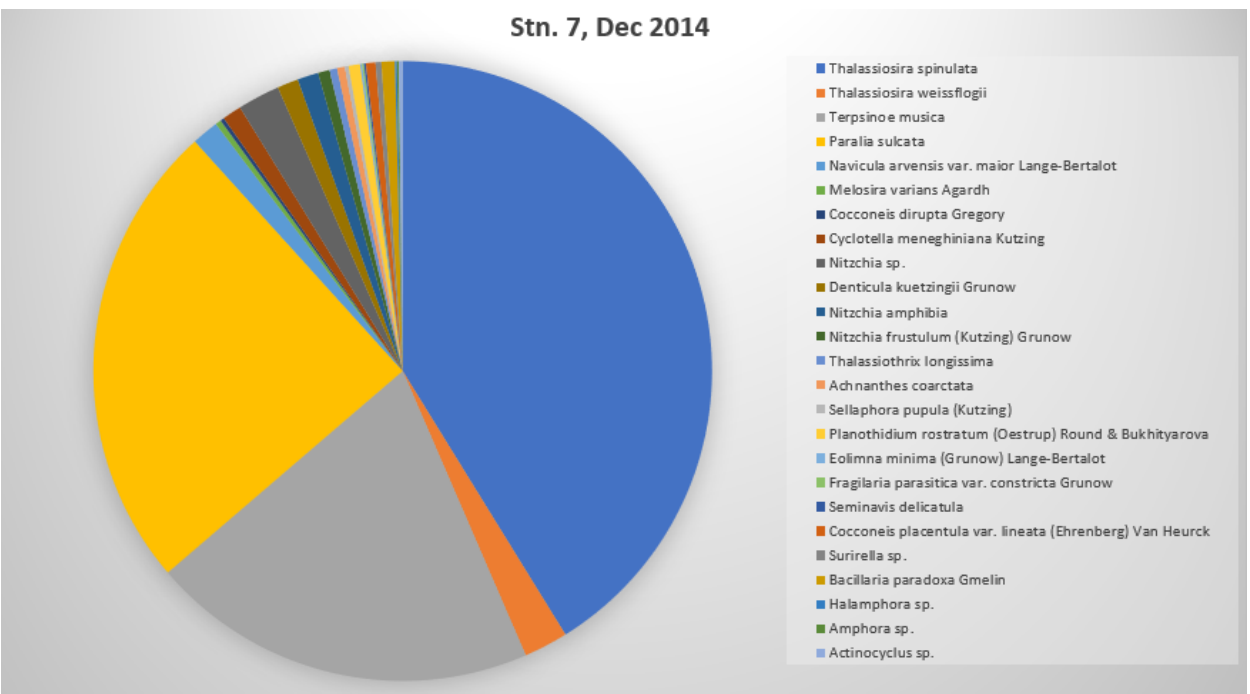


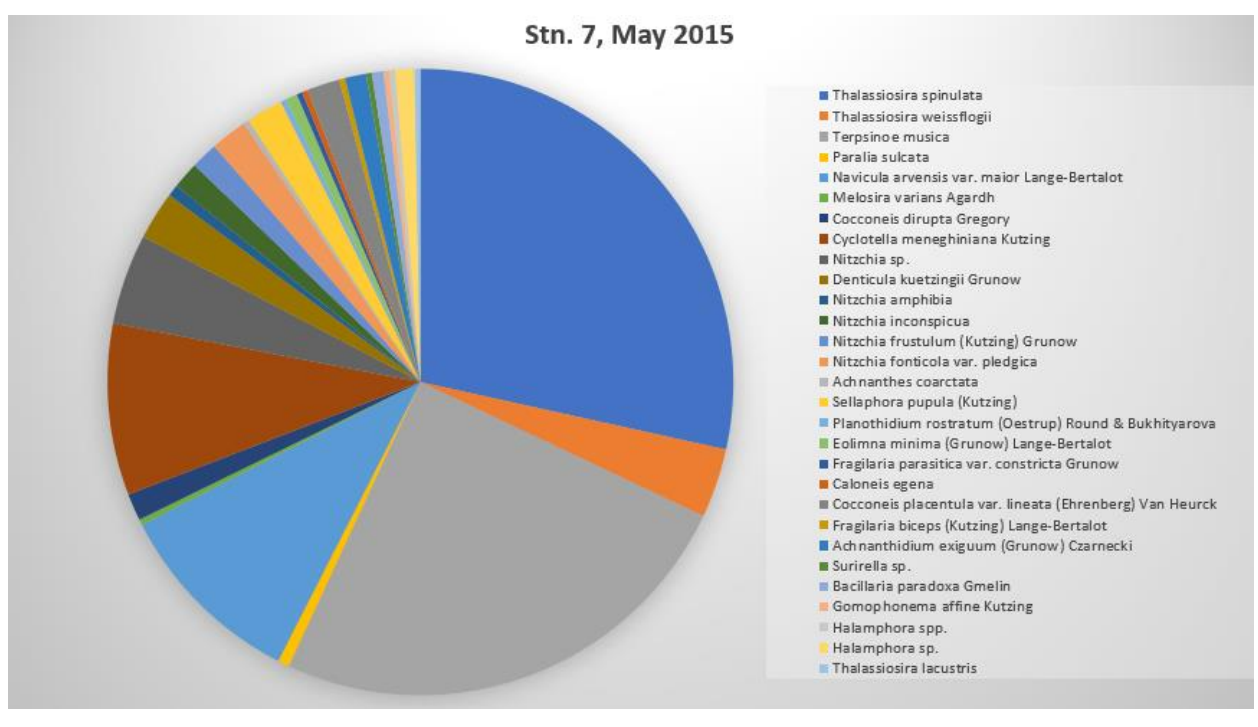
Appendix 1b. Stn. 7 population distributions.

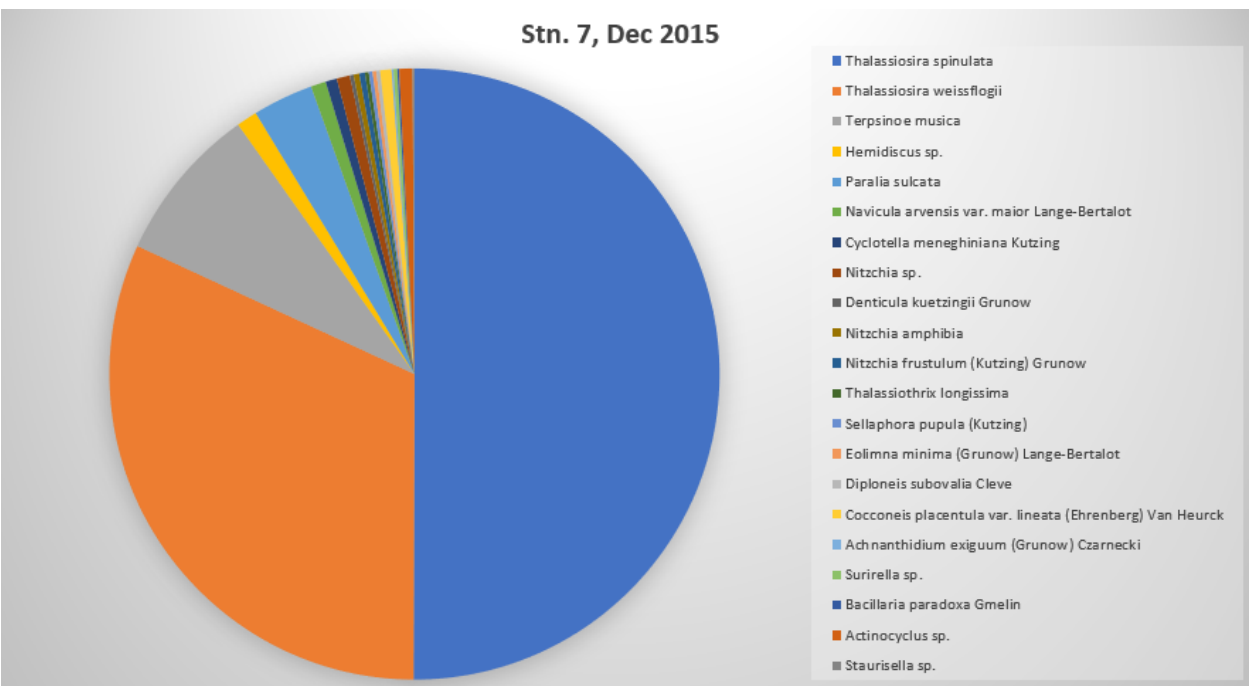




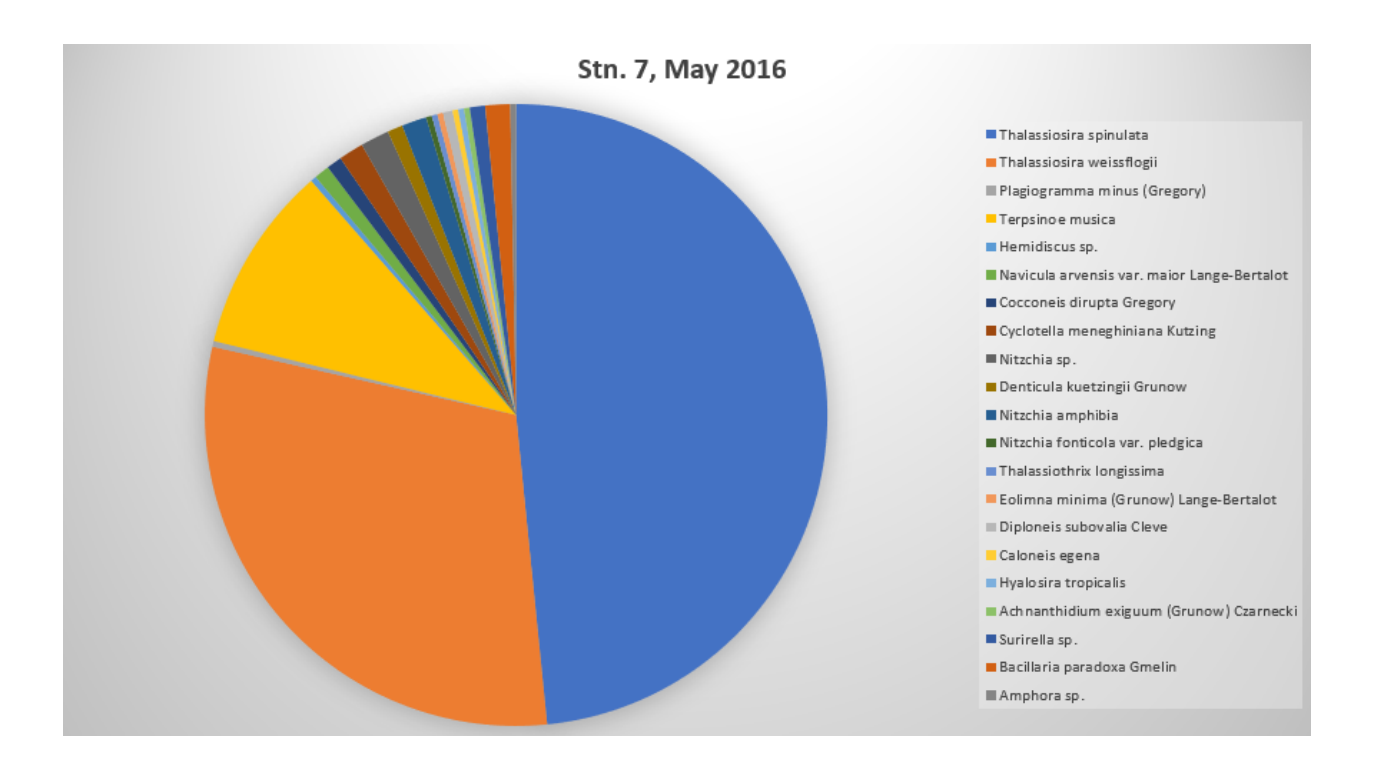


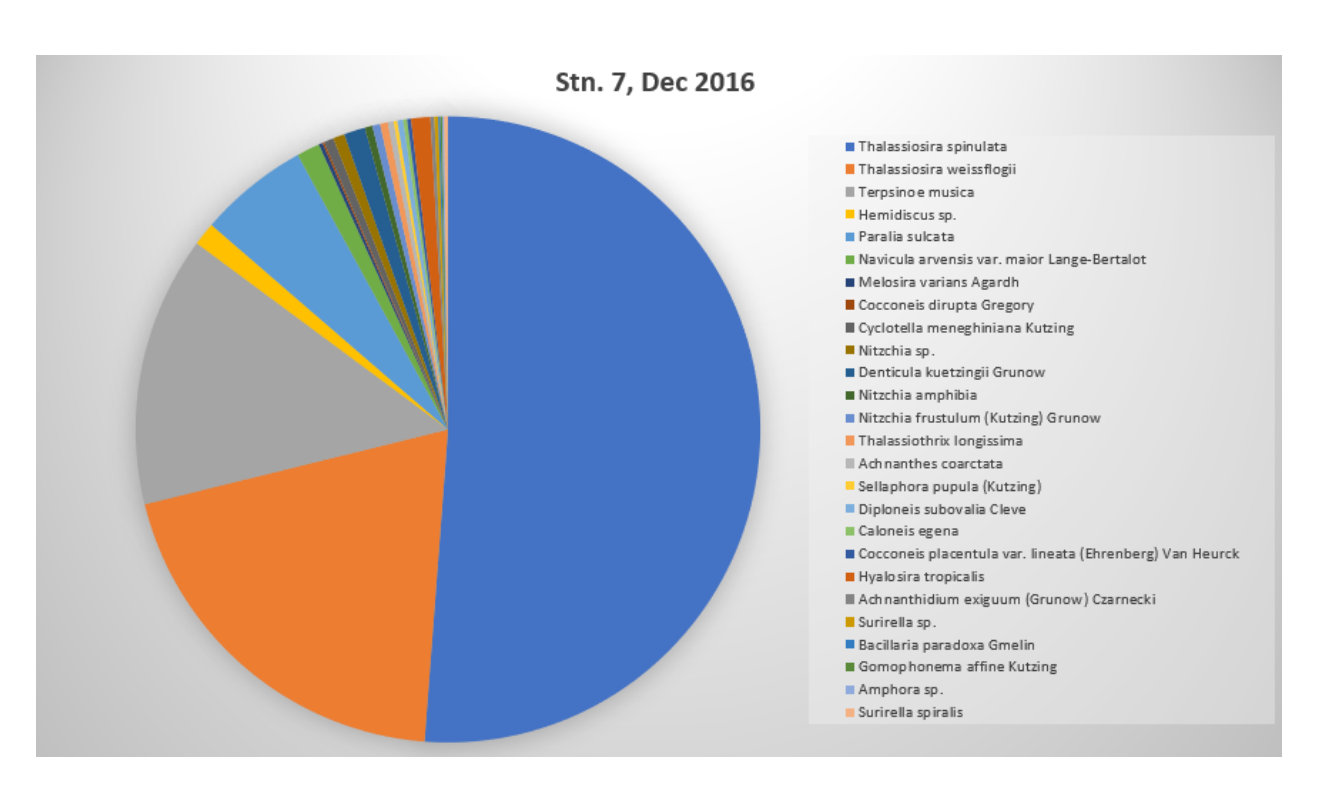


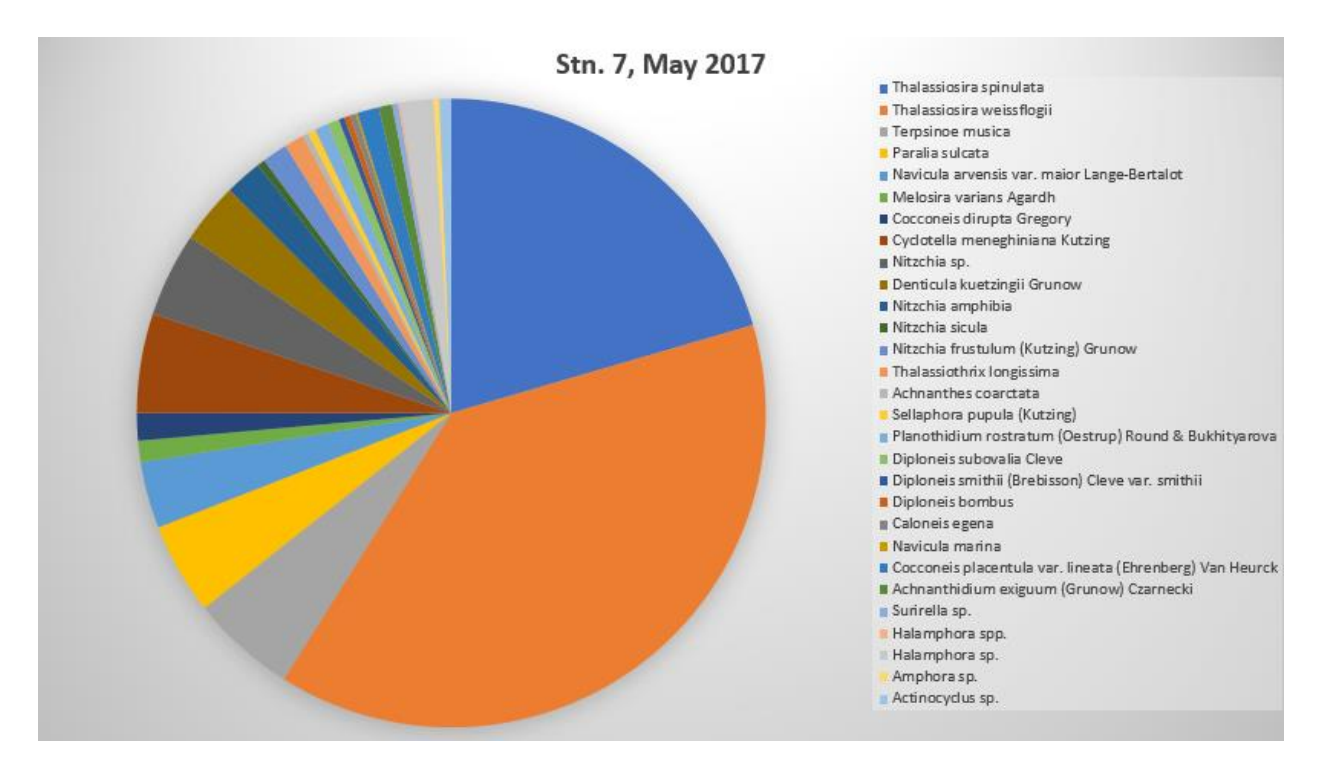




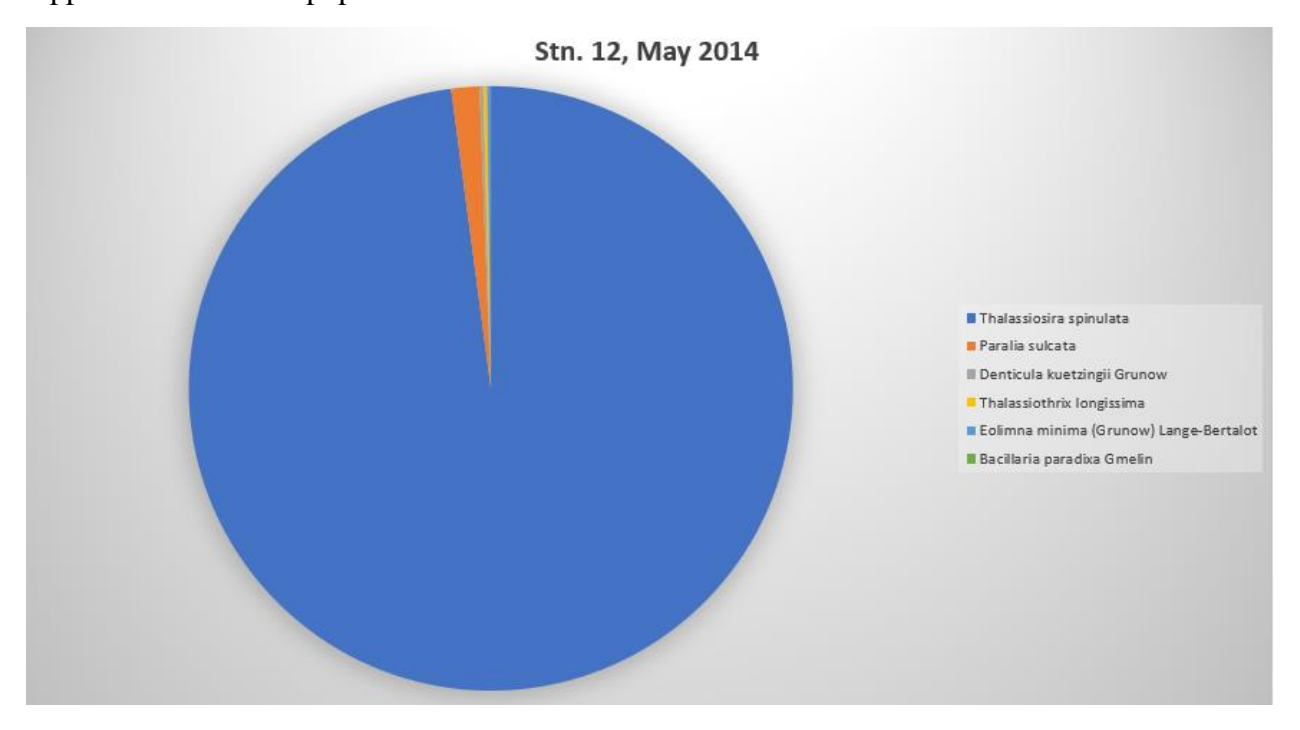
MSc Thesis – Katelyn Mountjoy; McMaster University – School of Earth, Environment and Society

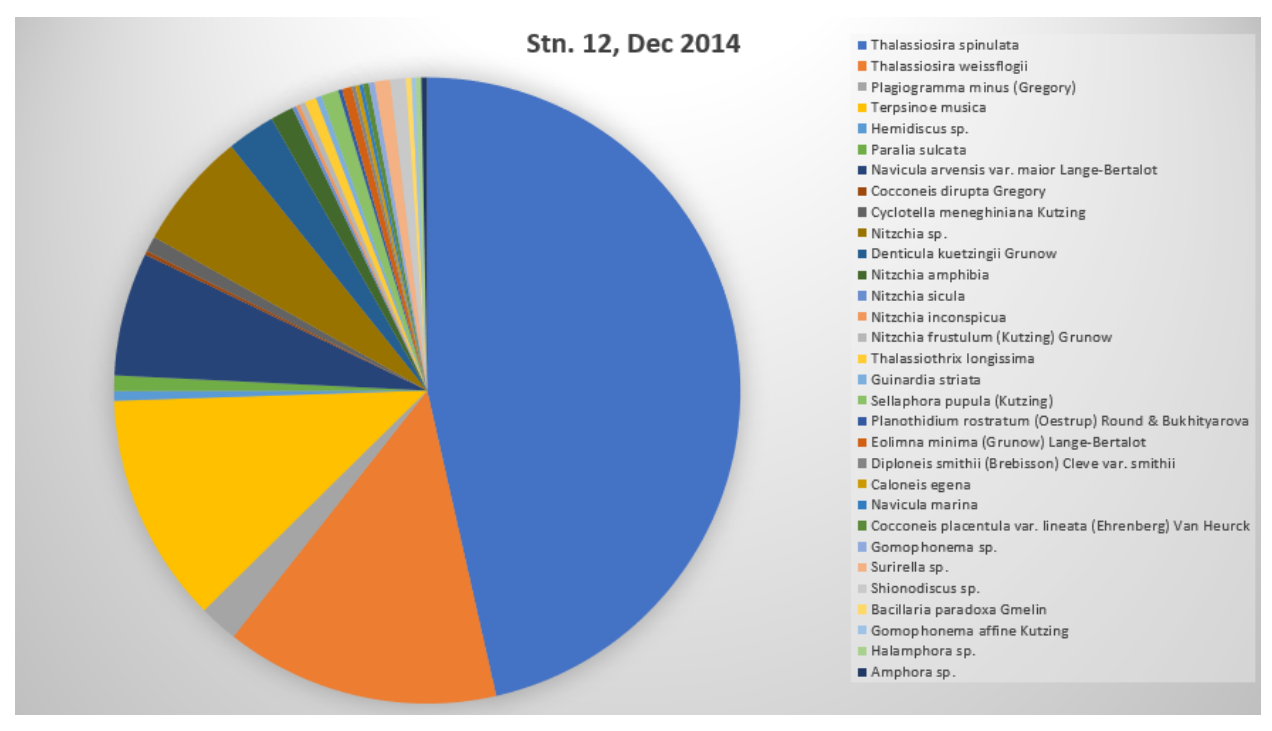


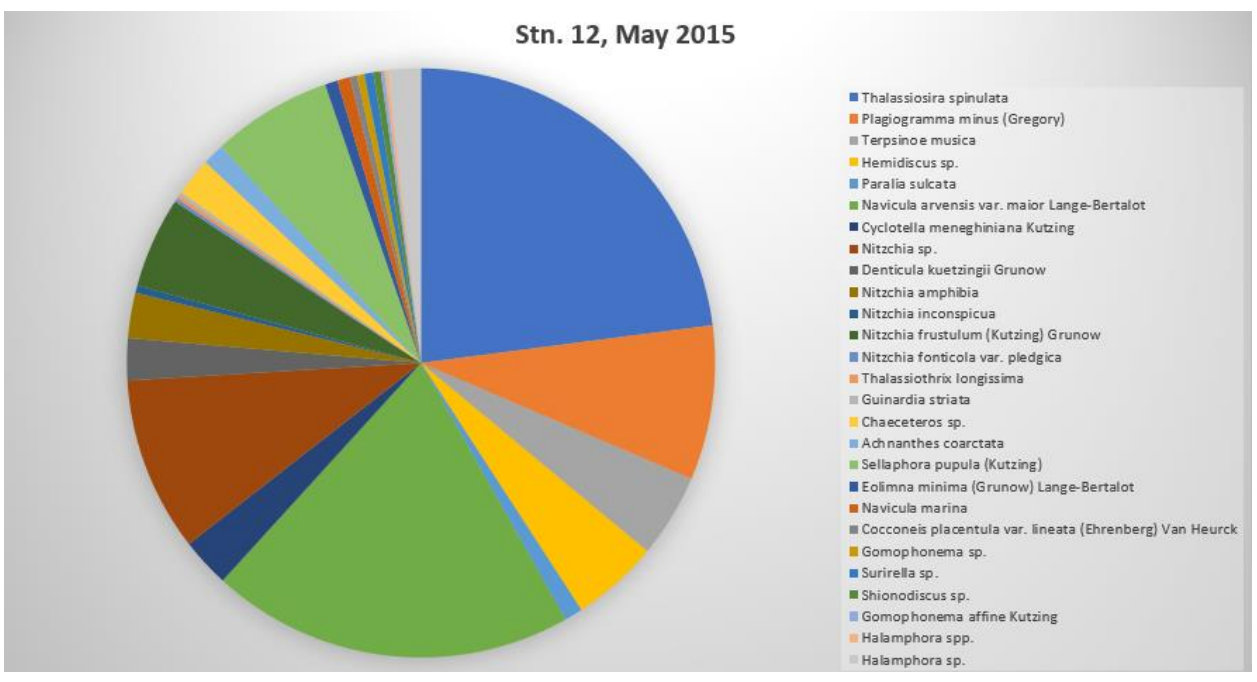


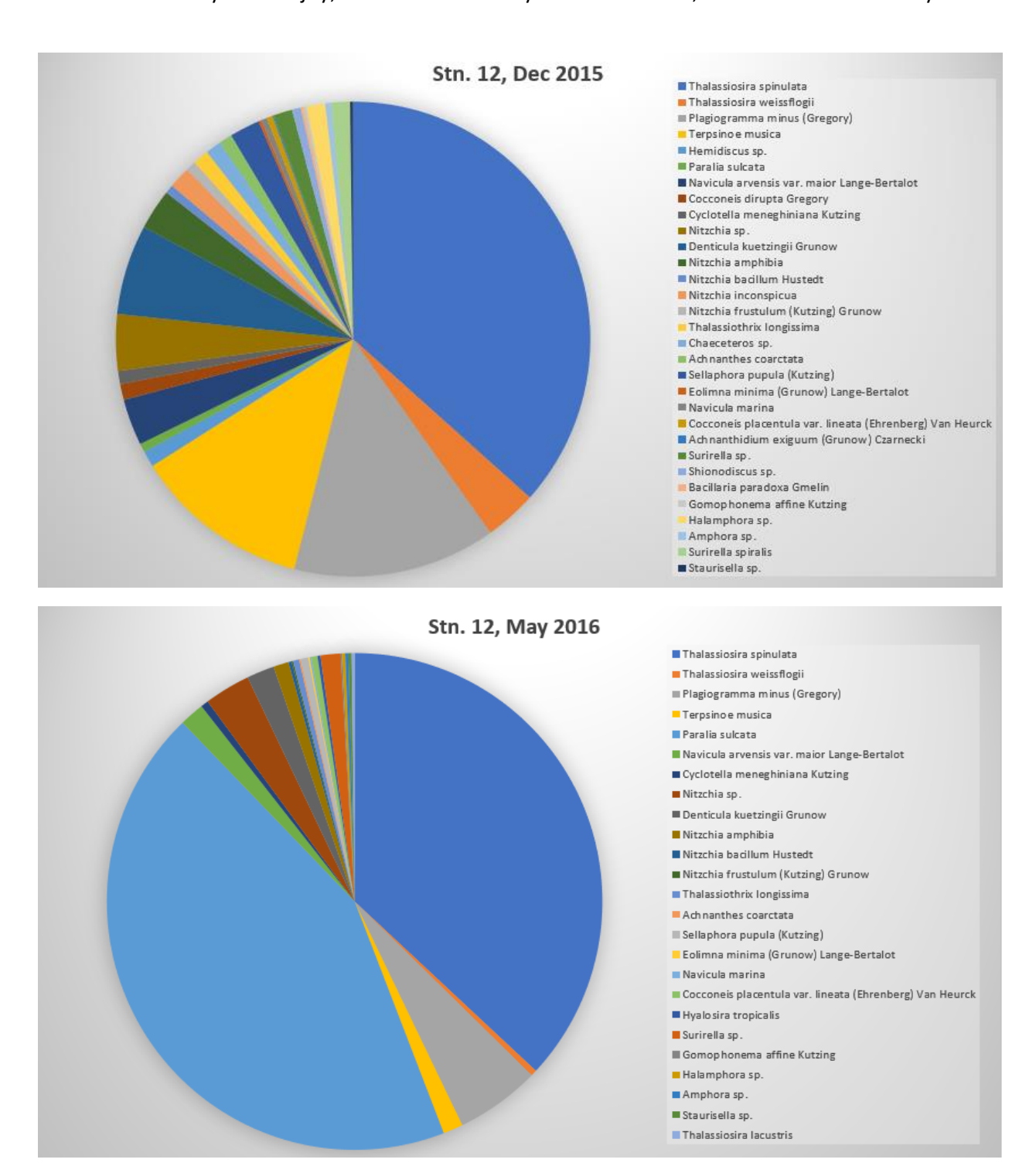


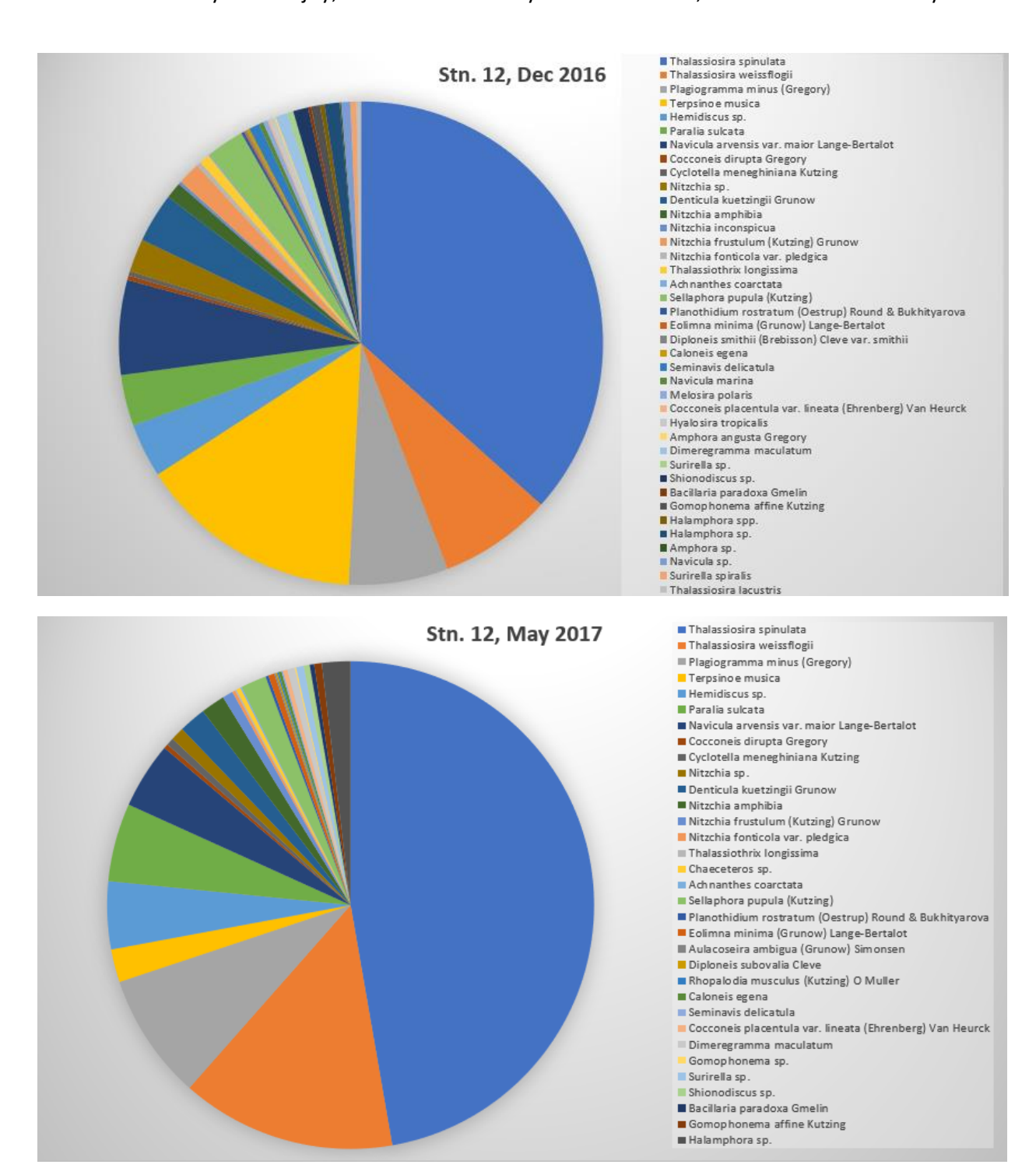
Appendix 1c. Stn. 12 population distributions.



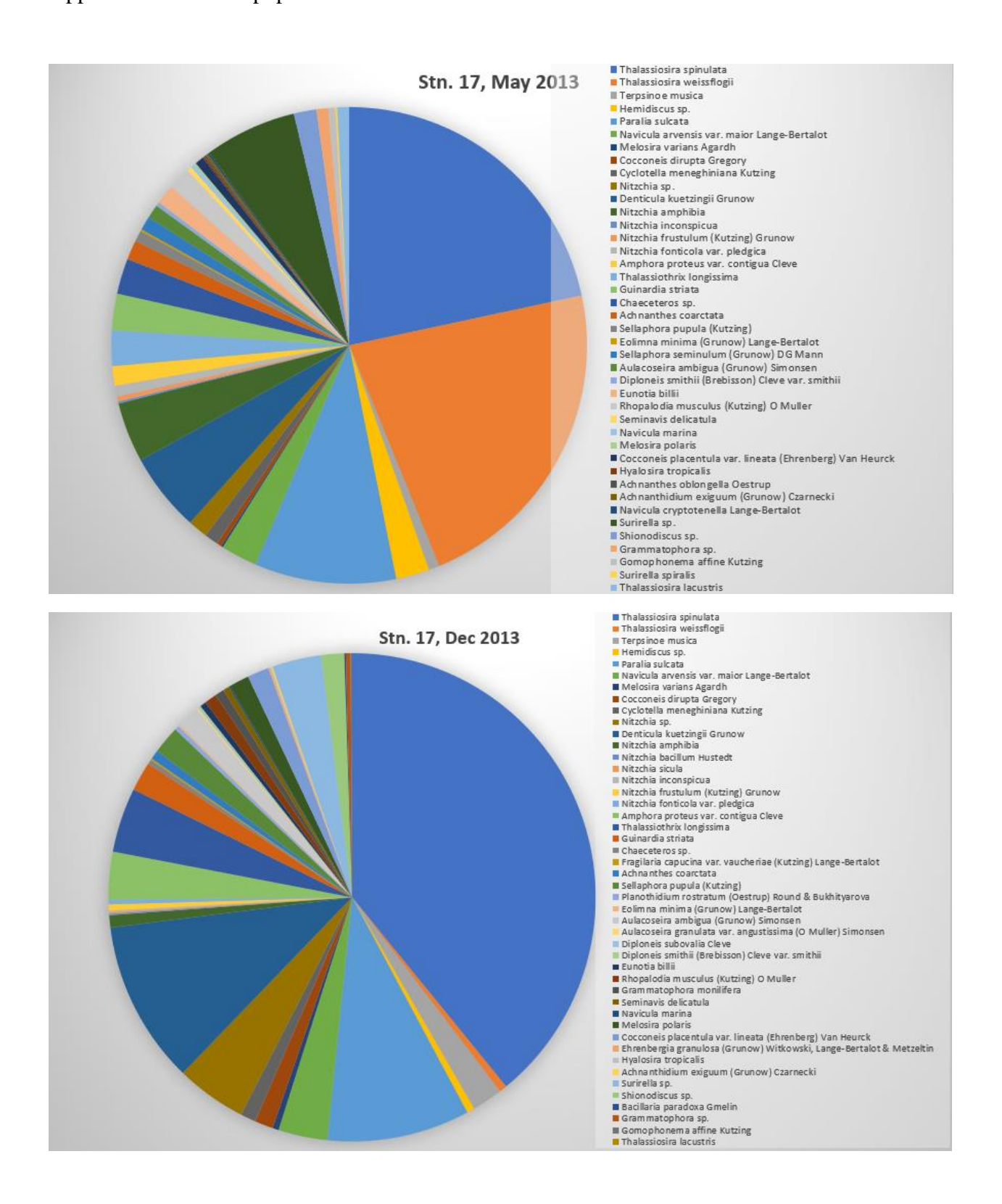


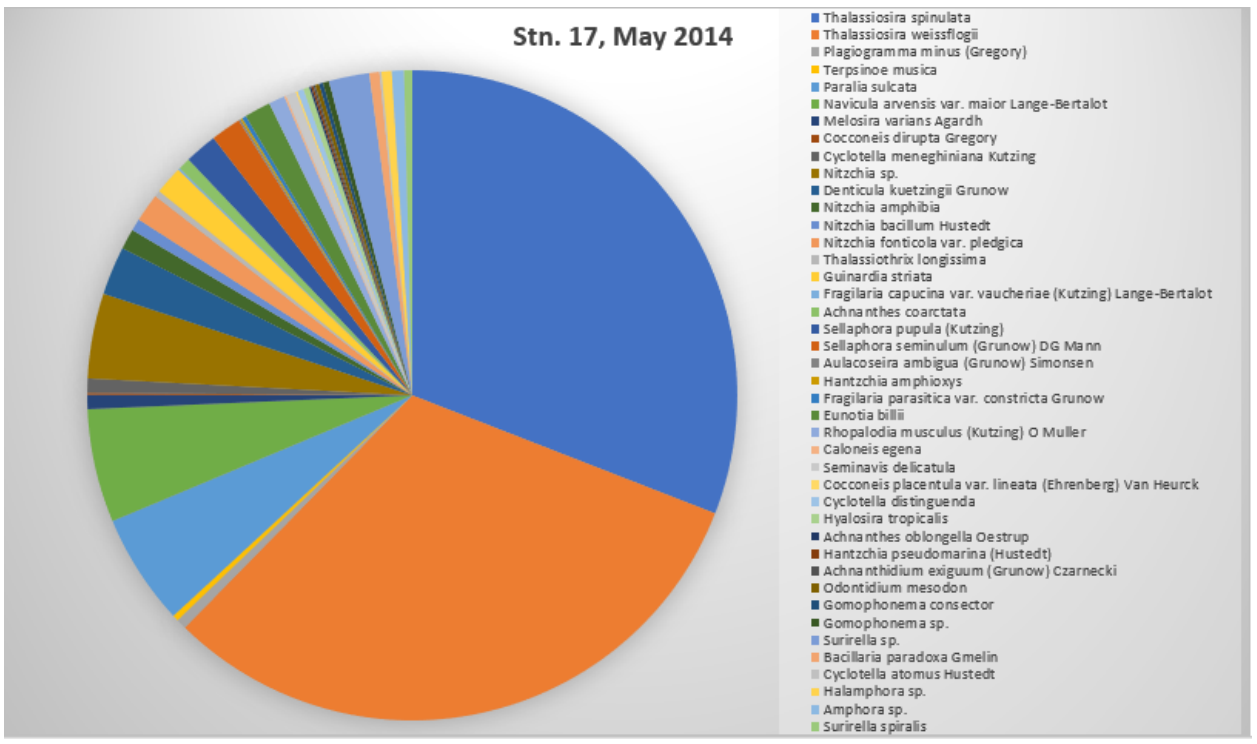


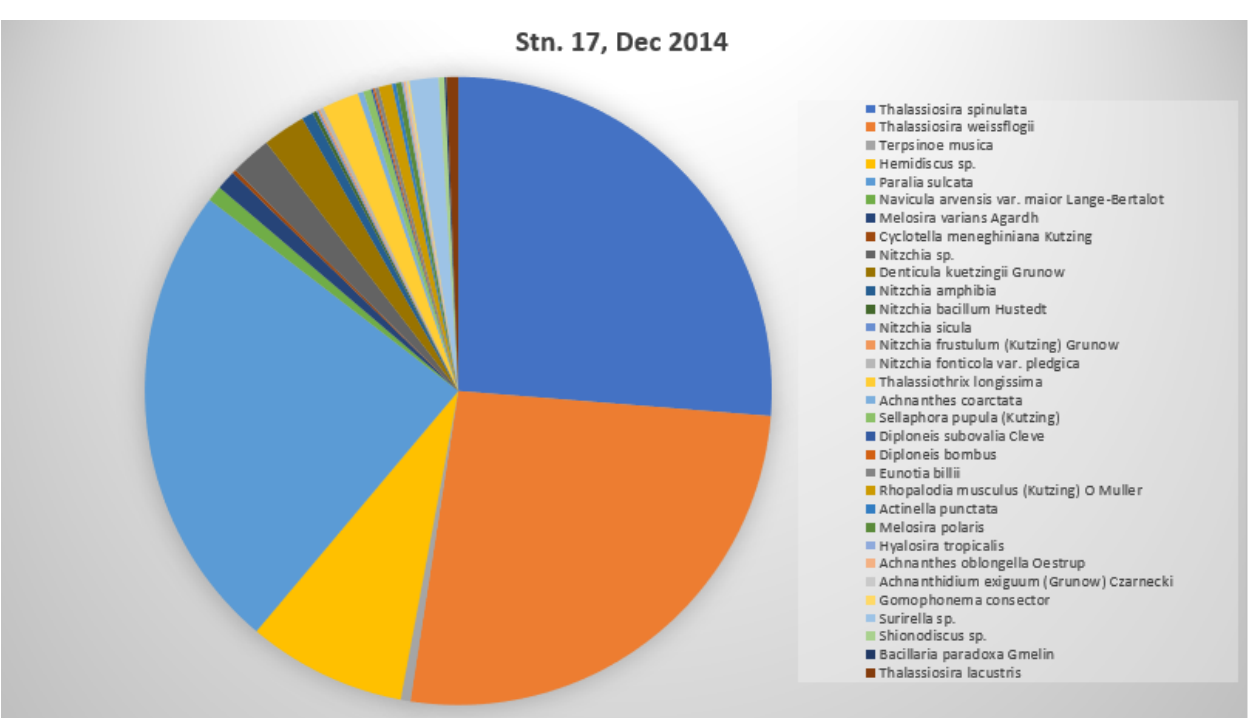


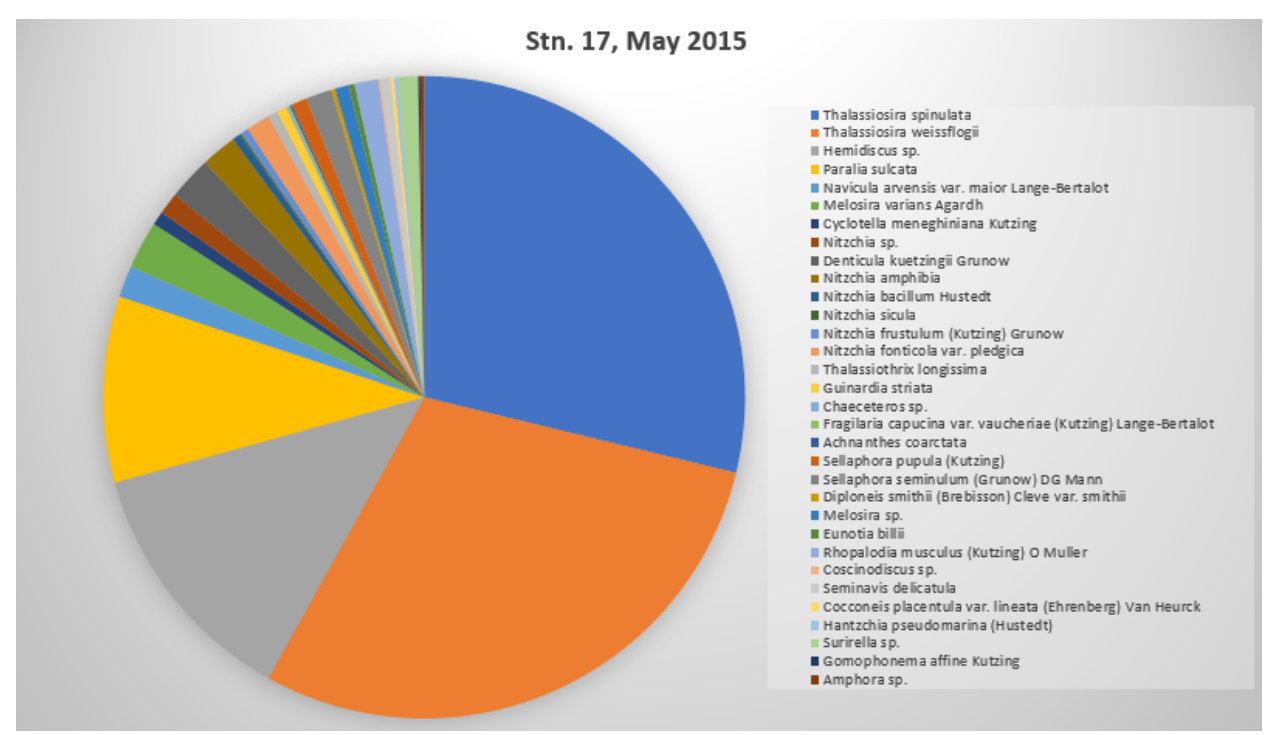


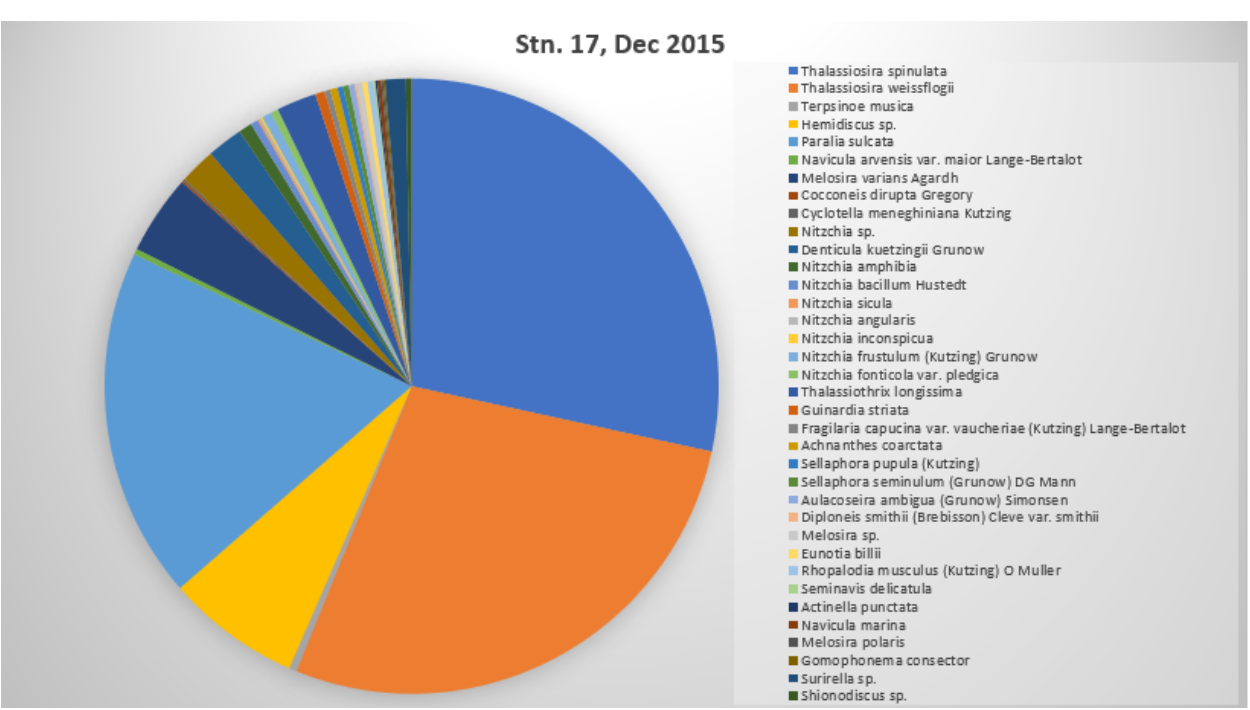
Appendix 1d. Stn. 17 population distributions.

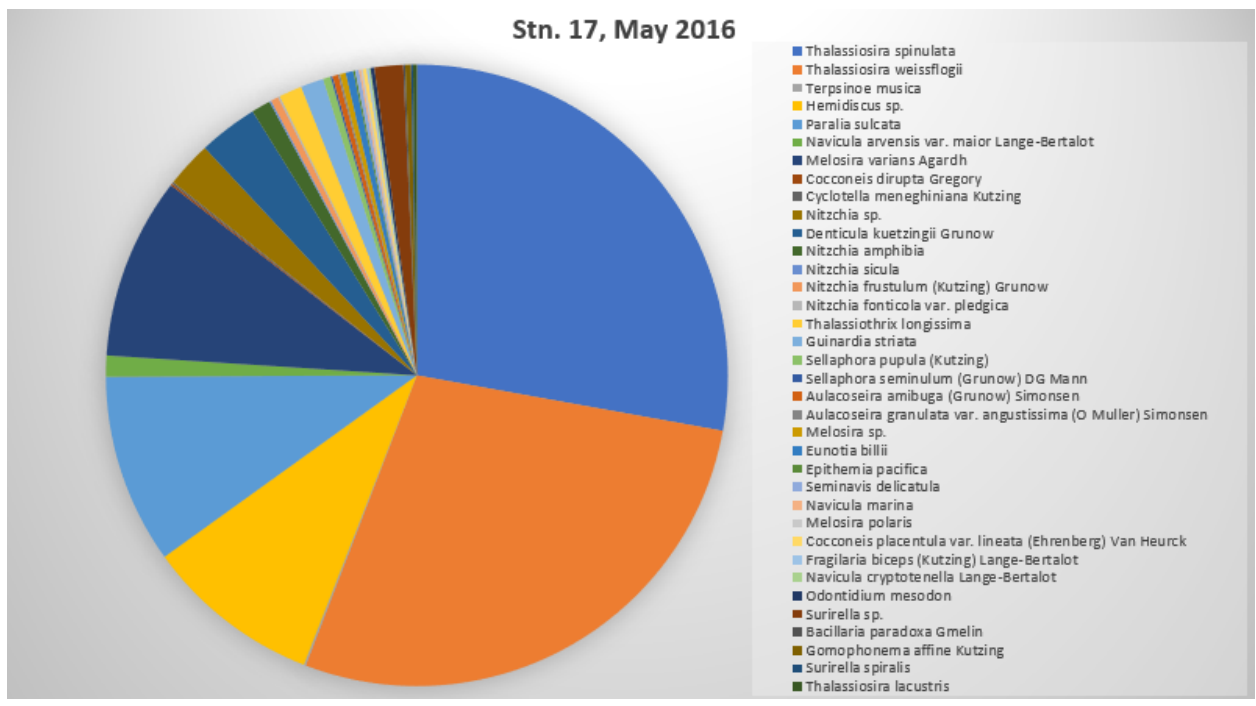


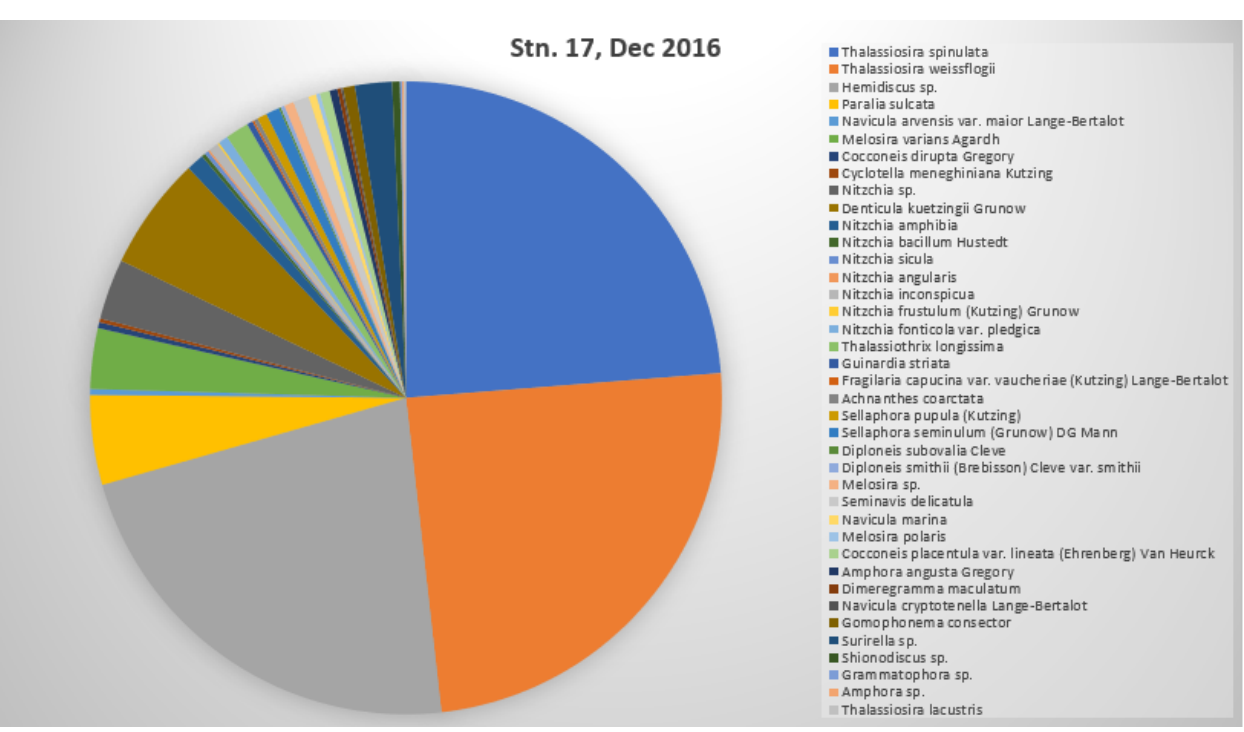


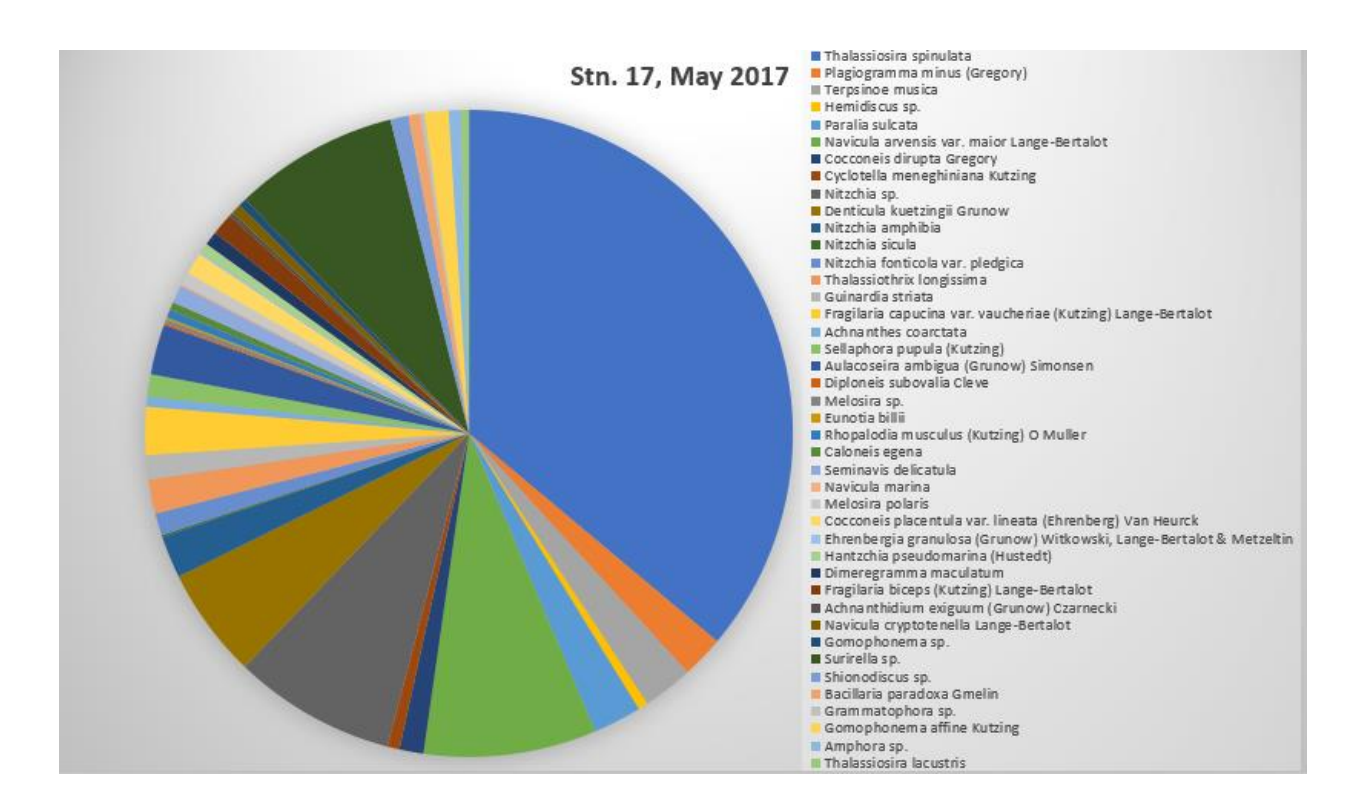




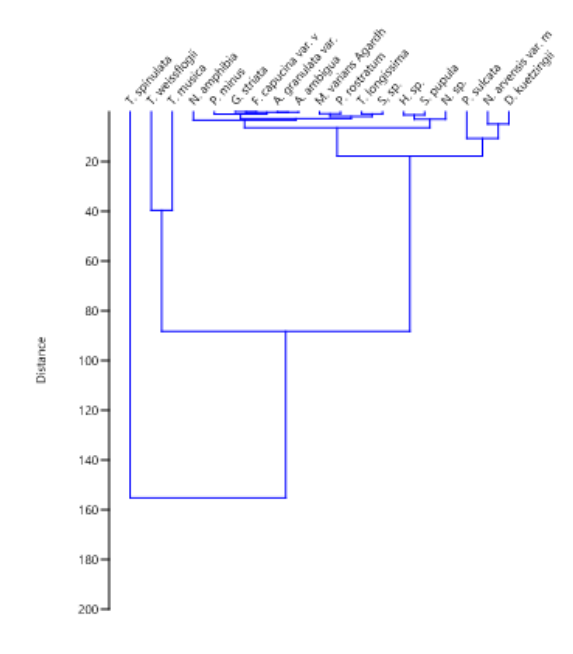




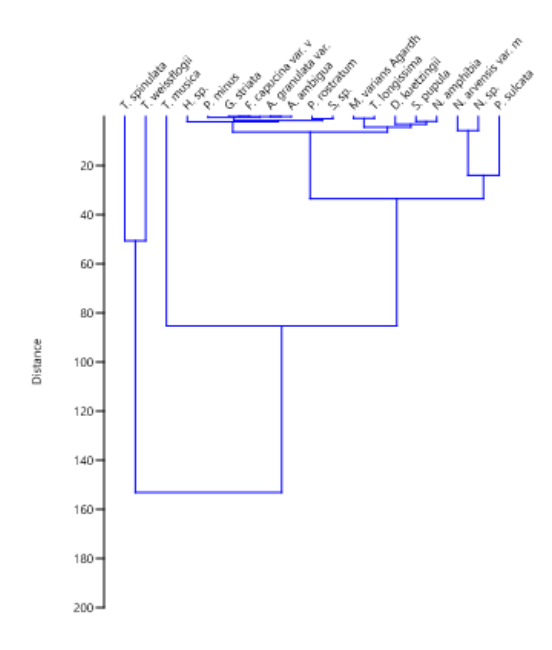




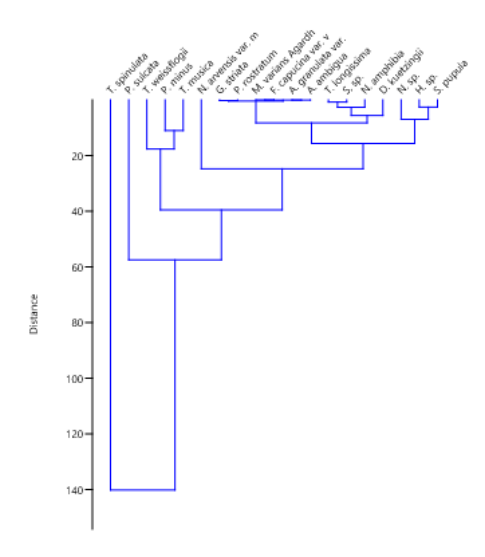
Appendix 2a. Expanded cluster analysis, stn. 2.



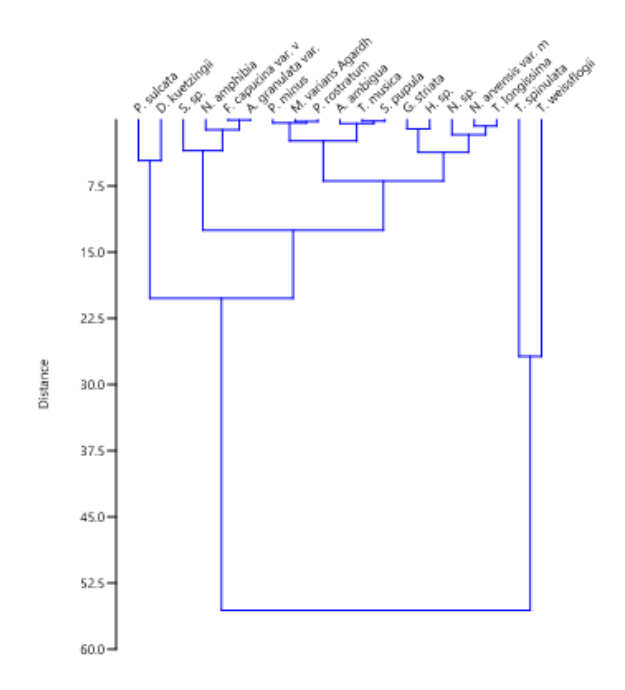
Appendix 2b. Expanded cluster analysis, stn. 7.



Appendix 2c. Expanded cluster analysis, stn. 12.



Appendix 2d. Expanded cluster analysis, stn. 17.



Appendix 3. Photographs of some of the most prevalent diatoms



Denticula kuetzingii Grunow

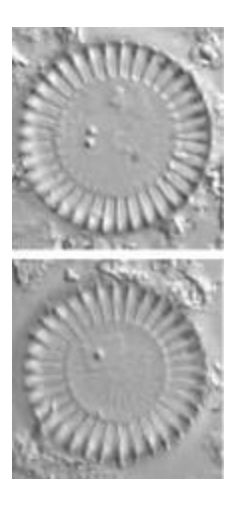
(Source: Taylor et al. 2007)



Navicula arvensis var. maior Lange-Bertalot

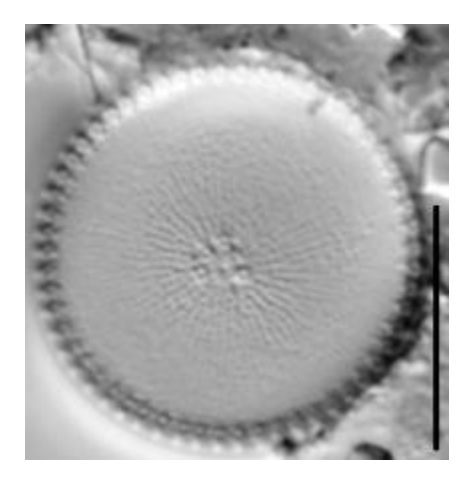
(Source: Taylor et al. 2007)

 $MSc\ Thesis-Katelyn\ Mountjoy; McMaster\ University-School\ of\ Earth,\ Environment\ and\ Society$



Cyclotella meneghiniana Kutzing

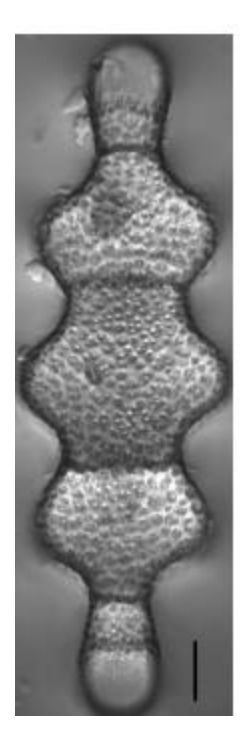
(Source: Taylor et al. 2007)

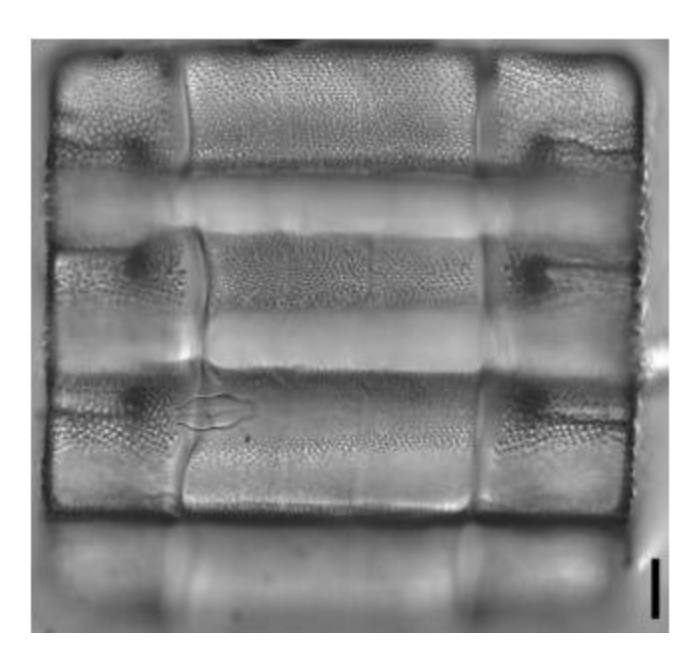


Thalassiosira weissflogii

(Source: Kociolek 2011)

 $MSc\ Thesis-Katelyn\ Mountjoy; McMaster\ University-School\ of\ Earth,\ Environment\ and\ Society$





Terpsinoe musica (Source: Wu 2013).